

Alma Mater Studiorum – Università di Bologna

DOTTORATO DI RICERCA

*Science for Conservation*

Ciclo XXII

Settore/i scientifico disciplinari di afferenza: CHIM/12

**PHYSICAL AND MINERALOGICAL CHANGES  
OF HUNGARIAN MONUMENTAL STONES  
EXPOSED TO DIFFERENT CONDITIONS:  
STONE-TESTING IN-SITU AND  
UNDER LABORATORY CONDITIONS**

Presentata da: **Magdalini Theodoridou**

Coordinatore Dottorato

**Prof. Rocco Mazzeo**

Relatori

**Prof. Ákos Török**

**Dr. Sándor Józsa**

**Esame finale anno 2009**

To my parents and Giannis

# Contents

1. Introduction.....	3
2. Brief Description of the Hungarian History Focused on the Middle Ages.....	5
3. Studied Site .....	8
3.1. Introduction.....	8
3.2. History and Construction Periods .....	8
3.3. Former Investigations .....	10
3.4. The Site Today.....	11
4. Studied Materials .....	14
5. Methods.....	17
5.1. In-situ Investigations.....	19
5.1.1. Mapping .....	19
5.1.2. Schmidt Hammer .....	19
5.1.3. Moisture Content .....	20
5.1.4. Drilling Resistance.....	21
5.2. Analyses under Laboratory Conditions .....	24
5.2.1. Petrographic Examination - Polarising Microscope .....	24
5.2.2. X-Ray Diffraction (XRD).....	24
5.2.3. Scanning Electron Microscope (SEM) .....	25
5.2.4. Porosimetry .....	25
5.2.5. Water Absorption.....	30
5.2.6. Determination of Sound Speed Propagation.....	31
5.2.7. Determination of Uniaxial Compressive Strength.....	32
5.2.8. Dynamic Modulus of Elasticity .....	32
5.2.9. Determination of Resistance to Frost Damage .....	33
5.2.10. Dynamic Mechanical Analyser.....	34
6. Results.....	36
6.1. In-situ Investigations.....	36
6.1.1. Mapping .....	36
6.1.2. Schmidt Hammer and Moisture Content .....	53
6.1.3. Drilling Resistance.....	59
6.2. Analyses under Laboratory Conditions .....	65
6.2.1. Petrographic Examination - Polarising Microscope .....	65

6.2.2.	X-Ray Diffraction (XRD) .....	70
6.2.3.	Scanning Electron Microscope (SEM) .....	70
6.2.4.	Porosimetry .....	72
6.2.5.	Water Absorption .....	85
6.2.6.	Pulse velocity, Strength, Elasticity and Artificial Frost Weathering ...	89
6.2.7.	Dynamic Mechanical Analyser .....	97
7.	Discussion .....	99
8.	Conclusions .....	109
9.	References .....	111
10.	Acknowledgements .....	124

# 1. INTRODUCTION

---

The presented thesis is a result of a three-year research within the frames of the EPISCON project (European PhD in Science for Conservation), coordinated by the University of Bologna and hosted by the Eötvös Loránd University of Budapest. The whole project was financially supported by the Marie Curie Actions, part of the 6<sup>th</sup> framework programme's Human Resources and Mobility (HRM) of the European Union.

The first objective of this research project was to further contribute to the existing knowledge about the studied site, the Ruin Garden of Székesfehérvár, with a focus on the identification of the different lithotypes and their distribution in the several parts of the monument built at different periods. The second objective was the characterization of the historical building stones, including information about the physical state of the materials, their properties and the identified decay forms. Finally, for a better understanding of the behaviour of the three most important identified lithotypes, a thorough investigation was carried out on specimens from existing local quarries with similar characteristics.

The current research, following its main objectives, was divided in three main parts. The first one concerned the National Memorial Place that was going to be studied. Therefore, it started with a thorough survey of the Ruin Garden of Székesfehérvár, focusing on the historical importance, the architecture of the monument and the different construction periods. A bibliographical survey on several libraries, several fieldtrips and discussions with the archaeologist in charge of the monument contributed to this first aim. The second step of this first part of the research was the identification of the different building stones and their distribution in the remaining parts of the monument. After macroscopic in-situ observations, several samplings were executed concerning the petrographic study of the building stones that were used during the construction.

The second part of the research activities focused on the investigation of the main identified lithotypes of the historical materials based on the physical and mechanical properties. The methods that were used for the identification of the material properties were based on both destructive and non-destructive techniques, under laboratory conditions and in-situ.

Finally, as a further step for understanding the behaviour of the three most relevant materials, additional samples were taken from local quarries with similar physical and mineralogical characteristics. The large number of samples tested under laboratory conditions, led to a fuller knowledge of the selected materials' behaviour.

Parts of this research have been already published related to the description of the historical studied site and the research methodology (Theodoridou 2008), the identification of the historical materials and their possible provenance (Theodoridou 2007, Theodoridou et al. 2008a) and the physical and mechanical properties of the historical materials (Theodoridou & Török 2008, Theodoridou et al. 2008b).

## 2. BRIEF DESCRIPTION OF THE HUNGARIAN HISTORY FOCUSED ON THE MIDDLE AGES

---

The state of Hungary is located in the Carpathian Basin of central Europe bordered by Austria, Slovakia, Ukraine, Romania, Serbia, Croatia and Slovenia. Its capital is the city of Budapest (see Fig. 2-1).



**Fig. 2-1: Map of Hungary**

Since 9 AD and until the end of the 4<sup>th</sup> century, the Western part of the Hungarian territory was occupied by the Roman Empire and the name of the province was Pannonia. During this period, the area experienced a flourishing civilization and the location of many of the most important Hungarian cities was defined already from that age as for instance the constitution of Aquincum, the capital of Lower Pannonia, which ruins can be found today within the borders of the city of Budapest. (Csorba et al. 2005)

The Magyars, seven nomadic Finno-Ugric tribes, started their migration from the Ural region which led them to the Carpathian Basin around 895. Árpád was the name of their leader who settles where the town of Székesfehérvár was later founded. The first dynasty of Hungary was named after him. The conversion into Christianity started by the grandson of Árpád, Prince

Géza around 970. Hungary was recognized as a Catholic Apostolic Kingdom under the kingship of István I (St. Stephen) who succeeded his father Géza after his death. King István received the Holy Crown from the Pope and was crowned in December 1000 in Esztergom. (Csorba et al. 2005)

In the Middle Ages, three were the most important centers in Hungary: Esztergom, Székesfehérvár and Buda and the triangle of them was considered to be the ‘middle of the country’ (Altmann et al. 1999). This could be attributed not only to the easy accessibility of the area from every other part of the country but also to the fact that the west part of the country, taking into consideration its division by the river Danube, seemed to have higher density in terms of population. The most important centre was Esztergom which was also the ecclesial centre of the country. The second centre was Székesfehérvár. The town was the place where most of the Hungarian kings were crowned and buried. Buda was the third centre which role is not well known for a long time. In the 13<sup>th</sup> century it became the most important town and royal residence. Already in the following century it started to be considered as the capital of the country though only at the beginning of the 15<sup>th</sup> century the royal household moved to Buda with Esztergom remaining the ecclesial and the ecclesiastical judicial centre and Székesfehérvár the place for the coronation and burial of most of the Hungarian kings not only during the Árpád dynasty but also for the dynasty of Anjou which followed.

In 1241 Mongols invaded the Hungarian territory after the Hungarian army was defeated in the battle of Mohi, resulting to a high number of victims of the Hungarian population. In 1242, Mongols left the country and King Béla IV began to rebuild the country including constructions of castles and fortifications as a defense against a possible second Mongol invasion.

King Matthias was one of the most important kings through the Hungarian History (1458-1490). He succeeded to unify the country politically and the period that lasted even after his death is known as the Golden Age of Hungary. Besides being a successful military leader, the famous mercenary ‘Black’ army was created during his kingship, he reorganized the state administration and carried out remarkable projects such as lots of construction work, supporting science and art and the establishment of the Corvina library which is still famous thanks to its huge size. Concerned about the danger of Turkish attacks he also turned his attention to military architecture (Lővei et al. 1998).



In 1526, the battle of Mohács was the first decisive victory of the Ottoman Empire in the Hungarian territory. In 1541, Buda was occupied by the Turks which led to the division of the country in three parts. Turkish occupation lasted 150 years in which many of the medieval settlements were demolished and the population growth was stunted.

## 3. STUDIED SITE

---

### 3.1. Introduction

Székesfehérvár is a city in central Hungary, located around 65km southwest of Budapest. In the Middle Ages (11<sup>th</sup> and 12<sup>th</sup> centuries), the city was a Royal residence and until the Turkish occupation in 1543, one of the most important cities of Hungary. This is also supported by the etymology of the city's name which translation into English is "white castle with the seat" with the word "seat" referring to the throne of the king.

The Ruin Garden of Székesfehérvár is a unique assemblage of monuments belonging to the cultural heritage of Hungary due to its important role in the Middle Ages as the coronation church for the kings of the Hungarian Christian Kingdom and the burial place for fifteen kings, several members of the royal families and later on, of the high nobility. It was also the home of the royal treasury and relics. It is comprised of a provostal church dedicated to Virgin Mary, so called today "Royal Basilica", royal tombs and related ecclesial and lay buildings. Since it has been nominated for "National Memorial Place", its present and future protection is required.

Its several reconstructions and expansions throughout Hungarian history introduce another aspect of the importance of the historical site. By a quick overview of the current state of the monument, the presence of several lithotypes can be found among the remained building and decorative stones. Therefore, the research related to the materials in order to understand their composition, structure, origin and behavior is crucial not only for the conservation of that specific monument but also for a series of other historic structures in the Hungarian territory.

### 3.2. History and Construction Periods

Between the 11th-15th centuries, the basilica was reconstructed several times. The Turkish occupation (1543-1688) was the beginning of the destruction of the church assemblage, which went on by using it as a storage facility and even its stones were used in the town's defence system until its final demolition during the 18th-19th centuries by that current bishop and the municipality of Székesfehérvár (Dercsényi D. 1943).

The first objective of this research project is to further contribute to the existing knowledge about the national monument of Székesfehérvár, with a focus on the identification of the different lithotypes and their distribution in the several parts of the monument built at different periods. Consequently, a deep comprehension of the ruins in terms of the different construction phases was needed. To that aim four fieldworks, literature survey, several discussions with the archaeologist in charge Piroska Biczó and photographic documentation contributed. According to all mentioned above, existing maps of the site were modified and enhanced in order to help the presentation and documentation of the research. The following description constitutes a summary based on existing bibliography (Biczó P. 2005).

### **11<sup>th</sup>-12<sup>th</sup> centuries**

The first phase of construction underwent during the 11<sup>th</sup> - 12<sup>th</sup> centuries, at the age of the Arpad Dynasty. It begun approximately in 1018, founded by King St. Stephen I (1000-1038), the first King of Hungary's Christian Kingdom who was canonised in 1083. Its size can be characterized by the number of the altars and side chapels which in the Árpád age were at least five but in later periods the number can be estimated at thirty-forty (Altmann et al. 1999). The royal basilica was in the axis of the building complex of the provostry with the palace of the provost and its lay buildings placed to the north, in accordance with the old town plans and the evidence of the excavation in 1979, and the cloister and the rooms belonging to the friary of the provost situated in the south of the basilica (Altmann et al. 1999). The church was modelled on Mediterranean and German Ottonian churches. It had a westwork entrance, a wide nave with two aisles and at the eastern façade, a wide semicircular apse is visible with smaller square rooms on both sides that could have been chapels or sacristy. According to contemporary sources this type of rooms, which recall earlier Byzantine-Italian models such as S. Apollinare in Classe in Ravenna, had an upper story, probably used as the house for the royal treasury, relics or the royal insignia (Lövei et al. 1998). In the main part, the spacious basilica is divided by rows of pillars or columns and a row of arcades providing access to the western façade, where we can see the part of the foundation of an added smaller structure.

## **12<sup>th</sup> century**

During the Arpadian Age, in the 12<sup>th</sup> century, the first rebuilding took place. It included the demolition of the arcades and the renovation of the supporting elements in the nave, reconstruction of the northern wall of the western structure and of the main walls in the southern part. In addition, some slabs are visible in the cloister of the southern part.

## **1<sup>st</sup> half of the 14<sup>th</sup> century**

Several Destructions by fires was the reason for the first gothic reconstruction that started in 1318, in the Age of the Anjou Dynasty. Further reinforcement of the 12<sup>th</sup> century pillars took place.

## **14<sup>th</sup>-15<sup>th</sup> centuries**

Another fire in 1327 led to the second Gothic reconstruction (14<sup>th</sup>-15<sup>th</sup> centuries) that included the rebuilding and enlargement of the pillars and the construction of a new tower in the western structure. The buttresses at the corners penetrated the 11<sup>th</sup> century walls.

## **2<sup>nd</sup> half of the 15<sup>th</sup> century**

The last expansion of the temple was implemented by King Matthias in the 2<sup>nd</sup> half on the 15<sup>th</sup> century. It changed the size and the proportions of the church, giving it an extra length of about thirty six meters towards the east and the nave was re-vaulted (Altmann et al. 1999). This construction was one of the most important commissions for the late Gothic royal workshop where Gothic and Renaissance styles were combined (Lővei et al. 1998).

### **3.3. Former Investigations**

Several studies has been carried out in the past decades related to the topography of the region and the historical background of the monument including archaeological investigations e.g. Dercsényi 1943, Fitz 1956, Fügedi 1967, Kralovánszky 1988, Siklósi 1992 & 1993. An intervention took place in the monumnet in the 1960's and the presence of cement mortar is related to it. The National Office for the Protection of Historic Monuments started the

analytical investigation of the territory in 1995. It contains the determination of the groundwater table and geological surveys of the ground (Maucha & Sárváry 1998 & Moyzes 1995) and first petrological and mineralogical investigation on samples of the building materials (Oravecz 1997, Tóth 1995 & Wojnárovits 1995). In the last ten years, new restoration activities included the exhumation of historic walls under the covered area in the Southern part of the site and the use of commercial restoration products such as Remmers mortar in many parts of the outdoor and uncovered areas.

### **3.4. The Site Today**

The Ruin Garden is located in the historical centre of the city of Székesfehérvár. In the 19<sup>th</sup> century, the excavation by Imre Henszlmann revealed the size of the main parts of the church. However, the ruins were still buried in the garden of the bishop palace located in the past western part of the temple. The next century excavations took place in the 30's by the architect Kálmán Lux. In the 60's, the process restarted under the supervision of the archaeologist Alán Kralovánszky and since 1993 the archaeologist in charge has been Piroska Biczó. The total site of the excavated ruins nowadays is approximately 4700 m<sup>2</sup>. The palace of the bishop still borders the excavation area today on the northwest part of the Ruin Garden.

For the 900<sup>th</sup> anniversary of St. Stephen's death, after the excavation between 1936 and 1938, the ruin garden was open to the public and the ruins were shown to the visitors in their original condition before any intervention (Altmann et al. 1999). In the eastern part of the remains of the Monostorbástya, a museum of stone carvings and the mausoleum were erected. The stone tomb, which has been called St. Stephen's sarcophagus after the published study by Varjú in 1930, is placed in the aforementioned mausoleum. The places are open to the public and a high number of tourists are visiting the site.

A European project has been approved for the rehabilitation of the entire city centre of Székesfehérvár including the renovation of the Ruin Garden. The main project related to the Ruin garden will be the construction of a new roof that will cover nowadays unprotected area. At the moment it is under design and no final decision has been made about the structure and shape of the roof system.



**Fig. 3-1: Views of the Ruin Garden: a) & b) parts of the uncovered area, c) & d) parts of the covered area.**

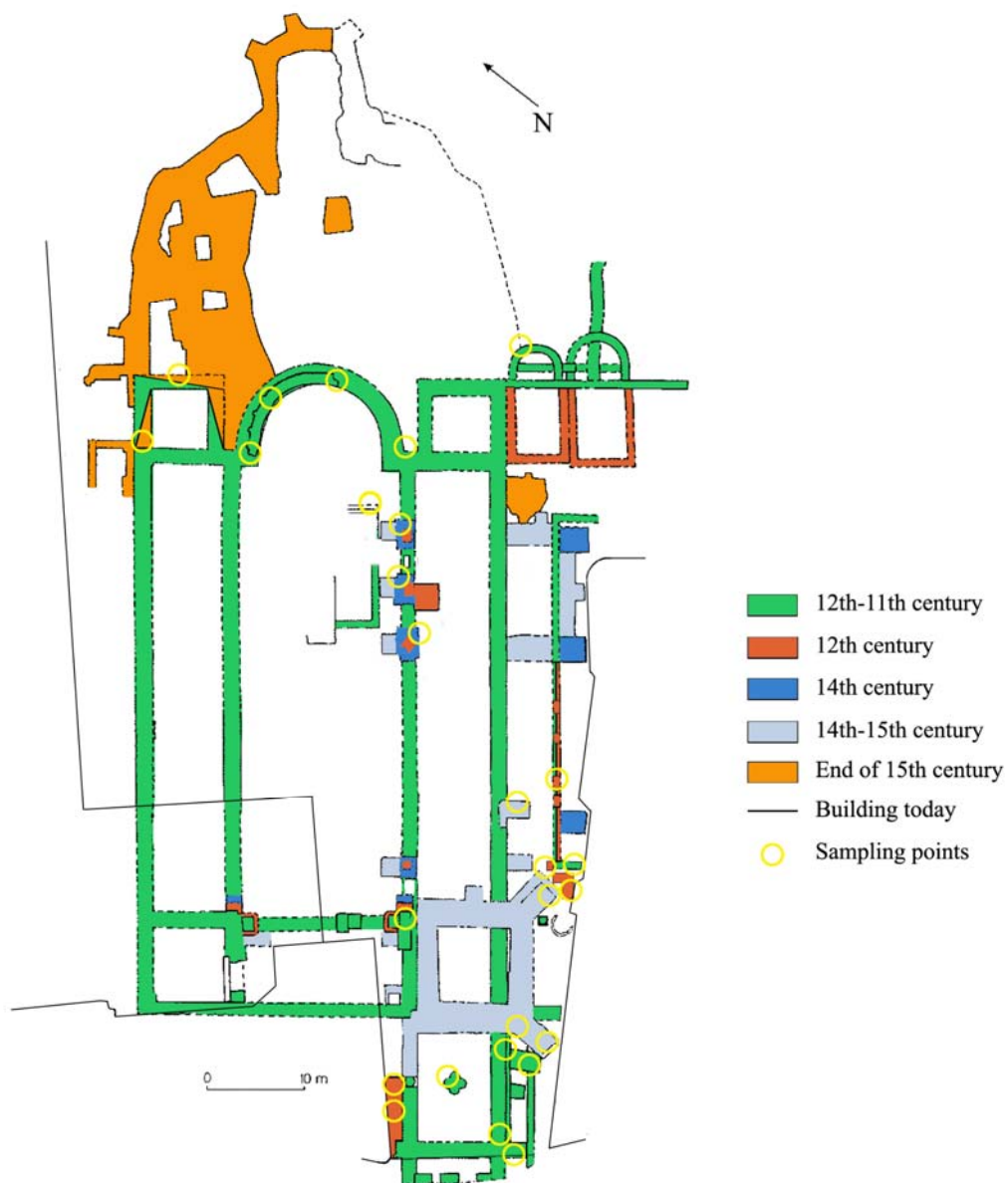


**Fig. 3-2: Map of excavated ruins of the Székesfehérvár Ruin Garden depicting their different periods of construction and the main sampling points (modified after Bartos et al. 2004)**

## 4. STUDIED MATERIALS

---

Three different groups of samples were studied for the implementation of this current study as they can be seen on Table 4-1 and Fig. 4-1.

The first group aimed at the identification of the different building stones and their distribution in the remaining parts of the monument. After macroscopic in-situ observations, two main samplings were executed concerning the petrographic study of the building stones that were used during the construction. The first one included samples taken from left over pieces. For the second one, building stones from the existing walls were sampled, considering the different lithotypes' distribution over the existing ruins. Small irregular samples were taken from a total of fifty seven building stones.

The second group was comprised of a selection of eight representative historical materials that took place for further and deeper investigations under laboratory conditions, taking into consideration the distribution of the material in the construction and the common decay phenomena: two Oolitic Limestones (OL & OL\_2), two Shelly Limestones (SL & SL\_2), a Sandy Calcarene (SC), a Red compact Limestone (RL), a Rhyolite (Rh) and a Marble (M). A total number of twenty five prismatic samples with dimensions of about 4 x 4 x 4 cm were used for this part of the study in addition with twelve smaller samples of about 2 x 2 x 2 cm that were used for the determination of total open porosity and the pore-size distribution.

Finally, as a further step for understanding the behaviour of the three most relevant materials, additional samples were taken from local quarries with similar physical and mineralogical characteristics: a medium-grained Oolitic Limestone (OL-Q1) and a coarse-grained Oolitic Limestone (OL-Q2) from Sóskút and a Red compact Limestone (RL-Q) from Tardos, Hungary (see Fig. 1-1). The specimens belonging to this final group of samples were hundred fifty nine cylinders of about 5 cm of height and 5 cm of diameter.



Group of Samples	Origin	Size	Total N.
1st	Monument	small & irregular	57
2nd	Monument	prismatic: 4x4x4 cm / 2x2x2 cm	25 + 3
3rd	Local Quarries	cylindrical : 5x5x5 cm	159

**Table 4-1: Groups of samples submitted to the tests and analysis of the current research**

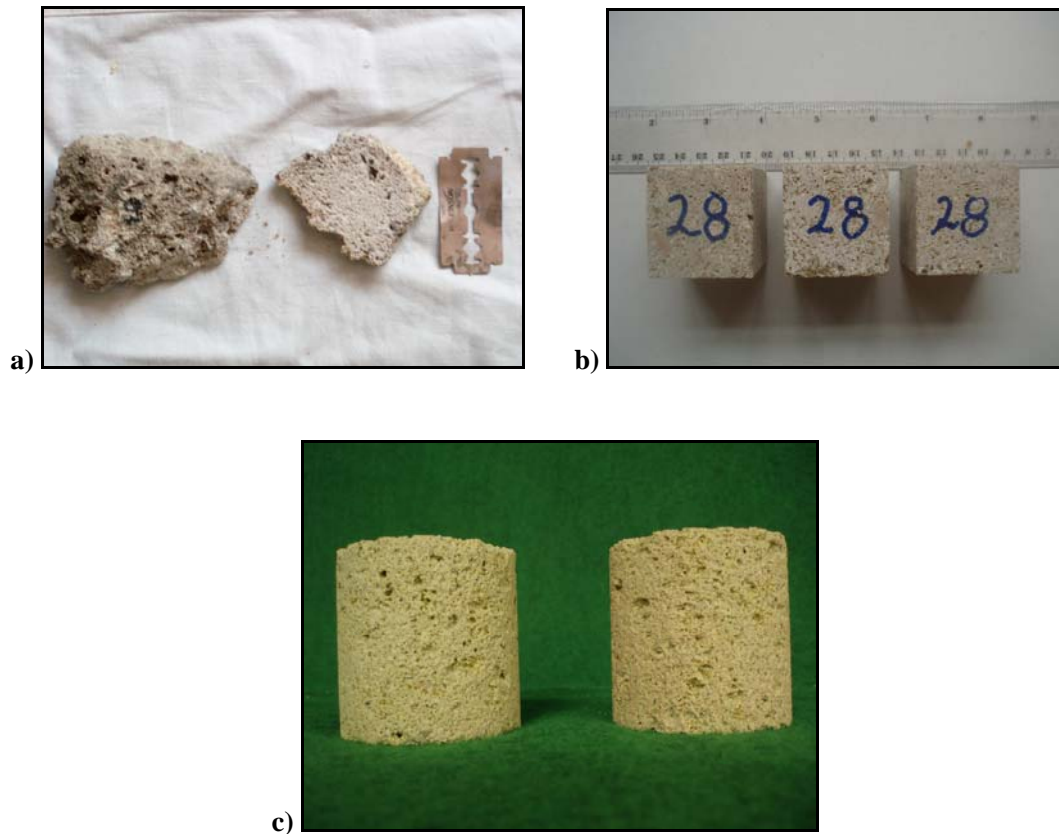


**Fig. 4-1: a) Irregular small sample from the monument (1<sup>st</sup> group), b) prismatic samples from the monument (2<sup>nd</sup> group), c) cylindrical samples from the local quarries**

The series of abbreviations that are used in the following text instead of the full names of the tested lithotypes are presented in the following Table:

Abbreviation	Full Name	Origin
Ool. L.	Oolitic Limestone	monument
Shelly L.	Shelly Limestone	monument
Sandy C.	Sandy Calcarenite	monument
Red L.	Red Limestone	monument
OL	Oolitic Limestone	monument
OL_2	Oolitic Limestone	monument
SL	Shelly Limestone	monument
SL_2	Shelly Limestone	monument
SC	Sandy Calcarenite	monument
RL	Red Limestone	monument
T	Travertine	monument
Rh	Rhyolite	monument
FL	Foraminifera bearing Limestone	monument
M	Marble	monument
OL-Q1	Oolitic Limestone	quarry
OL-Q2	Oolitic Limestone	quarry
RL-Q	Red Limestone	quarry

**Table 4-2: Abbreviations for the tested lithotypes**

## 5. METHODS

---

The current research, following its main objectives, is divided in three main parts. The first one concerned the National Monument that was going to be studied. Therefore, it started with a thorough survey of the Ruin Garden of Székesfehérvár, focusing on the historical importance, the architecture of the monument and the different construction periods. A bibliographical survey on several libraries e.g. the libraries of the Eötvös Loránd University (ELTE) and the Budapest University of Technology and Economics (BME), the library of the Hungarian National Museum (HNM) and a series of manuscripts from the archives of the museum, several fieldtrips and discussions with the archaeologist in charge of the monument contributed to this first aim. The second step of this first part of the research was the identification of the different building stones and their distribution in the remaining parts of the monument. Therefore, the first group of samples was indentified. After a macroscopic investigation, the sampled materials were specifically treated according to their individual characteristics in order to proceed to the procedure of thin-section making. General petrographic characteristics were achieved by microscopic investigation, carried out with polarising microscope. The main lithotype categories of the identified samples, as it is shown by the thin section analysis, in relation to the construction phases were also documented. In order to have a preliminary idea of the void space of the materials, the open porosity by vacuum assisted water absorption was determined on the small irregular samples.

The second part of the research activities focused on the investigation of the main identified lithotypes of the historical materials based on the physical and mechanical properties. The methods that were used for the identification of the material properties were based on both destructive and non-destructive techniques, under laboratory conditions and in-situ. As a first step, the in-situ micro-destructive and non-destructive investigations took place starting with the application of micro-drilling resistance measurements on selected ashlar of different lithotypes. Afterwards, selected wall sections were mapped regarding their different construction periods, the various lithotypes and the identified decay forms. On the selected wall sections, additional tests were carried out in-situ related to the surface strength of the blocks (Schmidt hammer) and their relative moisture content (Gann Hydromette Uni). On the second group of samples, several physical and mechanical properties were measured such as

open porosity by vacuum assisted water absorption, ultrasonic velocity, dynamic modulus of elasticity and uniaxial compressive strength. A further selection among those eight samples was done leading to a total of four samples (OL, SL, CS & RL); one sample of each stone type as mentioned above except for the Marble and Rhyolite due to their low frequency in use comparing with the other identified building stones. On those samples, total open porosity, pore size distribution by mercury and nitrogen absorption and micro-drilling resistance were measured as well.

Finally, the third group of samples was submitted to a series of analysis, petrographic and petrophysical ones. The large number of samples tested under laboratory conditions and in-situ, led to a fuller knowledge of the materials' behaviour. Apart from the methods used for the investigation of the historical materials, the analysis on the freshly quarried stone was extended by including the use of Scanning Electron Microscope, X-Ray Diffraction. Concerning the physical behaviour of the materials, water absorption at atmospheric pressure, capillary water absorption, dynamic modulus of elasticity and the resistance to frost damage were additionally determined.

The laboratory analyses were carried out in the following Institutions:

- Department of Petrology and Geochemistry, Eötvös Loránd University, Budapest, Hungary (ELTE)
- Department of Construction Materials & Engineering Geology, Budapest University of Technology and Economics, Hungary (BME)
- Laboratory of Building Materials, Department of Civil Engineering, Aristotle University of Thessaloniki (AUTH)
- Institute for the Conservation and Promotion of Cultural Heritage, National Research Council (CNR), Florence, Italy (ICVBC)
- Department of Civil & Environmental Engineering, Princeton University, New Jersey, United States of America

Table 5-1 summarises all the important information about the analytical methods that were used and the analysed materials.

## **5.1. In-situ Investigations**

### **5.1.1. Mapping**

In order to help the study of the Ruin Garden in Székesfehérvár, a series of maps was created based on in-situ investigations. Five wall sections were selected for the sake of the different lithotypes distribution and the different construction periods were the ruins belong to. The total mapped area covers about thirty m<sup>2</sup> of the existing walls surfaces. Three different kinds of maps were designed for each wall section. The first series of maps depicts the different construction periods of the selected section of the walls. The second series of maps shows the distribution of the different lithotypes over the wall which helps both to better evaluate the use of different stone types over the different construction periods and to correlate the different stone types to the various identified weathering forms. The last series of maps represent the visible weathering forms on the building materials. For the last category of mapping, the first classification was developed by the working group “Natural stones and weathering” (Fitzner et al. 1995) with several publications that followed e.g. Fitzner et al. in 1997, 2000, 2002, Viles et al. 1997, databases on the internet (University of Aachen, Queen’s University et al.) and the lately publishes glossary by ICOMOS-ISCS in 2008.

The new maps have proven to be very useful also for the further identification of the site e.g. the documentation of the in-situ measured results and their ensuing interpretation in relation with the existing climatic conditions.

### **5.1.2. Schmidt Hammer**

The Schmidt hammer is a non-destructive test that can be easily applied in-situ. There are different types of Schmidt hammers with their main difference found in the way to display the acquired results: with sliding pointers (N-34, L-9) or digitally (Digi 2). For this current research, the test was implemented by Schmidt hammer Digi 2 (Fig. 5-1) and it was carried out on the blocks of the five selected wall sections of the monument (see Fig. 5-4). During the test, a spring-loaded mass impacts the material and the rebound value is displayed digitally on the monitor. Ten values are acquired for each tested block and the extreme and mean values, in addition with the standard deviation is recorded.

The Schmidt hammer was originally developed for measuring the strength of hardened concrete (Schmidt 1951). Nevertheless, several studies have correlated its results for a prediction of several stone properties (Török 2008). The correlation of the rebound values with the rock compressive strength is the most commonly studied e.g. Miller 1965, Barton & Choubey 1977, Sachpazis 1990, Kahraman 2001. The use of the rebound values in the calculation of other mechanical properties has been also studied (Katz et al. 2000). Moreover, their state of weathering has been also estimated by evaluating the hammer values (e.g. limestones: Török 2003, Christaras 1996, Török et al. 2004, Bell 1993).



**Fig. 5-1: Schmidt hammer Digi 2**

### **5.1.3. Moisture Content**

An estimation of the structural moisture of the tested blocks can be very informative for the impact of climatic conditions on them. As a consequence, a connection of the results with the materials weathering is possible. Furthermore, the obtained values, even in the case of numerical and not absolute ones, can be used in comparison with other measuring points and a profile of relative moisture content can be drawn (Török Á. 2009). A Gann Hydromette Uni was chosen for an in-situ and non-destructive estimation of the structural moisture (Fig. 5-2). Based on the electrical resistance measuring principle, the electronic instrument displays the values on digital LCD readout. When the measured relative values are more than hundred

units, the material is considered wet. Ten measurements have been carried out on each tested block and the average value was calculated. The blocks that were measured belong to the five selected wall sections of the monument (see Fig. 5-4).



**Fig. 5-2: Gann Hydromette Uni**

#### **5.1.4. Drilling Resistance**

The DRMS cordless (Drilling Resistance Measurement System), produced by SINT Technology (Italy) and developed and validated within the European EC Hardrock Project (Tiano 2001), is the portable device that was used for performing the drilling resistance measurements in the stones (Fig. 5-4). The system is comprised of the drilling device and a Tablet PC where the acquired data is transmitted through a USB serial data connection and it can be saved and presented in different ways thanks to the installed software developed with LabVIEW™. The system can measure the actual drill position, the penetration force, rotational speed and penetration speed.

During the measurements, the necessary force for penetrating a certain depth in time is measured continually by the system, while the penetration rate and rotational speed are maintained constant. The rotational speed and the penetration rate are established by the operator and they can range from 20 to 1000 rpm and 1 to 80 mm/min in correspondence. The

value of the applied force that can be measured by the system is between 0 to 100 N. During the test, the outputs of the measurements are given in x-y plots of the drilling force along the depth profile and the data is registered in numeric values as well.

For our measurements, the operating conditions were 600 rpm for the rotational speed, 10 mm/min for the penetration rate and 10 mm the total depth of penetration. The diameter of the diamond drill bits that were used in our case was 5 mm.

As a first step, the four more important lithotypes from the monument and the three different types of the freshly quarried stone were tested at ICVBC. that were used for all the laboratory measurements were drilled at ICVBC as well. Three to nine drilling resistance measurements were carried out on each one of them depending on the heterogeneity of the stone.

A total of twenty various building stones of the ruins was subjected to the measurement system in-situ focused on different kind of limestones, marble and rhyolite.

Objective of this work was to gather further information about the various lithotypes and their state of weathering by means of in-situ micro-drilling, avoiding in this way further invasive sampling.



**Fig. 5-3: Application of DRMS in-situ**



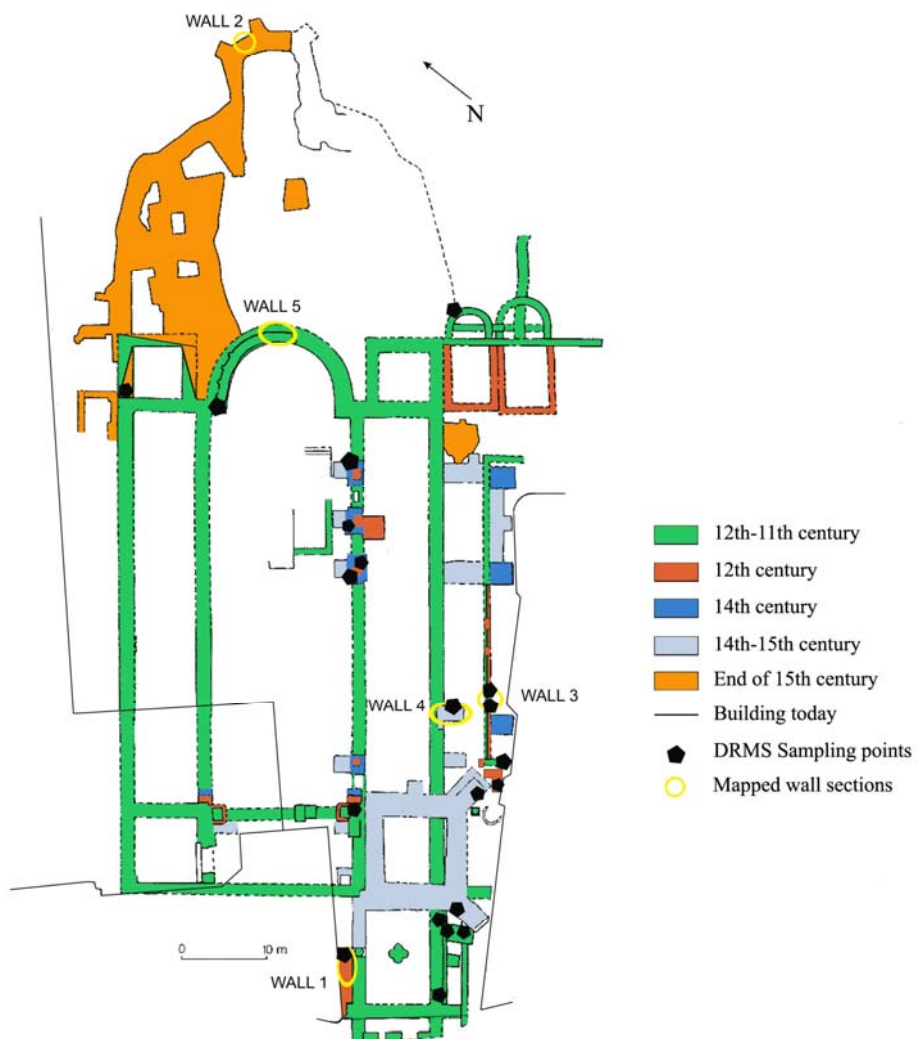


**Fig. 5-4: Excavated ruins and the DRMS application in-situ**

## **5.2. Analyses under Laboratory Conditions**

### **5.2.1. Petrographic Examination - Polarising Microscope**

The petrographic description of fifty seven sampled monumental stones and the three types of fresh stones from the quarries was done based on the EN 12407: 2000. The aim of this examination is the classification of the natural stone but also the observation of features that influence its chemical, physical and mechanical behaviour. The examination included macroscopic and microscopic investigation.

For the microscopic examination the polarised light microscopy was used. Polarising microscopy is used for revealing information about the texture, the minerals and the grains size of the observed materials. Thin sections were prepared at ELTE and BME. A portion of each material was mounted on a slide and mechanically reduced to a thin sheet of about  $(0.030 \pm 0.005)$  mm thickness. In case of less coherent samples e.g. oolitic limestone and in order to avoid disintegration while cutting, the samples were firstly impregnated in glue (bi-component epoxy adhesive Araldite: epoxyn resin with polyamine hardener Renshape Solutions REN HY 956) and cut without water.

The thin sections of the investigated building stones were observed at the Lithosphere & Fluid Research Laboratory at ELTE through a Nikon eclipse LV 100 POL. Microscopic photographic aspects of the thin sections were taken by a Nikon DS-Fi1 camera adjusted on the microscope and the software used for this reason was the NIS-Elements AR 2.20.

### **5.2.2. X-Ray Diffraction (XRD)**

The mineralogical composition of the three types of freshly quarried samples was further investigated by using the X-ray diffraction method on the crystal atoms of the minerals of each analysed sample. During the x-ray diffraction, an incident beam contacts the crystal atoms and therefore it scatters resulting in changes in radiation intensity. The diffraction pattern that is produced is used for the atomic structure of the crystals. The identity of the observed diffraction patterns is confirmed by the exact matching of the intensities of its peaks

with those that belong to reference materials. The fundamental of the basis was already discussed by A. W. Hull in 1919.

A small amount of the material to be tested was grounded in a porcelain mortar until it had powder consistency. The powder was considered to be fine enough passing through the 0.063 mm sieve. A Phillips diffractometer PW 3710 (Cu anode, 40 kV, 30mA and 5-70° T) was used for the implementation of the analyses at BME.

The advantages of X-ray diffraction are described by Suryanarayana et al. 1998:

- The powder diffraction method is determined by the exact atomic arrangement in a material.
- Its substance in a mixture produces its own characteristic diffraction pattern independently of the others.
- The X-ray diffraction pattern discloses the presence of a substance as that substance actually exists in the specimen.
- Only a small amount of the material is required for the analyses.
- The test is non-destructive on the prepared specimen.

### **5.2.3. Scanning Electron Microscope (SEM)**

The Scanning Electron Microscope (SEM) was used for assessing magnified images. During the preparation of samples, each sample was covered by a thin carbon film. The analysis was carried out at ELTE through an AMRAY 1830I SEM using the TESCAN SATELLITE TS1130 software and hardware for digital imaging. The acceleration potential was 20kV and the beam current about 0.8 nA. The specimens that were used belong to the four more important historical lithotypes.

### **5.2.4. Porosimetry**

The four more important lithotypes from the monument and the three from local quarries were selected for the porosimetric studies.

## Open Porosity

The goal of this measurement is to characterize the open porosity of the stone samples, determined by vacuum assisted water absorption. The method that was followed and it is described below is based on the EN 1936: 2006 for natural stone. Similar procedures have been also described by other associations such as the Rilem Recommendation CPC11.3 for the determination of water absorption by immersion under vacuum (Rilem CPC11.3 1984). The later Recommendation is for determining the absorption of hardened cement. Nevertheless, measurements based on this method have been successfully used during the identification of several other building materials. Under vacuum water can penetrate into pores with diameter larger than 100nm (Meyer et al. 1994).

The open porosity by vacuum assisted water immersion is defined by the difference between the mass of the given specimen of stone immersed in water under vacuum and the mass of the same specimen when dried, expressed in terms of the volume of the dry specimen.

The specimen was dried in a ventilated oven at  $(70 \pm 5)$  °C for 24 hours. The mass  $m_d$  of the dried specimen was measured. Right after the determination of the  $m_d$ , the specimen was immediately placed in a vacuum tank in which the air pressure was then lowered up to  $(2.0 \pm 0.7)$  kPa in order to eliminate the air contained in the open pores of the specimen. After a period of at least 2 hours, demineralised water was transferred from its initial tank into the tank in which the specimen was placed and the amount of water was sufficient to submerge the specimen, completely covering it with at least 20 mm water. The same pressure was maintained during the introduction of water. As soon as the specimen was fully submerged, the vacuum was maintained for at least 2 hours before the pressure was raised to the atmospheric value. The measurement of the wet mass  $m_s$  took place 24 hours after the vacuum was abolished. Before each weighing, the surface of the specimen was dried with a damp tissue so as to have water saturated surfaces. At that time, the specimen was also weighed while it was submerged in water, with a precision of at least 0.1%. This value is called  $m_h$ .

The absorption of water by immersion under vacuum is obtained from the expression:

$$P_o = \frac{m_s - m_d}{m_s - m_h} \times 100$$

in which:  $m_d$  is the dry mass expressed in grams;  $m_s$  is the mass of the specimen saturated with water and  $m_h$  is the apparent mass of specimen submerged in water, after water absorption in vacuum, expressed in grams.

Based on the results of the aforementioned test, the calculation of the specific gravity  $SG$  of the tested materials is possible and it is expressed by the following equation:

$$SG = \frac{m_d}{m_h - m_s}$$

The method was applied to all of the three groups of samples (see table 4-1) at AUTH.

### **Total Open Porosity**

The total open porosity was determined at ICVBC according to the method described by Barsotelli et al. 2001. Three specimens of about 2 x 2 x 2 cm were prepared for each type of the four more important lithotypes coming from the monument and for each lithotype coming from the quarries. After the preparation, the specimens were dried at 60 °C and the dry weight  $W_d$  was determined. Using the Quantachrome helium pycnometer, the real volume of the specimens  $V_r$  was measured and their bulk volume  $V_b$  was determined by a Chandler Engineering mercury pycnometer. The total open porosity  $P$  is given by the following equation as a percentage:

$$P = \frac{V_b - V_r}{V_b} \times 100$$

Furthermore, on the basis of the results from the helium and the mercury pycnometers, the real density  $\gamma_r$  and the bulk density  $\gamma_b$  of the specimens were calculated dividing the dry weight with the real volume and the bulk volume correspondingly:

$$\gamma_r = \frac{W_d}{V_r} \quad \text{and} \quad \gamma_b = \frac{W_d}{V_b}.$$

## **Pore Size Distribution**

Two methods were selected for the investigation of the pore-size distribution of pore sizes in the materials. In the first method the results were achieved by nitrogen adsorption and in the second one by mercury intrusion.

### ***Nitrogen Adsorption***

The adsorption of gas is a method for the determination of the physisorption isotherms of an inert gas in a solid. Nitrogen is commonly used for this method (Sing 2001). By the nitrogen adsorption method nitrogen intrudes the specimen under progressively increased pressure. The higher pressure is applied, the more nitrogen molecules are condensed on the surfaces of the specimen pore space. The surface of the material is determined by measuring the number of nitrogen molecules which intrude the material necessary to cover in one layer all the surface of the material. By BET (Brunauer–Emmett–Teller) method the registered data of the nitrogen isotherms can give information about the sizes of the material's pores. In our case, the results are presented as the cumulative pore volume in which nitrogen was adsorbed versus the pore size in the range of pore diameter from 0.001 to 0.2  $\mu\text{m}$ .

The method was implemented at AUTH through a Quantacrome Nova 2000 apparatus on the four most important lithotypes found in the studied monument and the three freshly quarried ones. Each sample that was used for the analysis had a mass in the range of 1 - 2 grams in dry condition.

### ***Mercury Intrusion Porosimetry (MIP)***

The principle of Mercury Intrusion Porosimetry is that a non wetting liquid, one with a contact angle greater than 90°, will only intrude capillaries under pressure (Abell et al. 1999).

The samples are introduced into a chamber, the chamber is evacuated and mercury surrounds the samples. A progressively increased pressure is applied to mercury which penetrates firstly the bigger pores of the stone sample and successively the smaller ones. After achieving the highest rate of intrusion, mercury has been shown to penetrate the interior of the sample (Winslow & Diamond 1970, Beaudoin et al. 1979).

The relationship between the pore size and the applied pressure, with the assumption that the pore is cylindrical is expressed by the Washburn equation (Washburn 1921):

$$P = \frac{-4\gamma \cos \theta}{d}$$

where  $P$  the absolute applied pressure,  $\gamma$  the surface tension of the liquid which in our case is mercury,  $\theta$  the contact angle of the liquid (mercury) and  $d$  the diameter of the capillary.

The intruded volume at each pressure increment determines the pore size distribution and the total intruded volume gives the total open porosity. The registered data is presented as the cumulative open porosity versus the mean diameter.

A ThermoQuest mercury Porosimeter was used at ICVBC, utilising the Pascal 140 and 240 unities. Three cubic specimens of about 2 x 2 x 2 cm of each lithotype coming from the monument were tested in order to compute the mean values and three specimens for each lithotype coming from the quarries. Furthermore, the total mercury porosity  $PHg$  was computed as the total porosity determined by the mercury porosimeter in the dimensional radius' ranges from 0.0037 to 150  $\mu\text{m}$  (diameter: 0.0074-300  $\mu\text{m}$ ), the so-called mesoporosity (Barsottelli et al. 2001, Barosttelli et al. 1998).

### 5.2.5. Water Absorption

Megjegyzés [U1]:

#### Water Absorption by Capillarity

The capillary suction was measured at BME based on the EN 1925: 1999. Dry samples were submerged in  $(3 \pm 1)$  mm of water and the capillary-rise absorption was measured in function of the time.

Three cylinders of each of the three types coming from the quarries were cut with a diameter and height of about 50 mm. The samples were firstly dried to constant weight at the temperature of  $(70 \pm 5)$  °C. The samples were placed in a tank on a net support and they were submerged in water until the depth of  $(3 \pm 1)$  mm. The level of the water was maintained at that level during the measurement, adding water when it was necessary and closing the tank to avoid evaporation in case of slow capillary absorption. The capillary-rise absorption was marked in each certain interval of time which was initially very short and later longer. The capillary-rise absorption in mm was plotted versus the lapsed time.

#### Water Absorption at Atmospheric Pressure

The scope of this method is to determine the water absorption of the natural stone samples by immersion in water at atmospheric pressure. The procedure of the measurement is based on the EN 13755: 2001.

Three specimens of each of the three types of stones coming from the quarries were submitted to this test at BME. The specimens were cylindrical of about 50 mm diameter and about 50 mm height. They were dried to constant mass at the temperature of  $(70 \pm 5)$  °C. Their dry mass  $m_d$  was measured. The samples were placed in a tank on special supports and then tap water was added until the specimens were completely immersed to a depth of  $(25 \pm 5)$  mm of water. In each certain interval of time which was initially very short and later longer, the specimens were taken out of the water, quickly wiped with a damp cloth and then weighted within 1 min to an accuracy of 0.01 g ( $m_i$ ). After the measurement, the specimens are immediately immersed again in water to continue the test up to constant mass of specimens.



The result of water absorption at each interval was expressed as a percentage to the nearest 0.1 % by the following equation:

$$A_i = \frac{m_i - m_d}{m_d} * 100$$

The test was stopped after sixteen days. The mass of the last weighing is the saturated one  $m_s$  and based on this, the total water absorption at atmospheric pressure  $A_b$  after sixteen days of immersion was calculated by the aforementioned equation replacing  $A_i$  with  $A_b$  and  $m_i$  with  $m_s$ .

#### **5.2.6. Determination of Sound Speed Propagation**

The measurement aimed the calculation of the velocity of propagation of sounds of ultrasonic longitudinal waves in natural stone according to the European standards (EN 14579: 2004). All tested stone samples were measured by placing the two transducers on opposite face and directly opposite to each other in order to have a direct transmission and the maximum energy propagated.

Measurements were carried out on the second and third group of samples (see Table 4-1). The former one was tested at AUTH through a Matest C369 ultrasonic pulse velocity tester, while the later ones at BME through a Pundit one. The historical samples were submitted to the measurement only air-dried. Regarding the freshly quarried materials, the measurement was carried out on air-dried samples in addition with water saturated ones before, after and during the artificial frost weathering that was implemented under laboratory conditions.

The fluctuation of the velocities is of a certain importance in the final correlation of the results in order to estimate the identity or the physical characteristics of the stones such as strength, porosity and behaviour through the weathering process.

### 5.2.7. Determination of Uniaxial Compressive Strength

Uniaxial Compressive Strength tests were performed according to EN 1926: 2006 on samples from the second and third group (see Table 4-1).

The load was applied on the specimen at a constant stress rate of  $(1 \pm 0.5)$  MPa/s. The maximum load on the specimen was recorded to the nearest 10kN and the ratio of the failure load of the specimen and its cross-sectional area before testing determined the uniaxial compressive strength.

The historical specimens (second group-see Table 4-1) were tested through a Mohr & Fedehaff AG Nr 5359 machine besides the red compact limestone which was tested through a Matest C056 machine at AUTH. The specimens from the three freshly quarried samples (third group-see Table 4-1) were tested at BME, through a DRMB 200 machine with recording of lateral and axial displacement. The last measurement was applied not only on air-dried samples, as the European Standard indicates, but also on water saturated freshly quarried samples before any artificial weathering and after eight and twenty-four cycles of the freeze-thaw test.

### 5.2.8. Dynamic Modulus of Elasticity

Based on all the results obtained by the determination of the sound speed propagation, elastic properties can be determined non-destructively and with a relatively low cost comparing with the elastic properties measured by mechanical load (Weiss 2006). The dynamic modulus of elasticity can be calculated as it has been described in ASTM C597:

$$E_d = V^2 \frac{[\rho(1 + \nu)(1 - 2\nu)]}{(1 - \nu)}$$

where  $E_d$  the dynamic modulus of elasticity,  $V$  the ultrasound pulse velocity,  $\nu$  the dynamic Poisson's ratio and  $\rho$  the density of the tested material.

In general, the principle of this test, as it has been mentioned by Qasrawi H. Y. in 2000, the velocity of sound in a solid material,  $V$ , is a function of the square root of the ratio of its modulus of elasticity,  $E$ , to its density,  $\rho$ :

$$V = f \sqrt{\left( \frac{gE}{\rho} \right)}$$

where  $g$  is the gravity acceleration.

#### **5.2.9. Determination of Resistance to Frost Damage**

The method that was used in order to assess the freeze-thaw cycle's effect on natural stone was based on the EN 12371: 2001.

Twelve specimens of each one of the three types of freshly quarried stones (third group-see Table 4-1) were submitted to the test. Exact values about their dimensions, mass  $M_d$  and ultrasound pulse velocity were measured in dry conditions. Afterwards, the specimens were completely immersed in water according to the standards. The apparent mass in water  $M_h$  and the mass in air  $M_s$  (the specimen is surface dried after removal from the water) in addition with the ultrasound pulse velocity were measured for each specimen also after immersion. Each cycle consisted of six hour freezing period in air at -12 °C, followed by a six hour thawing period during which the specimens were immersed in water. The aforementioned measurements were repeated after each freezing-thawing cycle and the total number of cycles was twenty four for the specimens that did not fail before the end of the test. After the completion of eight cycles, six specimens of OL-Q2 and RL-Q and only three of the OL-Q1 (due to the early failure of this lithotype) were put aside in order to be tested under uniaxial compressive load. The behaviour of the specimens during the test was evaluated by the observed changes in the measured values and also by visual inspection.

#### **5.2.10. Dynamic Mechanical Analyser**

The Dynamical Mechanical Analysis measures the mechanical properties of materials in function of time and temperature. In our case, the cooling experiment was carried out in order to analyze stress generated during thermal cycles without any load application. Three small prismatic specimens of about 12 x 6 x 6 mm belonging to the freshly quarried red limestone were subjected to the test. The specimens had been immersed in water over five days before the beginning of the measurement. The changes in length and temperature were measured during the test. The measurement was carried out at the Princeton University through a Perkin – Elmer DMA7 analyser.

Test Method	Relevant Suggested Methods	Number of analysed samples	Location of analyses
Mapping	-	5 wall sections	in-situ
Schmidt Hammer	-	142	in-situ
Moisture Content	-	142	in-situ
Drilling Resistance Measurement System	-	20 (in-situ) & 7 (lab)	in-situ & ICVBC
Petrographic Determination	EN 12407: 2000	60	ELTE & BME
Scanning Electron Microscope	-	7	ELTE
X-Ray Diffraction	-	3	BME
Open Porosity	EN 1936: 2006	59	AUTH
Total Open Porosity	-	15	ICVBC
Nitrogen Adsorption	-	7	AUTH
Mercury Intrusion Porosimetry	-	15	ICVBC
Water Absorption by Capillarity	EN 1925: 1999	7	BME
Water Absorption at Atmospheric Pressure	EN 13755: 2001	9	BME
Ultrasonic Pulse Velocity	EN 14579:2005	181	BME & AUTH
Uniaxial Compressive Strength	EN 1926:2006	88	BME & AUTH
Dynamic Modulus of Elasticity	ASTM C597	181	BME & AUTH
Frost Resistance	EN 12371:2002	36	BME
Dynamic Mechanical Analyser	-	3	Princeton University

**Table 5-1: Methods of analysis and tests, relevant standards, total number of analysed samples and location of the analyses where ELTE the Eötvös Loránd University, BME the Budapest University of Technology and Economics, AUTH the Aristotle University of Thessaloniki and ICVBC the Institute for the Conservation and Promotion of Cultural Heritage.**

### 6.1. In-situ Investigations

#### 6.1.1. Mapping

The several construction periods where certain blocks of building stones belong to are demonstrated in the figs 1-5. This depiction on the five selected wall sections together with maps showing the distribution of the different lithotypes (Figs. 6-1, 4, 7, 10 & 13) highlights the complexity of the monument.

As it is well represented by the selected wall sections, several types of limestones such as Oolitic, Travertine and Bioclastic ones are the most widely used lithotypes in the different construction periods of the monument (Figs. 6-2, 11 & 14). Rhyolite is also widely used in some construction periods (Figs. 6-5 & 8). The use of granite in the last construction period is also remarkable (Fig. 6-5). Details about the distribution of the several identified lithotypes in the remained walls can be seen in Figs. 6-2, 5, 8, 11 & 14.

Several weathering forms were observed on the various lithotypes as it is represented on the Figs. 6-3, 6, 9, 12 & 15.

On the Oolitic Limestone have occurred the most severe weathering processes in comparison with the other lithotypes of the monument. Individual fissures visible by naked eye were observed (e.g. Figs. 6-3 & 6). Detachment of grains also occurred such as crumbling and granular disintegration (e.g. Figs. 6-3, 12 & 15). Further detachment of thin layers of in general a millimetric scale (multiple scaling) can be seen for instance on the blocks of Oolitic Limestone of wall 4 (Fig. 6-12). Exogenic deposits in combination with materials derived from the stone created black and white crust in different blocks of the aforementioned lithotype (e.g. Figs. 6-3 & 12). Detachment of the black crust was observed in the case of fine-grained Oolitic Limestone (e.g. Fig. 6-3).

In the case of Bioclastic Limestone minor cracks were noted with a dimension smaller than 0.1 mm, the so called hair cracks, crumbling and erosion that leads to smoother shapes due to loss of material such as rounding and roughening of the surfaces (e.g. Fig. 6-9). In the case of blocks of Bioclastic Limestone totally exposed to the exterior environment (e.g. Fig. 6-6), black crust and biological colonization (moss, lichens and plants) is also observed.

The same forms of biological colonization are observed on the blocks of Travertine which are exposed to the outdoor environmental conditions in addition with cracks (e.g. Fig 6-15). Network of small interconnected depressions of millimetric to centimetric scale (microkarst) were also observed on the exposed Travertine. The latter decay form is a result of surface dissolution due to exposure to water run-off.

The Red Limestone appears to be the most durable one among the different types of limestones. Only minor alterations were observed on these blocks such as decolourization of the surface (e.g. Fig. 6-9) and a few cracks.

In some cases of granitic blocks exposed to the environmental conditions (e.g. Fig 6-6), major cracks and multiple flaking (scaling in thin scales of millimetric thickness) have occurred.

Rhyolite seems to be relatively resistant to weathering processes besides a few hair cracks observed in relatively small blocks (e.g. Fig. 6-9).

Additionally, salt efflorescence (e.g. Fig. 6-3) and biological colonization are phenomena observed on the historical mortar of the ruins. Especially the latter one is intense in the areas that are close to the ground (e.g. Figs. 6-3, 9 & 12). In few cases, the presence of algae is expanded to the adjacent blocks of Rhyolite (e.g. Fig. 6-6) and Travertine (e.g. Fig. 6-12).

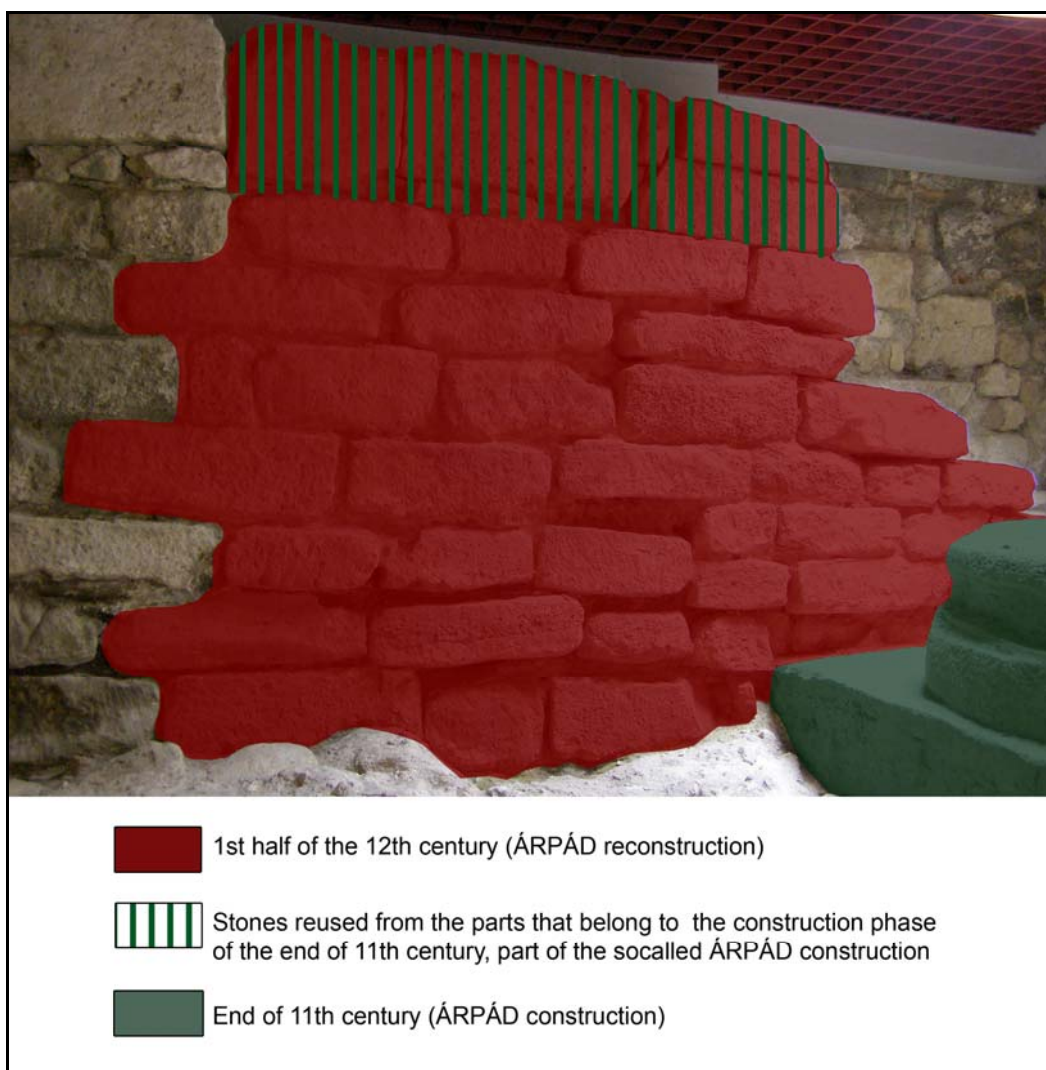


**Fig. 6-1: Wall 1 – Map of construction periods**



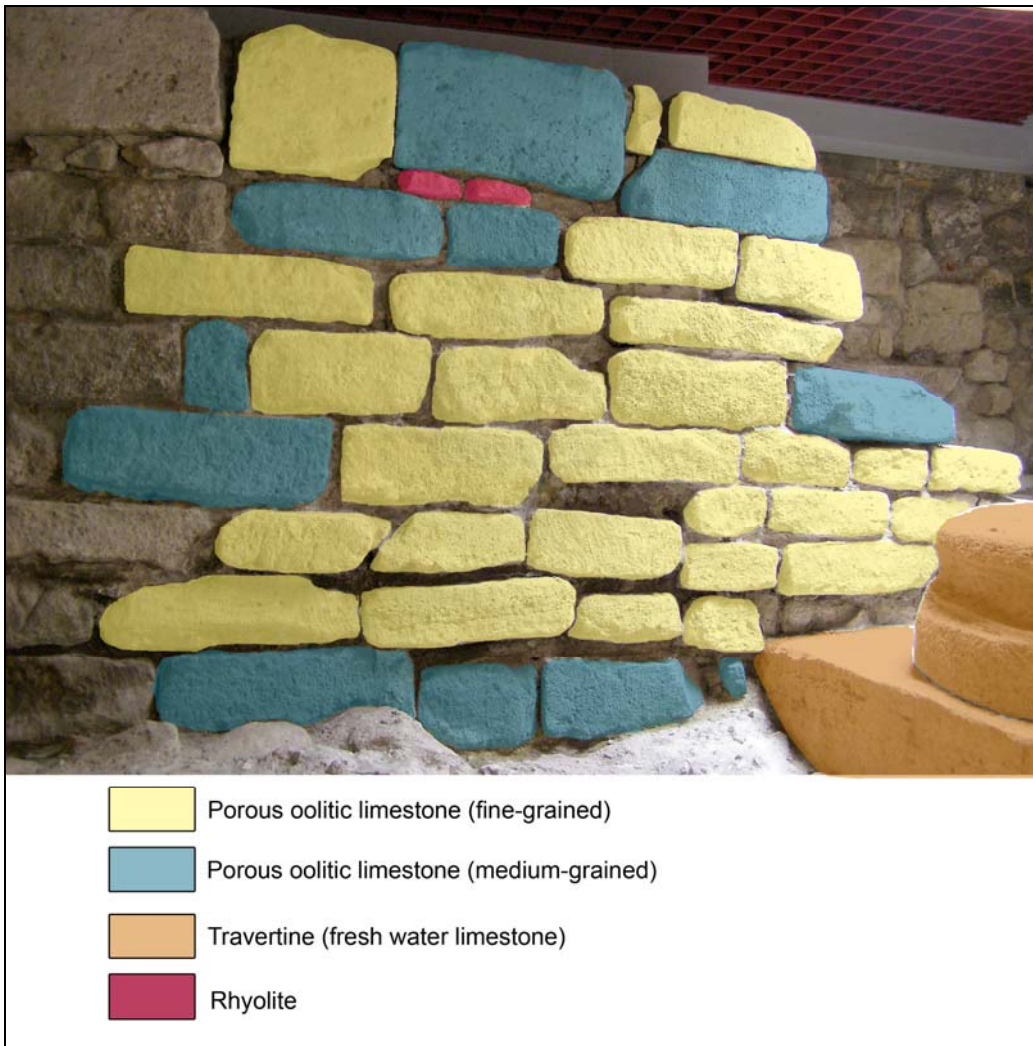


**Fig. 6-2: Wall 1 – Map of lithotypes**

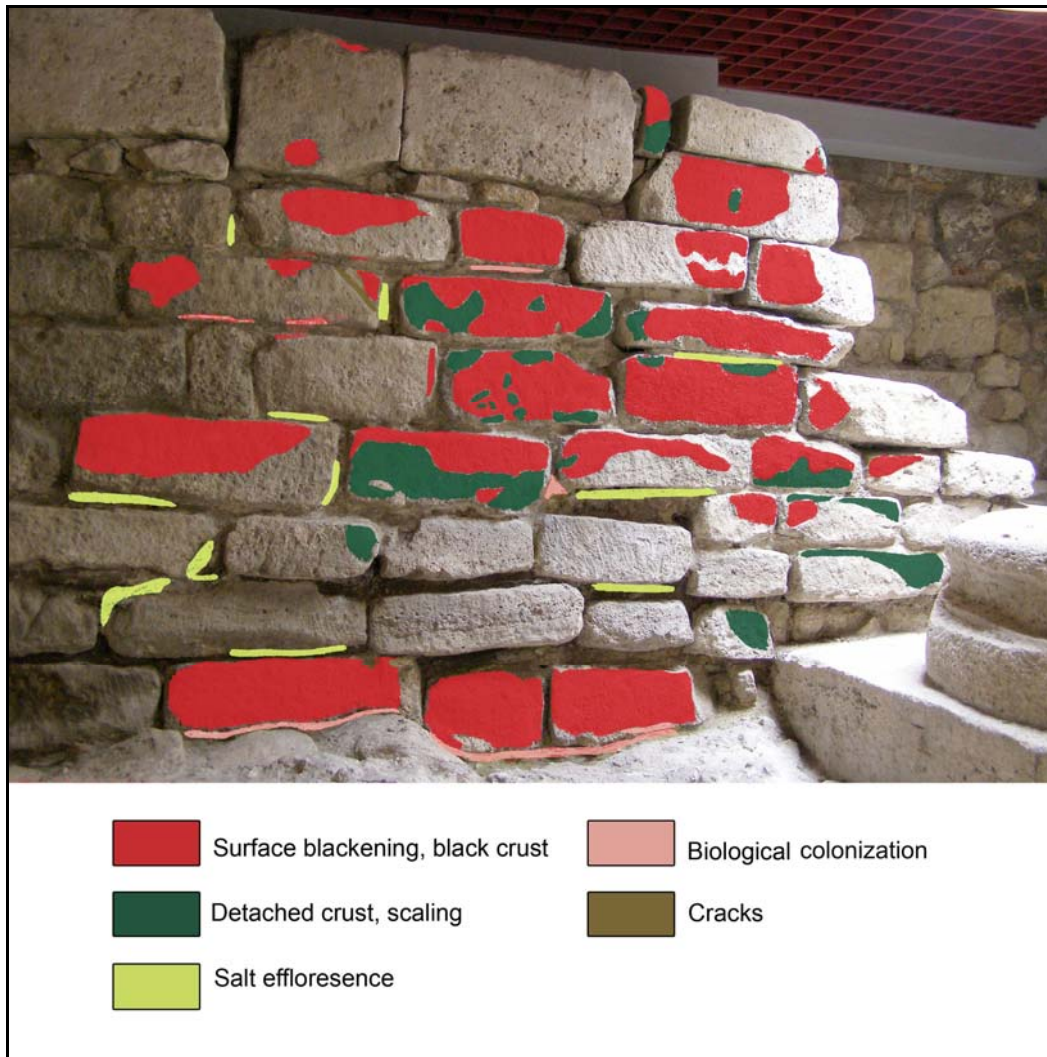


**Fig. 6-3: Wall 1 – Map of weathering forms**



**Fig. 6-4: Wall 2 – Map of construction periods**





**Fig. 6-5: Wall 2 – Map of lithotypes**

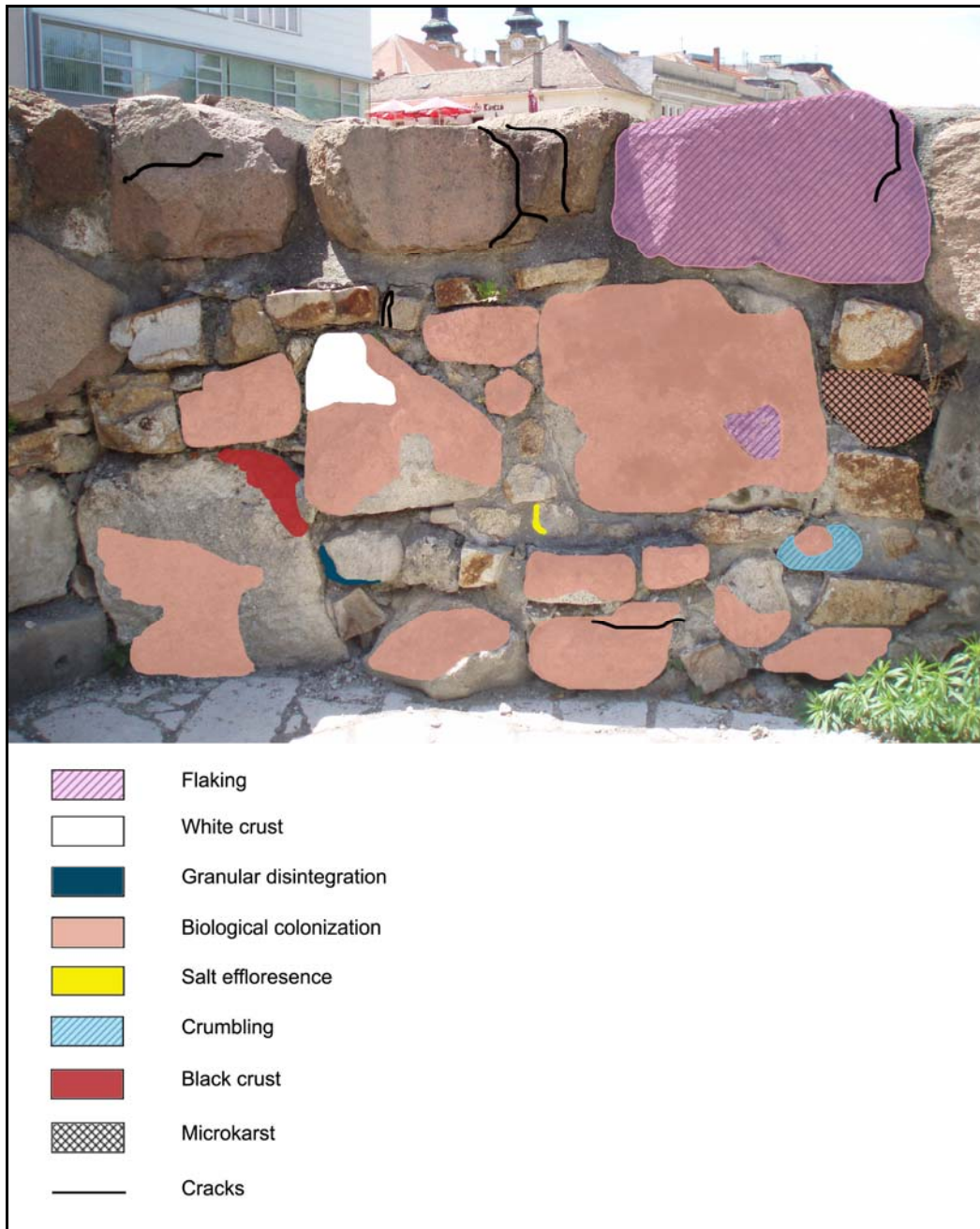
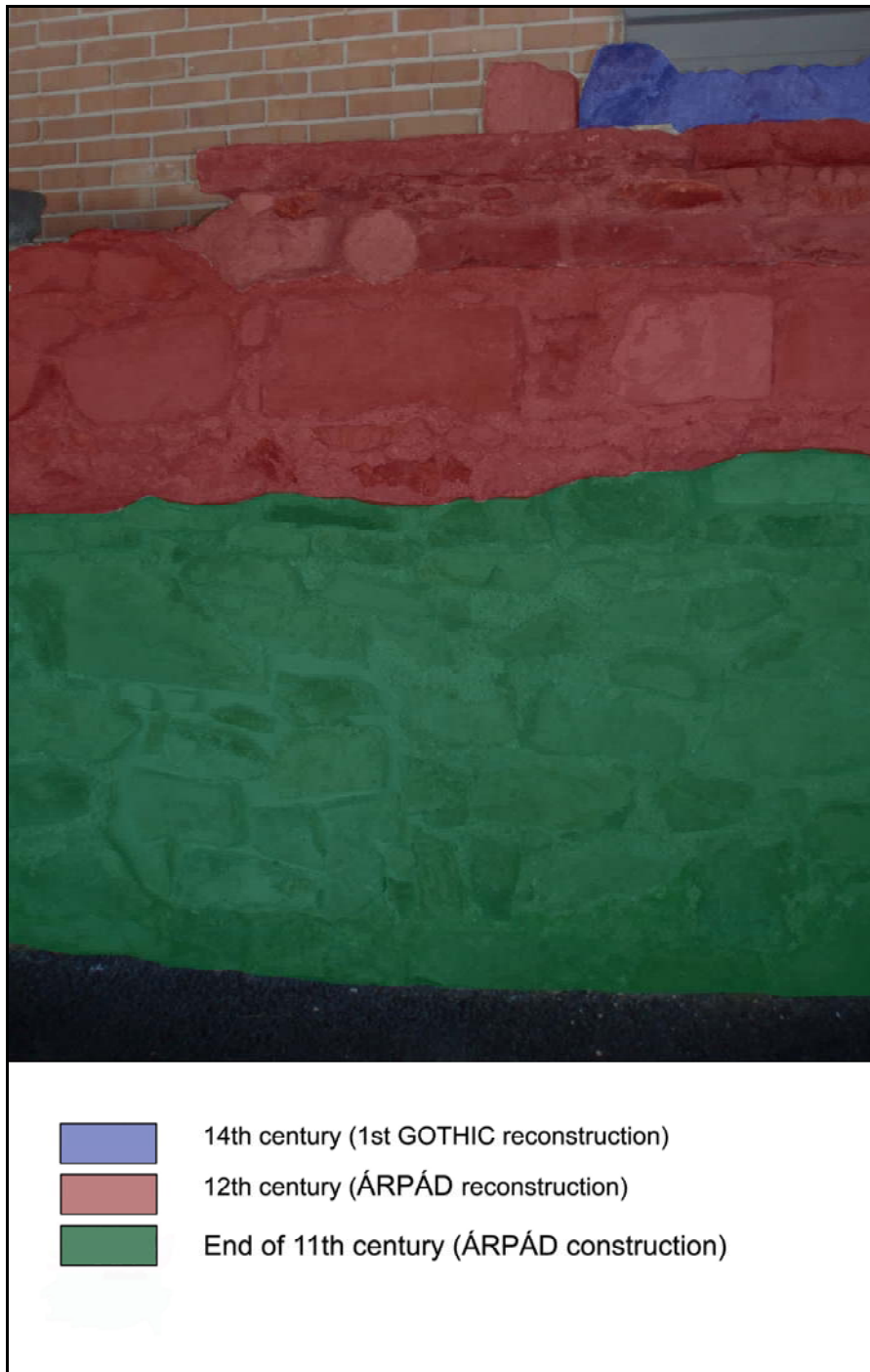
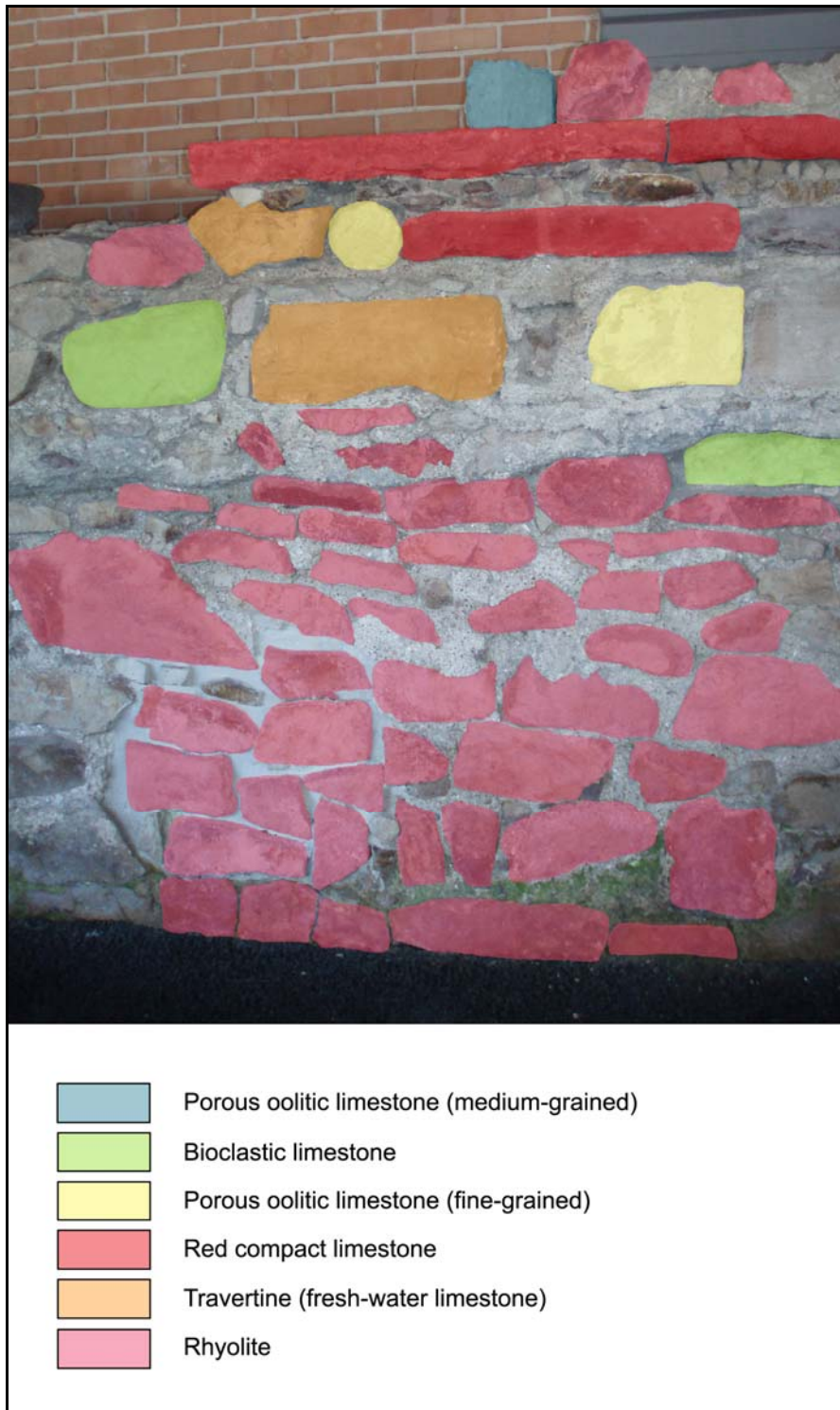


Fig. 6-6: Wall 2 – Map of weathering forms



**Fig. 6-7: Wall 3 – Map of construction periods**





**Fig. 6-8: Wall 3 – Map of lithotypes**

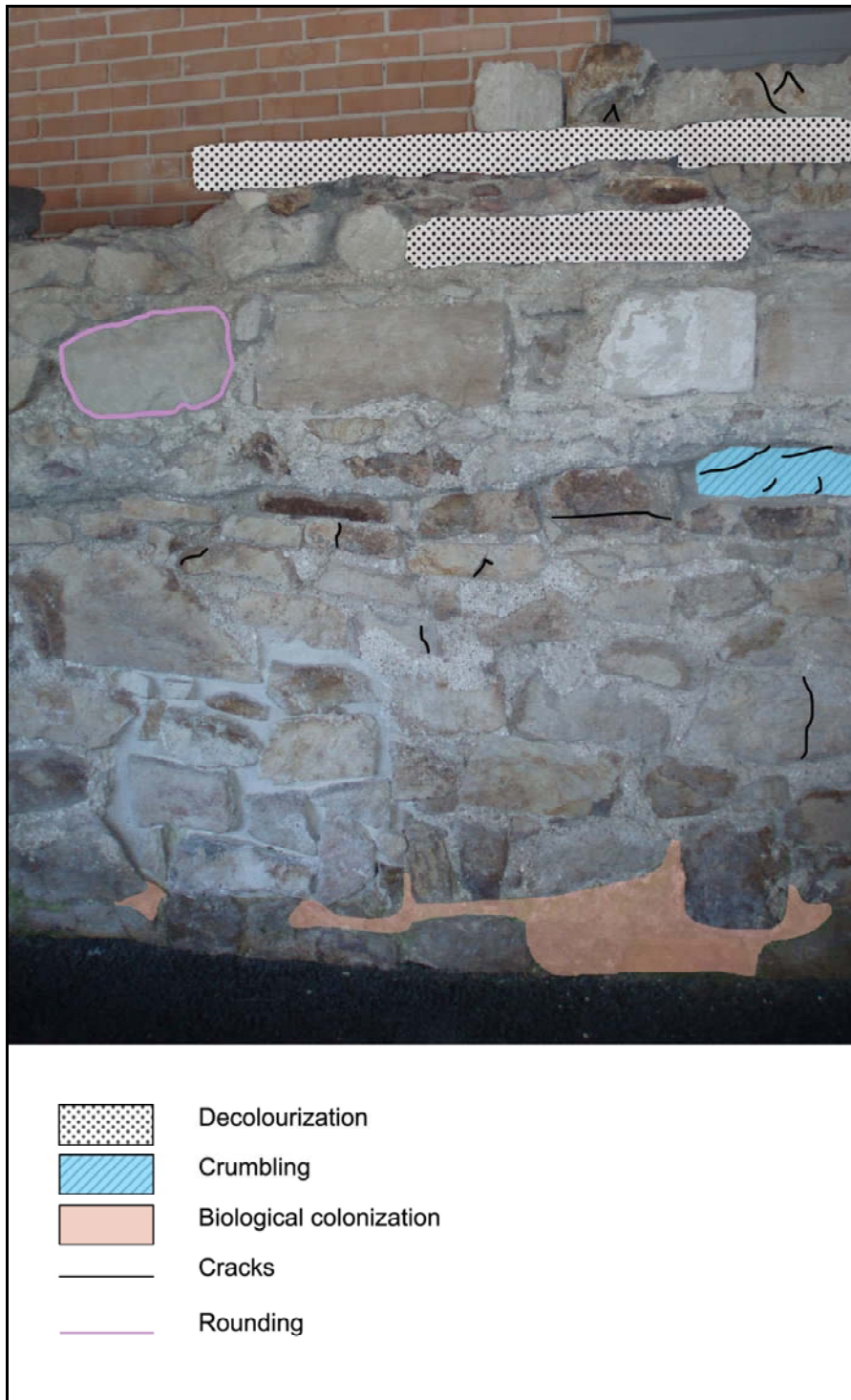


**Fig. 6-9: Wall 3 – Map of weathering forms**





**Fig. 6-10: Wall 4 – Map of construction periods**

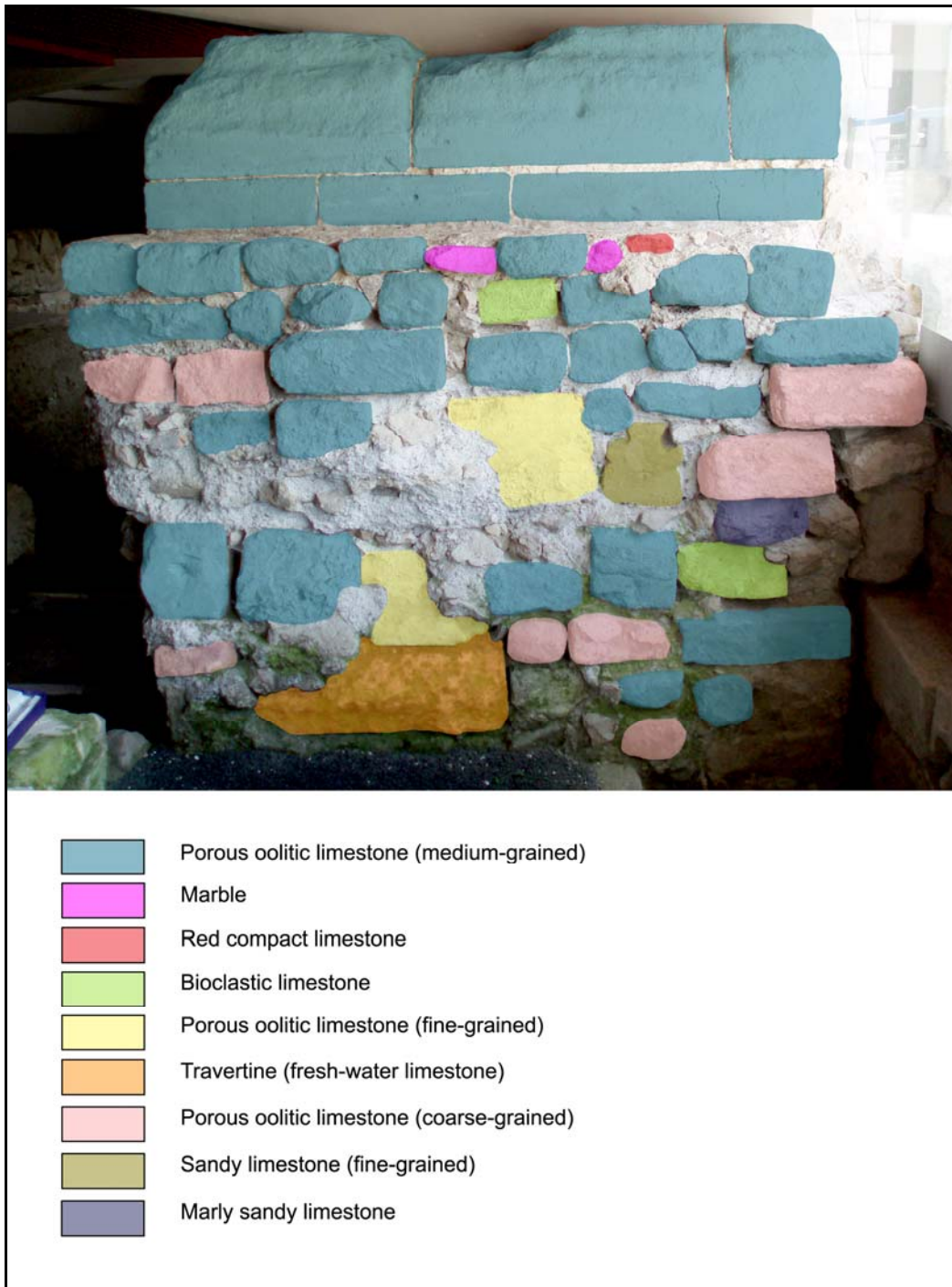


**Fig. 6-11: Wall 4 – Map of lithotypes**

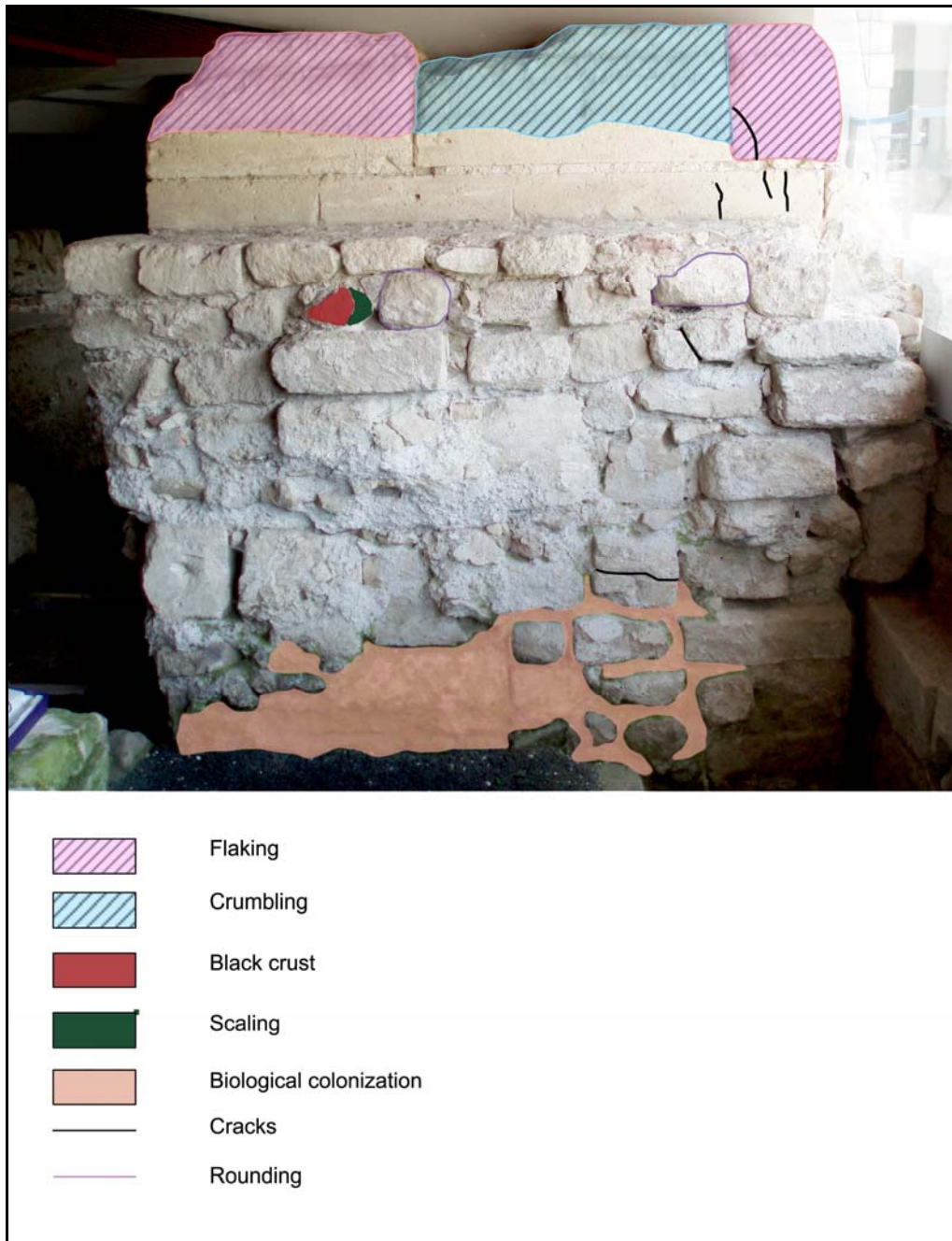
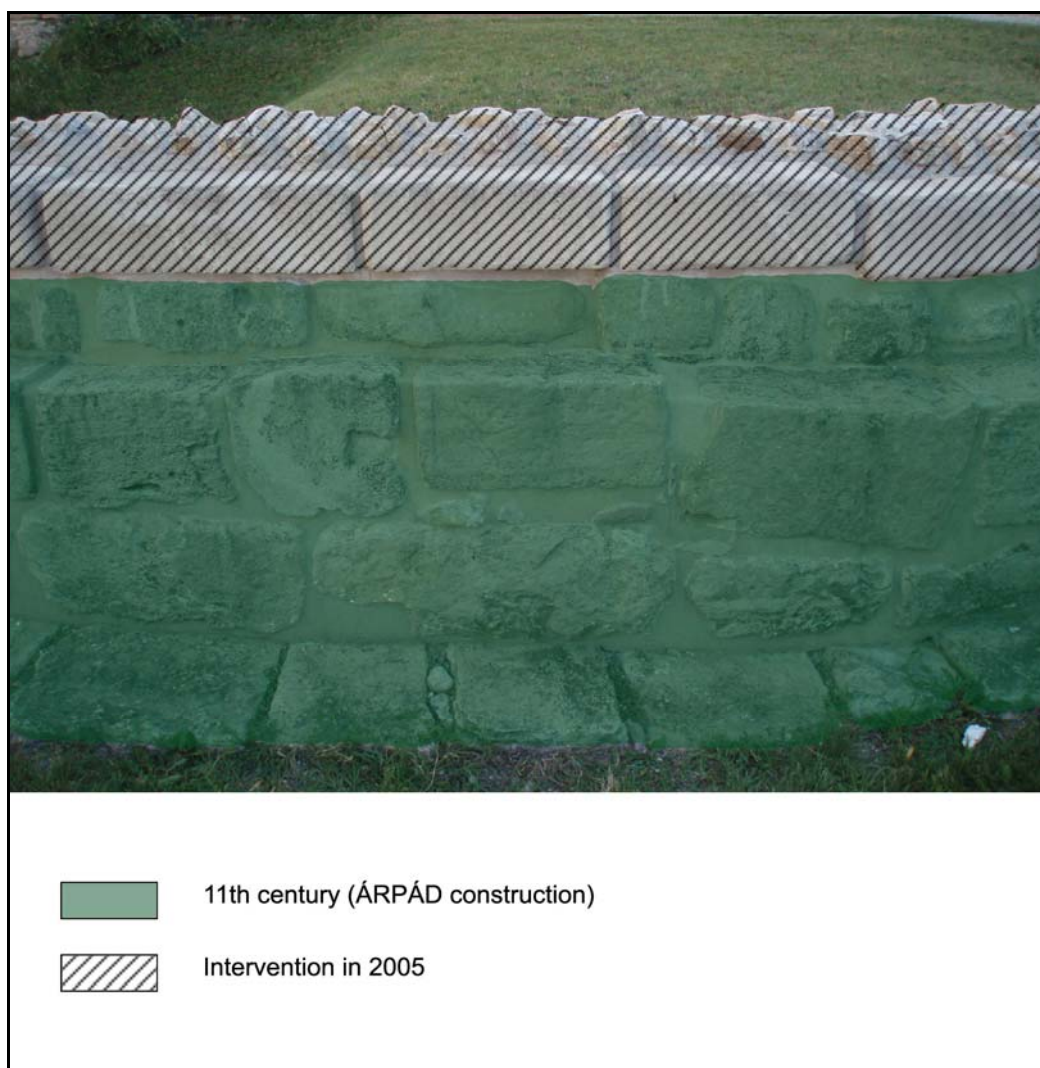
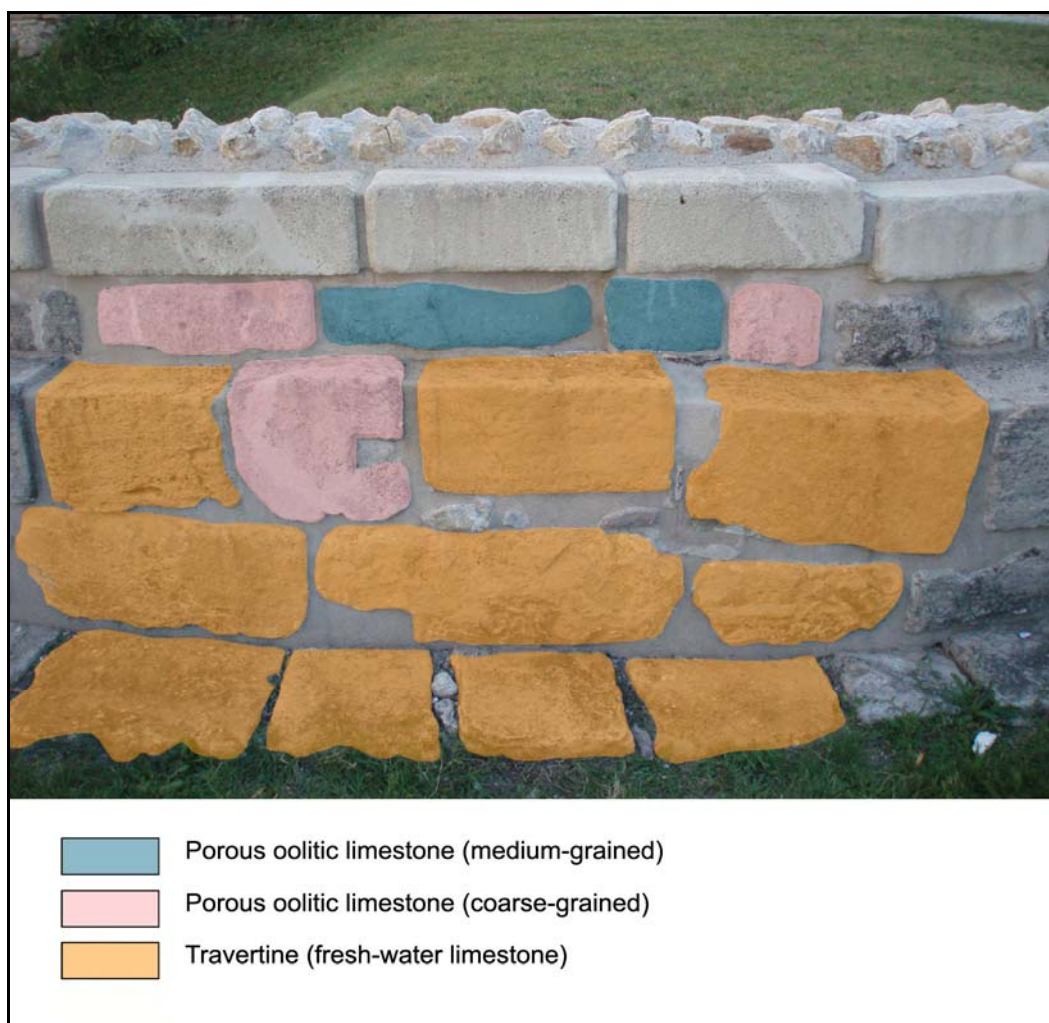


Fig. 6-12: Wall 4 – Map of weathering forms





**Fig. 6-13: Wall 5 – Map of construction periods**



**Fig. 6-14: Wall 5 – Map of lithotypes**

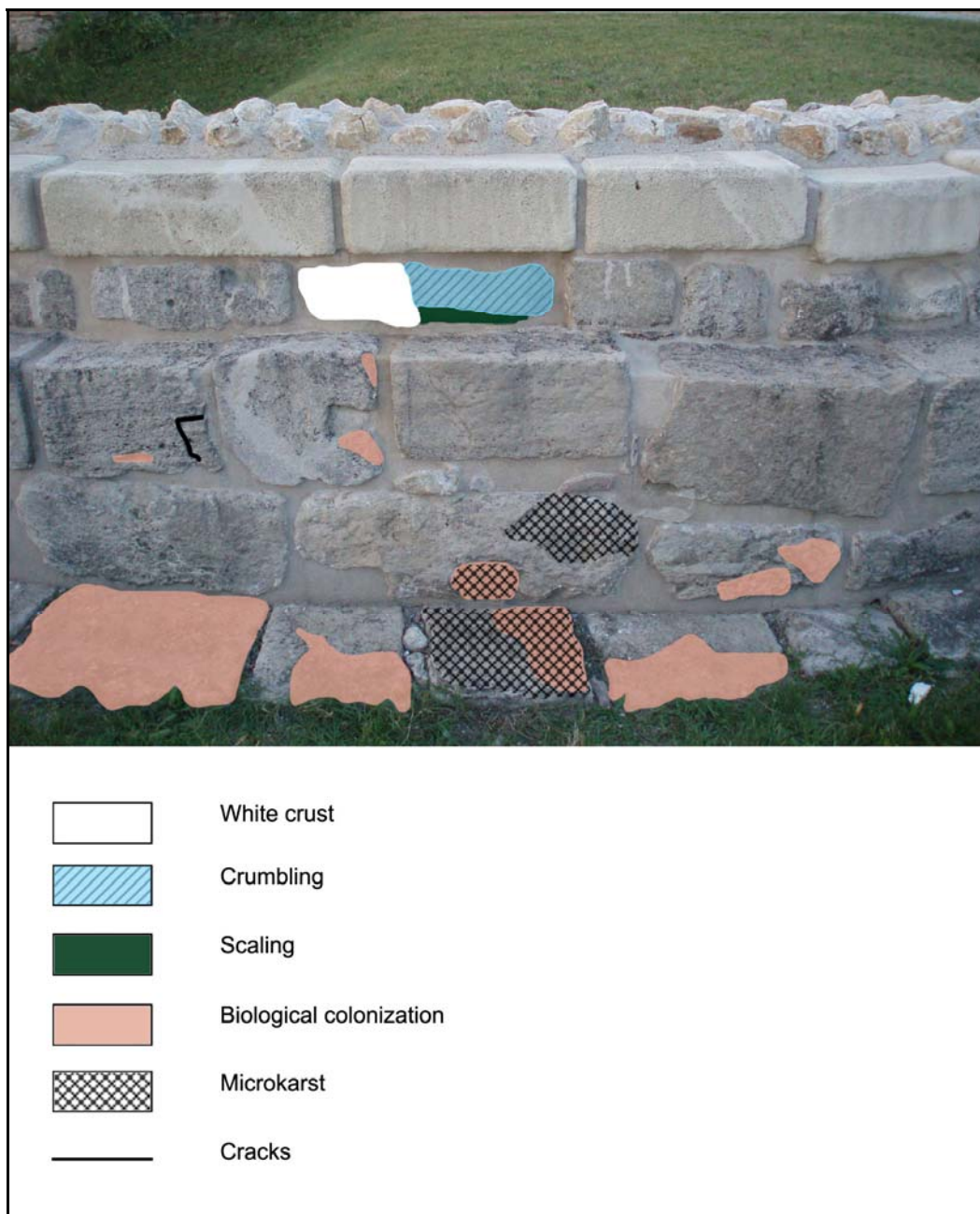


Fig. 6-15: Wall 5 – Map of weathering forms

### **6.1.2. Schmidt Hammer and Moisture Content**

The Schmidt hammer values and the moisture content measure on the blocks of the selected walls are presented in the Figs. 6-16, 17, 18, 19 & 20. The Schmidt hammer values are higher for the more compact stones such Rhyolite and Granite with the Red Limestone performing also relatively high rebound values. Most type of Limestones performed relatively low values with the Oolitic one generally showing lower values than the Travertine.

The moisture content values are also presented on the Figs. 6-16, 17, 18, 19 & 20. The fluctuation of the values for the same lithotype is related to the influence of the different environmental conditions on the stone materials; blocks of the same lithotype showed higher moisture values in case of being located in shadow areas, especially in the covered parts of the monument. For instance in the case of wall 1 (Fig. 6-16), the blocks which are on the right part of the wall, where the sunlight passes through a transparent glass located on the right top of the ceiling, gave lower moisture values than the blocks that are constantly in the shadow part of the wall . Moreover, in all cases blocks of the same lithotype located close to the ground, had higher moisture content than the ones located further from it.



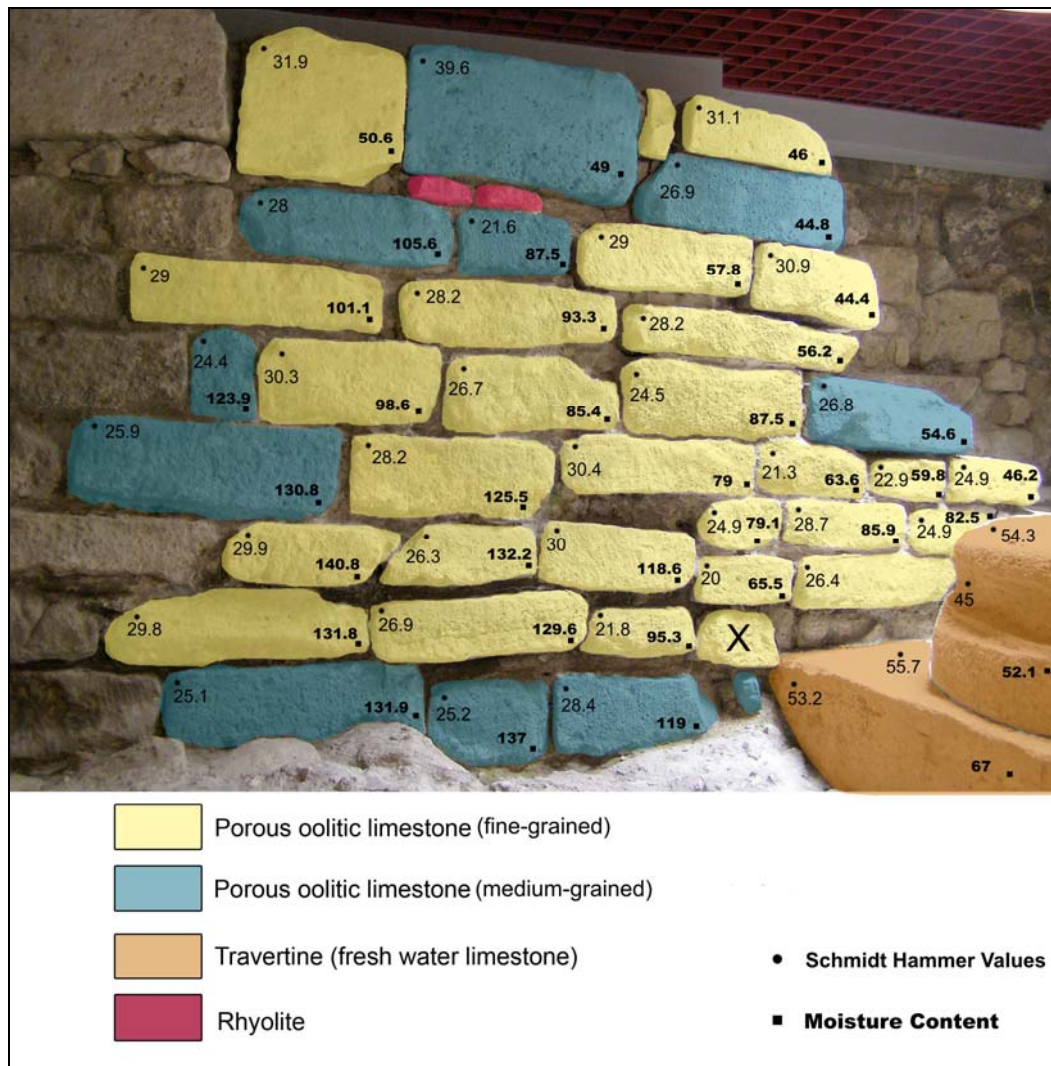


Fig. 6-16: Wall 1 – Schmidt Hammer & Moisture content Values



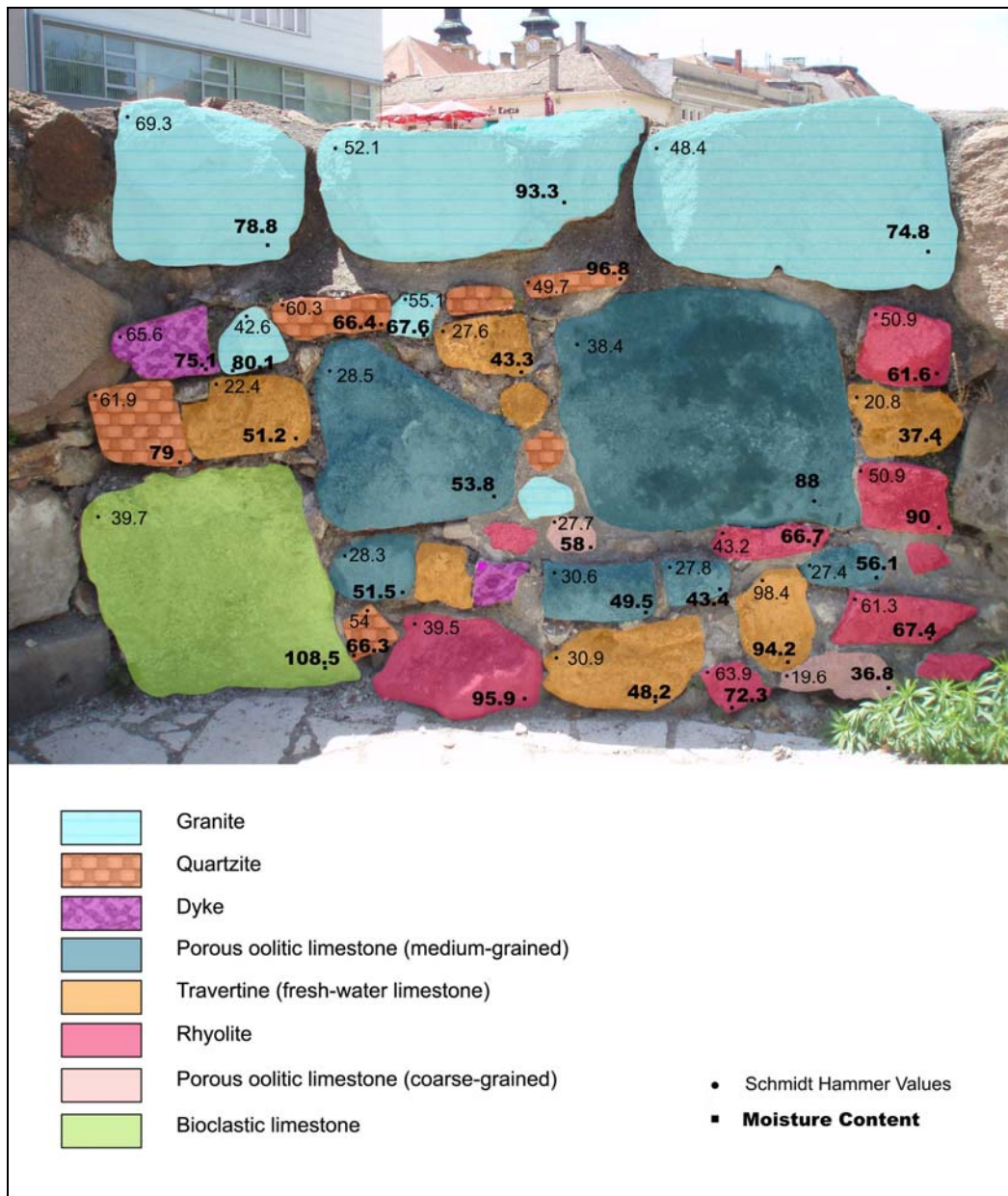


Fig. 6-17: Wall 2 – Schmidt Hammer & Moisture content Values

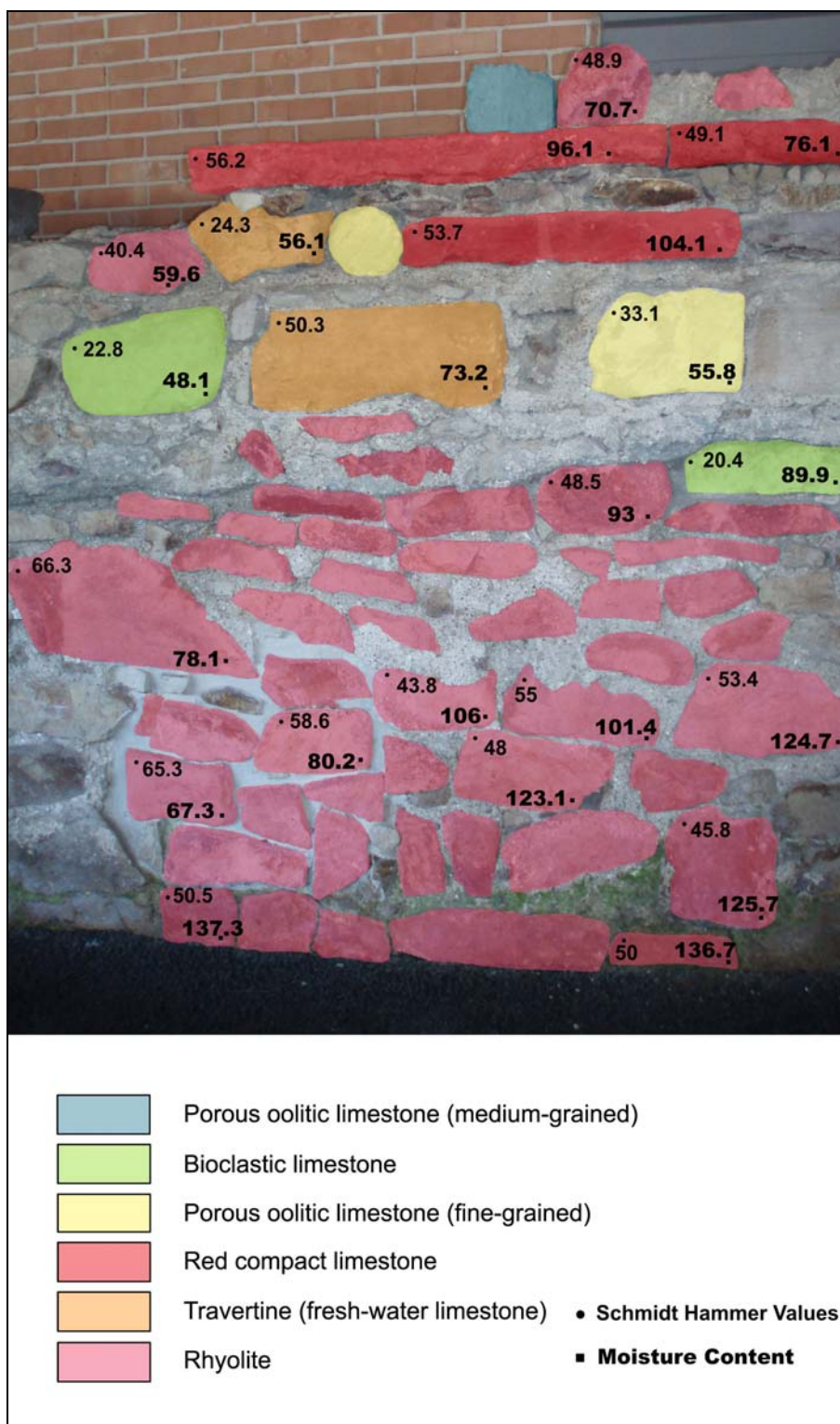


Fig. 6-18: Wall 3 – Schmidt Hammer & Moisture content Values

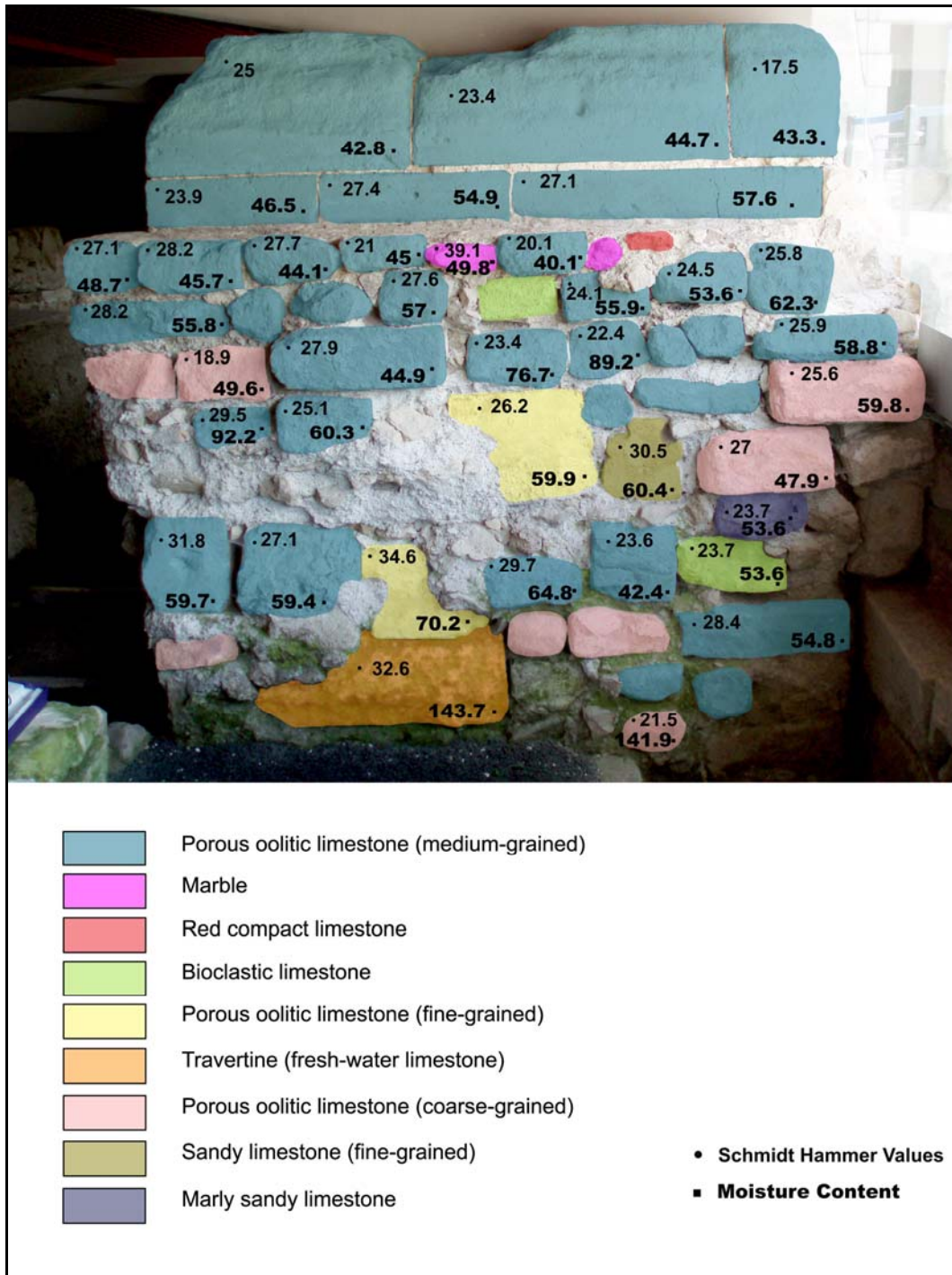


Fig. 6-19: Wall 4 – Schmidt Hammer & Moisture content Values



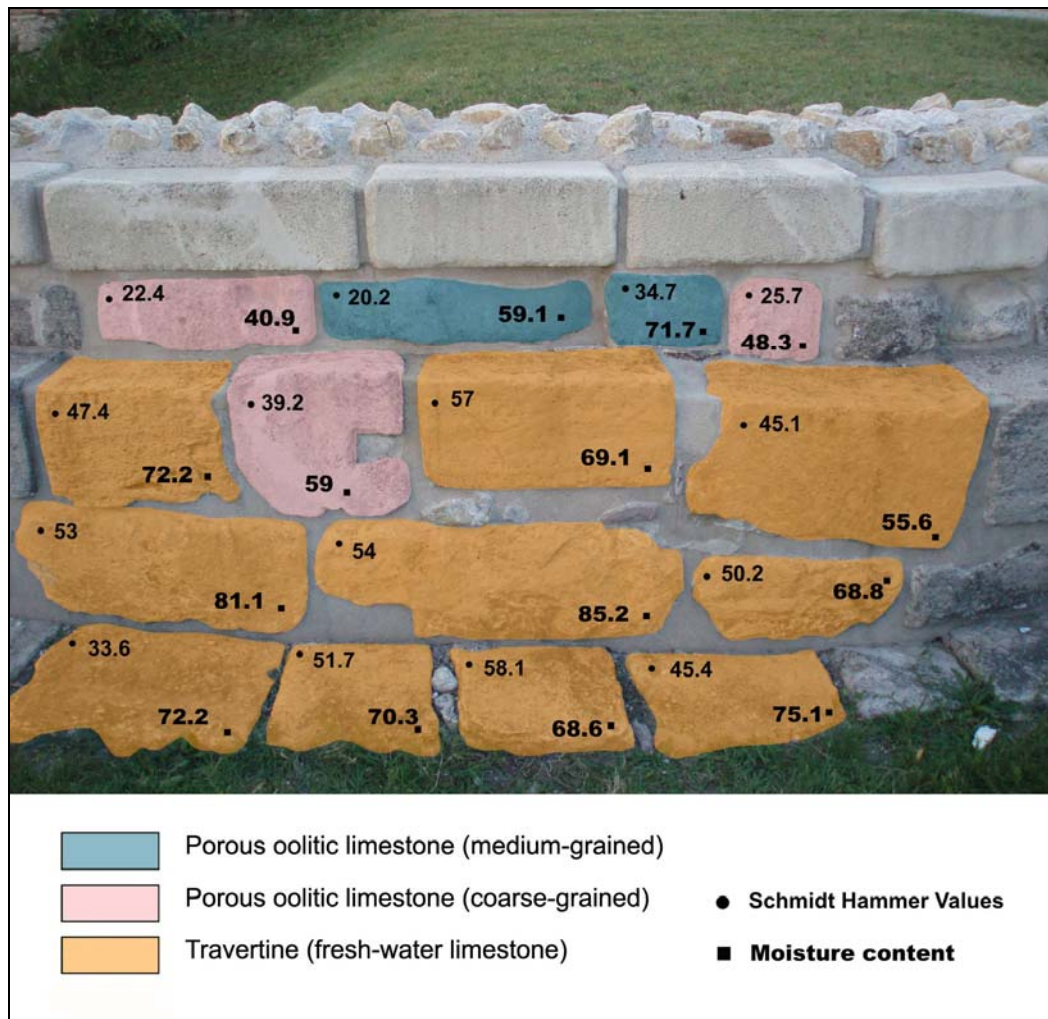
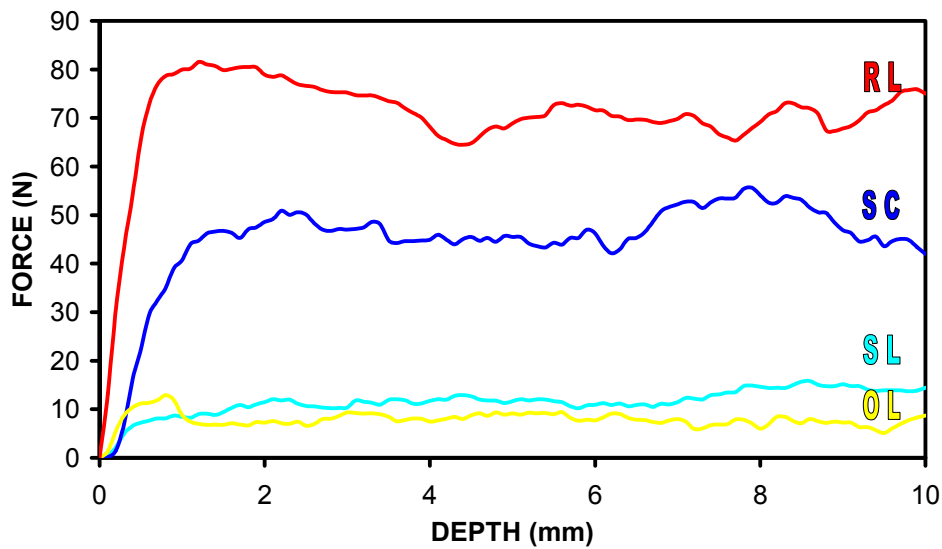


Fig. 6-20: Wall 5 – Schmidt Hammer & Moisture content Values

### 6.1.3. Drilling Resistance

In the Fig. 6-21 the average values of the demanded force in order to drill 10 mm from the surface to the interior of the specimens are presented. The specimens belong to the four selected lithotypes coming from the monument and they were measured under laboratory conditions. The average values correspond to nine drilling measurements for the Oolitic Limestone (OL), the Shelly Limestone (SL), the Sandy Calcarenite (SC) and to three for the Red Limestone (RL) due to its better homogeneity. As it is shown in the Fig. 6-22, the OL has an average value of demanded drilling force equal to 7.8 N, the SL 11.4 N, the SC 44.5 N and the RL 70.1 N.



**Fig. 6-21: Profiles of the average values of demanded drilling forces versus the drilled depth from the surface to the interior of the material for the four historical samples tested in the laboratory: Oolitic Limestone (OL), Shelly Limestone (SL), Sandy Calcarenite (SC) and Red Limestone (RL)**

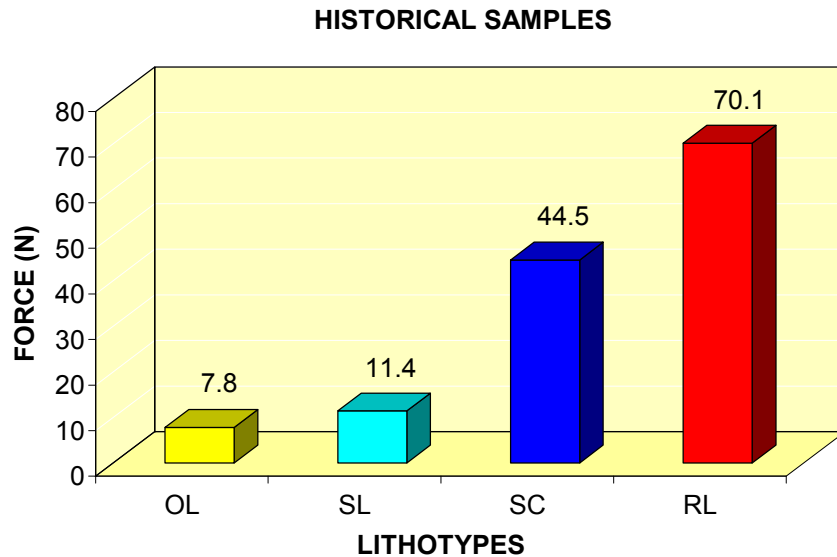


**Fig. 6-22: Average demanded force values for the historical specimens (OL, SL, SC and RL) tested under laboratory conditions (see Table 4-2, p. 16 for abbreviations)**

Similarly to the Figs. 6-21 and 6-22, the Figs. 6-23 and 6-24 show the profiles and the average force values for the freshly quarried stones. The average values correspond to three drilling measurements on each one of the three specimens that were tested for every different lithotype: the medium-grained Oolitic Limestone OL-Q1 and the coarse-grained Oolitic Limestone OL-Q2. The measurements on the specimens of the Red Limestone RL-Q were not completed with success due to the high drilling resistance of the stone and the limitations of the measuring system. The OL-Q1 shows an average demanded drilling force of 4.7 N and the OL-Q2 of 9.8 N.

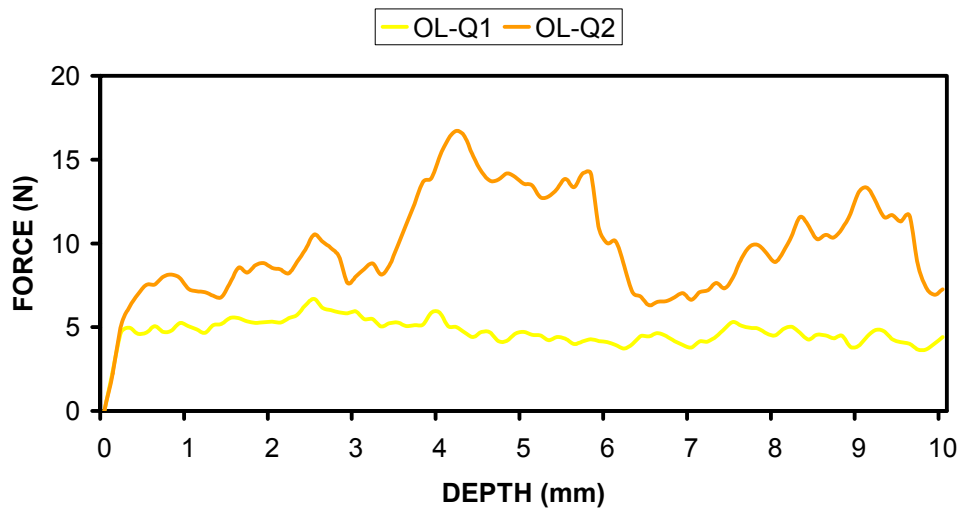


**Fig. 6-23: Profiles of the average values of demanded drilling forces versus the drilled depth from the surface to the interior of the material for the two freshly quarried samples tested in the laboratory: medium-grained Oolitic Limestone (OL-Q1) and coarse-grained Oolitic Limestone (OL-Q2)**

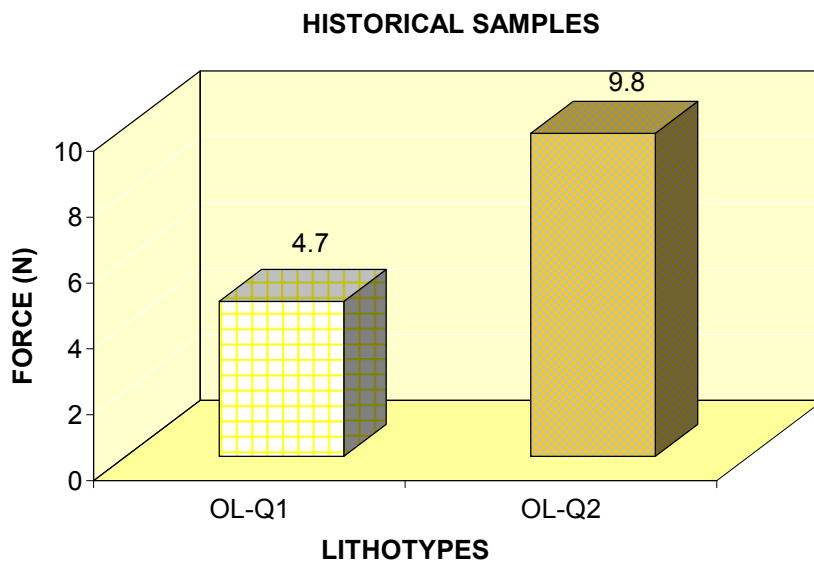


**Fig. 6-24: Average demanded force values for the freshly quarried specimens (OL-Q1 and OL-Q2) tested under laboratory conditions (see Table 4-2, p. 16 for abbreviations)**

During the in-situ application of the Drilling Resistance Measuring System (DRMS), twenty different blocks belonging to different lithotypes were tested (Table 6-1).

Lithotypes	Sample Codes	N. of Samples
Ooidal Peloidal Limestone	8, 10, 12, 26, 27	5
Shelly Limestone	14, 18A, 13	3
Polimict Sandy Calcarenite	1A, 1B, 20	3
Red Bio-micritic Limestone	22, 25A, 25B	3
Foraminifera-bearing Limestone	11, 21	2
Travertine	4B, 5	2
Quartz-porphyre Rhyolite	2	1
Marble	23	1
Total number of tested blocks		20

**Table 6-1: Tested blocks in-situ by DRMS**

In the Figs. 6-26 & 28 the representative profiles for each tested lithotype in-situ are presented. Three drilling measurements were carried out on each block with an exception of the Quartz-porphyre Rhyolite (Rh) shown on Fig. 6-28, where the measurement could not be completed due to its higher drilling resistance than the potential of the measuring system. The average demanded drilling forces of the first four more important lithotypes are shown on the Fig. 6-27. Looking at the profiles of the Ool. L. (Fig. 6-25) and in particular to the one belonging to the block that is exposed to the exterior environmental conditions (block 27), the highest drilling resistance is observed at approximately the first 1.5 mm of the drilling depth which is followed by lower values measured in the interior part of the material. This is not the same for the Ool. L. located in the protected areas of the monument (blocks 8 & 10). The profiles of the Shelly L., Sandy C. and Red L. (Figs. 6-26) and of the other measured lithotypes (Fig. 6-28) showed an increase in the drilling resistance during the approximately top most 2 mm.



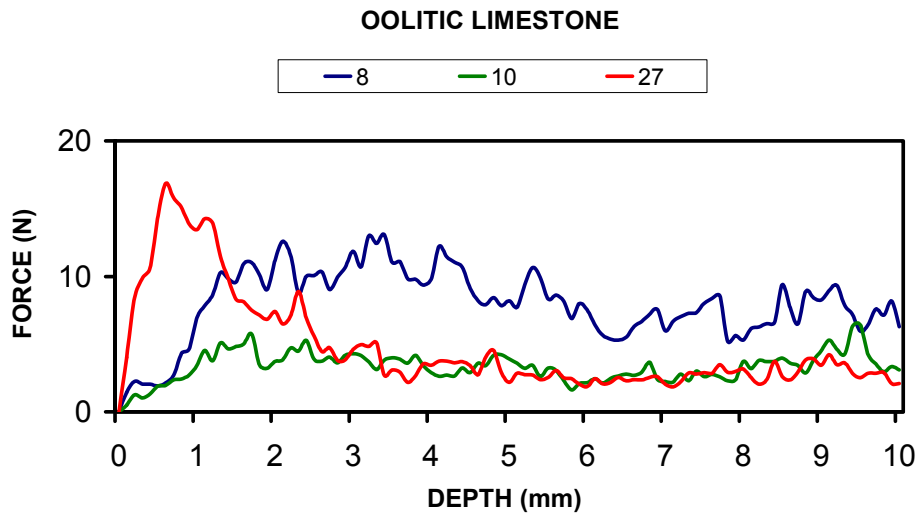


**Fig. 6-25: Profiles of the average values of demanded drilling forces versus the drilled depth from the surface to the interior of the material for representative blocks of Oolitic Limestones (Ooidal Peloidal Limestones) tested in-situ**

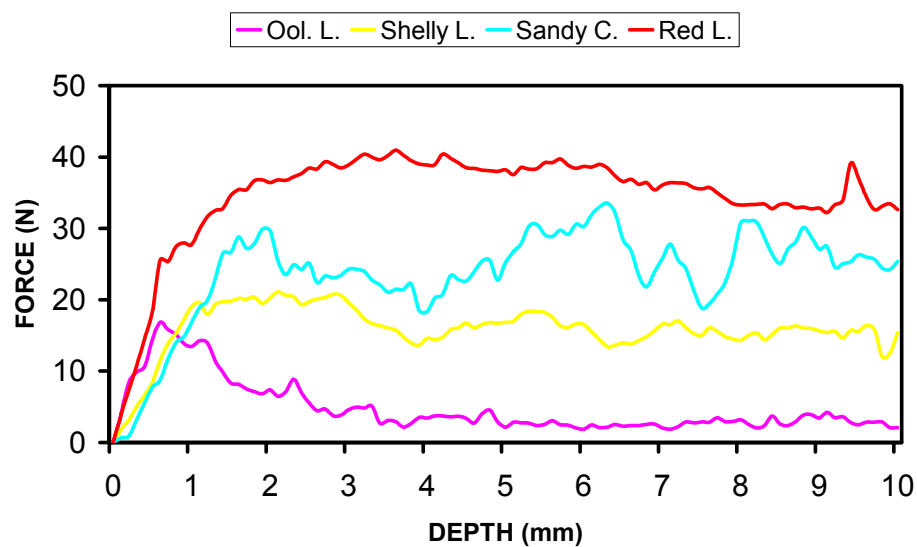


**Fig. 6-26: Profiles of the average values of demanded drilling forces versus the drilled depth from the surface to the interior of the material for representative blocks of the four more important in-situ measured lithotypes: Oolitic Limestone (Ool. L.), Shelly Limestone (Shelly L.), Sandy Calcarentie (Sandy C.) and Red Limestone (Red L.)**

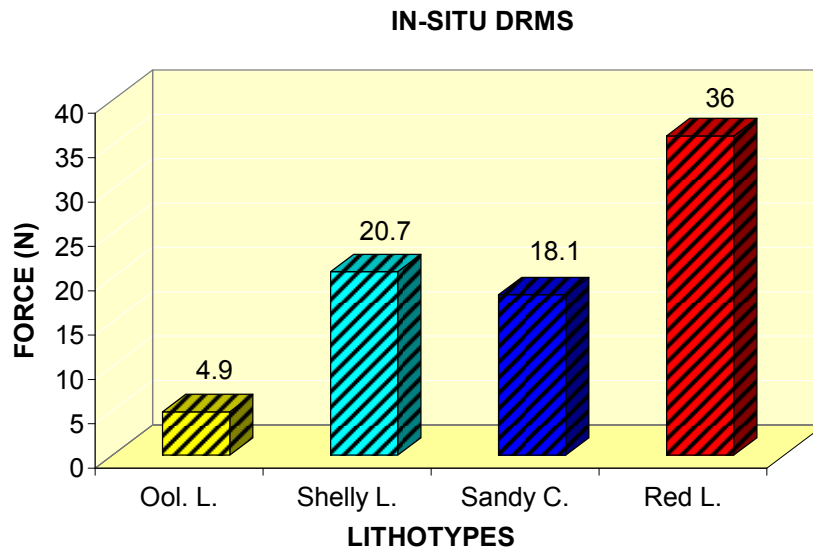


**Fig. 6-27: Average demanded force values for the four more important in-situ measured lithotypes: Oolitic Limestone (Ool. L.), Shelly Limestone (Shelly L.), Sandy Calcarentie (Sandy C.) and Red Limestone (Red L.)**

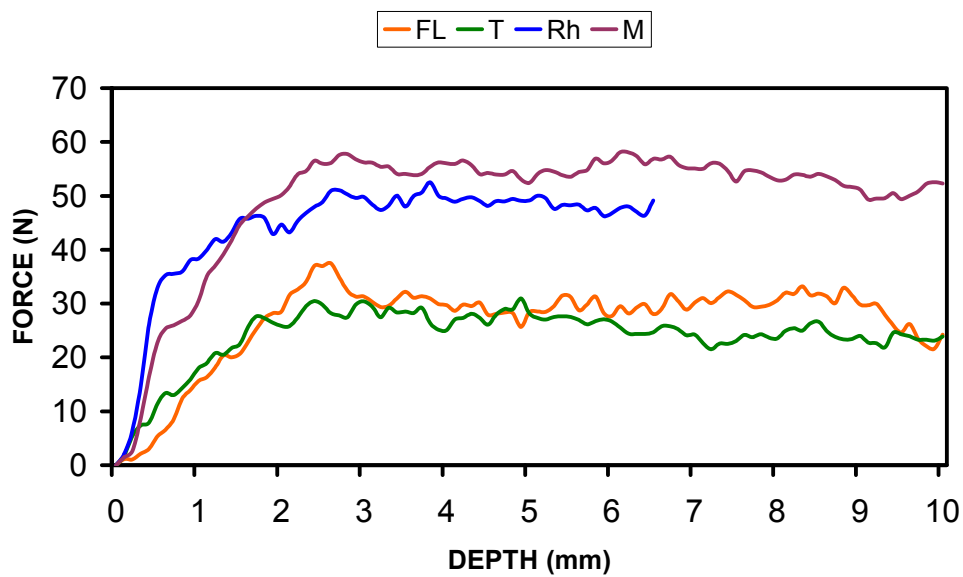


**Fig. 6-28: Profiles of the average values of demanded drilling forces versus the drilled depth from the surface to the interior of the material for representative blocks of the rest four in-situ measured lithotypes: Foraminifera-bearing Limestone (FL), Travertine (T), Rhyolite (Rh) and Marble (M)**

## **6.2. Analyses under Laboratory Conditions**

### **6.2.1. Petrographic Examination - Polarising Microscope**

#### *Ooidal-peloidal Limestone*

The micro-fabric is dominated by coated carbonate grains of various size. Micro-oncoids of 1 mm in scale and ooids of 0.1 mm in diameter are the most common carbonate particles. The nuclei of these grains are either small silt-sized quartz grains or carbonate grains. The oncoids are irregularly coated with micrite envelopes. Small size micritic peloids also occur. Besides the coated carbonate grains shell fragments and foraminifers are the most common compounds. The cement is governed by sparitic calcite therefore the micro-fabric is oncoid-ooid-peloid grainstone.

#### *Shelly Limestone*

The micro-fabric of the limestone is characterized by the dominance of carbonate mud. In terms of microfacies it is considered as a foraminifer bearing shelly limestone (wackestone). Besides shell fragments micritic intraclast also occur. Moldic porosity is dominated by dissolution pores of shells.

#### *Polimict Sandy Calcarenite*

Sandy calcarenite is composed of a mixture of sand-sized particles. Angular quartz grains predominate while other particles such as lithic fragments of limestones and bioclasts are less common. The quartz grains are often fractured and dissected by micro-cracks. The matrix of the calcarenite is composed of micritic calcite. Bioclasts are represented by red algae fragments.

#### *Red bio-micritic Limestone*

The micritic limestone has a wackestone microfabric. In the micritic matrix it contains a few amounts of thin bivalve shells of pelagic origin. The shell fragments are recrystallized.

Besides shells small amount of pelagic foraminifers and calcite spherules also occur. Stylolitic veins with limonitic stainings are also very common. Scattered iron-oxi-hydroxide (limonitic) and hematite contribute to the reddish colour of the stone.

### *Travertine*

The travertine is characterized by various micro-fabric. One common type is the phytoclastic packstone to floatstone with the predominance of bioclasts, such as phytoclasts. The matrix is dominated by recrystallised micro-sparitic calcites. The porosity is given by intragranular and interparticle pores. Large pores in phytoclasts also occur. Oncoidal packstones and grainstones are less common, but strongly recrystallised pelloidal wackestones to packstones are more frequent.

### *Rhyolite*

Rhyolite is characterized by cumulo porphyric holocrystalline mico-fabric. The matrix is composed of glassy constituents that show micrographical textures around the porphyric crystals. Feldspars (plagioclases and K-feldspars) and quartz dominates while other crystals such as mica are less common. The plagioclase crystals are strongly weathered (sericitized). No micro-pores were visualized under the microscope.

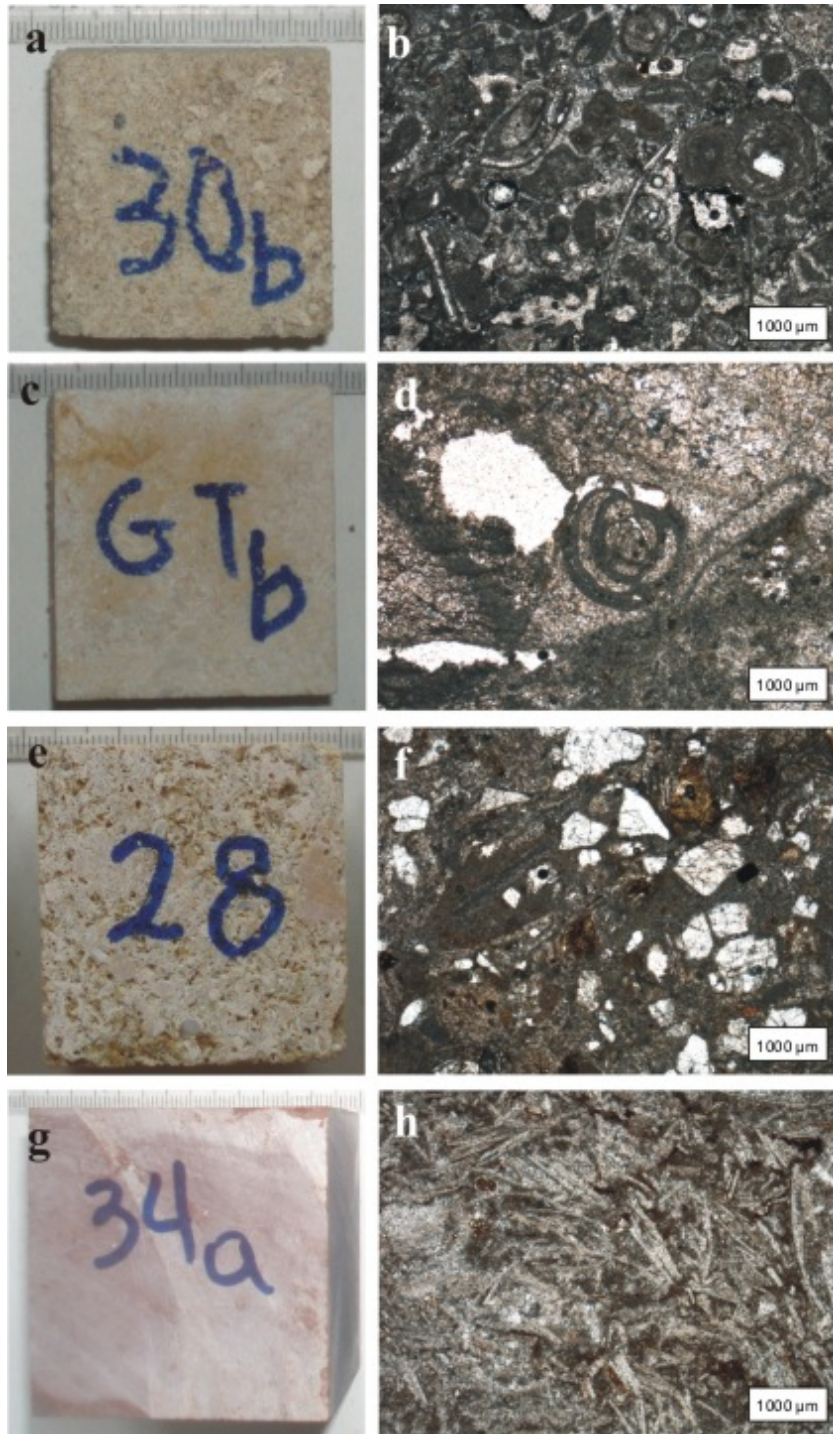


**Fig. 6-29: Macroscopic and microscopic aspects of historical samples: a) & b) Ooidal-peloidal Limestone (OL), c) & d) Shelly Limestone (SL), e) & f) Polymict Sandy Calcarenite (SC) and g) & h) Red bio-micritic Limestone (RL)**

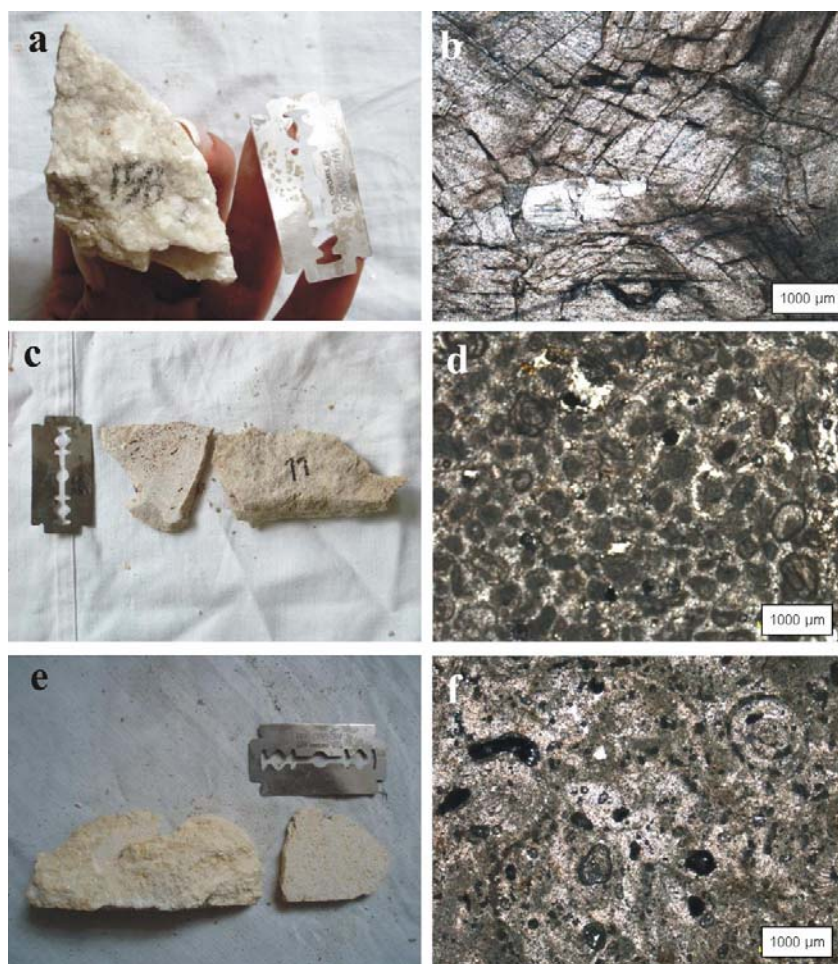


**Fig. 6-30: Macroscopic and microscopic aspects of historical samples: a) & b) Marble, c) & d) Foraminifera-bearing Limestone and e) & f) Travertine**



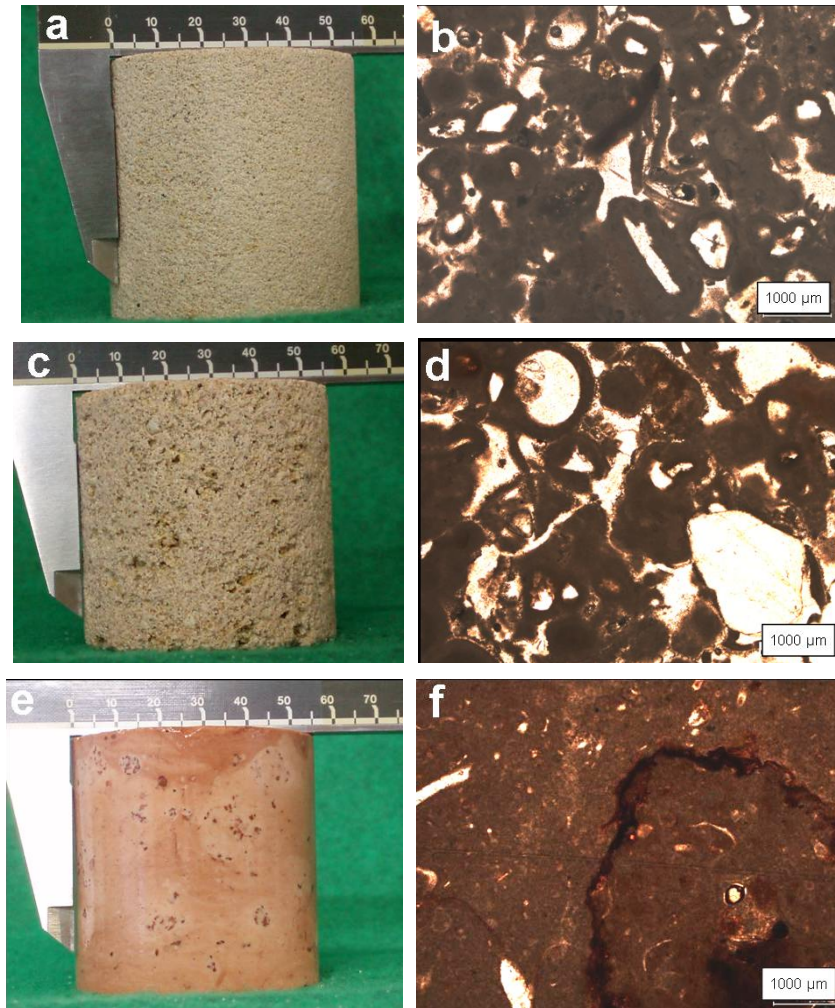







**Fig. 6-31: Macroscopic and microscopic aspects of freshly quarried samples: a) & b) medium-grained Oolitic Limestone (OL-Q1), c) & d) coarse grained Oolitic limestone (OL-Q2) and e) & f) Red Limestone (RL-Q)**

In Table 6-2 the samples that were taken from the walls of the monument are divided according to their lithotype. The construction period that they belong to is depicted in different colours. The use of Ooidal-peloidal Limestone is found in most of the construction periods. The use of Shelly Limestone through the several construction periods is also relatively wide while Red Limestone appears only in the reconstruction that took place in the 12<sup>th</sup> century according to the results of the relative sampling and marble in the first construction period.

Lithotypes	Total N. of Samples	Samples code
Ooidal Peloidal Limestone	9	24, 7, 10, 17, 8, 9, 27, 12, 26
Shelly Limestone	6	18A, 13, 3, 4A, 14, 19
Polimict Sandy Calcarene	4	1B, 1A, 28, 20
Red Bio-micritic Limestone	4	22, 29, 25A, 25B
Travertine	4	5, 18B, 6, 4B
Marble	3	15A, 15B, 23
Foraminifera-bearing Limestone	2	11, 21
Quartz-porphyre Rhyolite	1	23
Silica-cemented Red Sandstone	1	16

	11 <sup>th</sup> -12 <sup>th</sup> centuries		12 <sup>th</sup> century
	14 <sup>th</sup> century		14 <sup>th</sup> -15 <sup>th</sup> centuries
	end of 15 <sup>th</sup> century		

**Table 6-2: Division of samples from the 2nd sampling according to the general category of lithotypes and the period of construction they belong to**

### 6.2.2. X-Ray Diffraction (XRD)

The XRD showed the prevailing presence of calcite in the medium-grained Oolitic Limestone from the quarry (OL-Q1). Quartz was also detected in addition with muscovite and clay minerals (illite and montmorillonite). No feldspars were detected in this type of stone.

Calcite is the main mineral also for the coarse-grained Oolitic Limestone (OL-Q2). Quartz was identified in this material as well. The presence of feldspars (microcline and albite) and clay minerals belonging to the group hydromicas was also identified.

The main difference of the Red Limestone (RL-Q) in comparison with the aforementioned OL-Q1 and OL-Q2 is the absence of quartz. Calcite is the main mineral of its composition and the presence of saponite is under question due to its very weak peak.

### 6.2.3. Scanning Electron Microscope (SEM)

When comparing the micro-fabric of the samples from the monuments and quarries under the SEM it is visible that the samples from the monuments show some alterations. The Oolitic Limestone is composed of micritic to micro-sparitic calcite crystals. The calcite crystals of



the freshly quarried samples (OL-Q1) show clear crystal faces with no dissolution features, while the samples from the monuments (OL) display various forms of surfaced alterations. Besides micro-cracks small crystal aggregates and secondary calcite crystal growth was detected on weathered samples of the monument by using SEM (Fig 6-32).

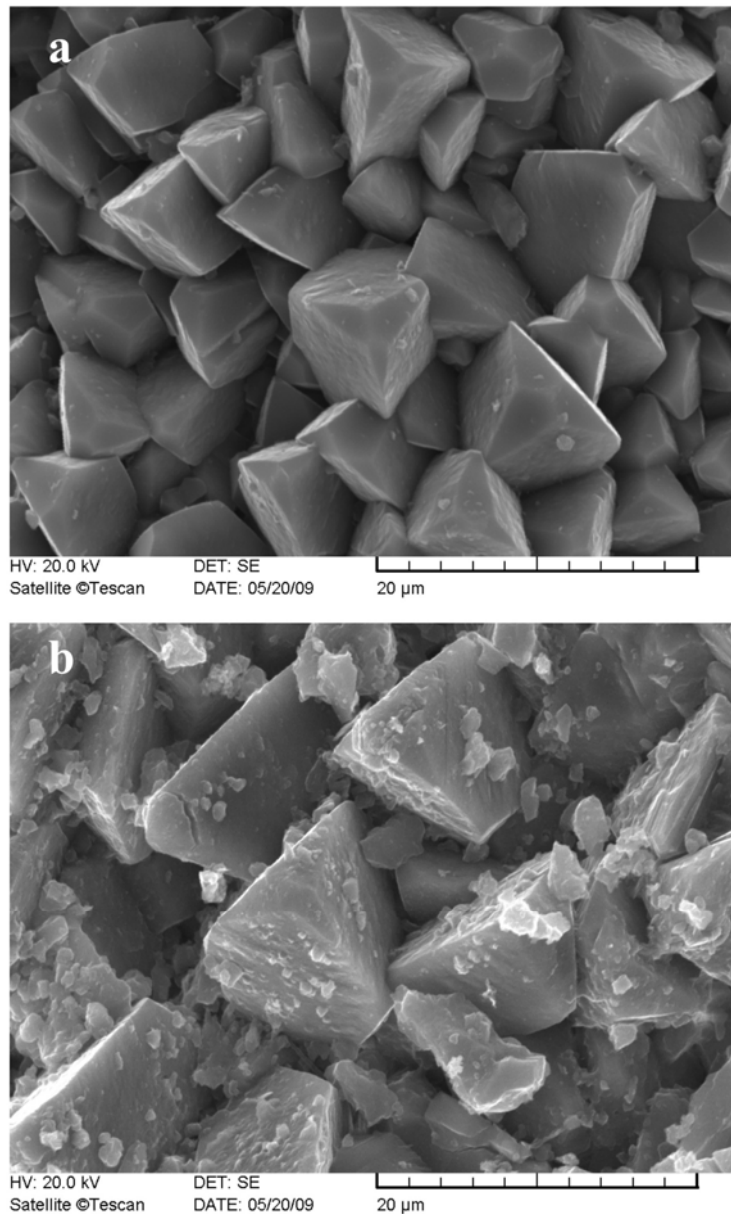


**Fig. 6-32: Microscopic aspects by SEM: a) fresh medium-grained Oolitic Limestone (OL-Q1), b) Oolitic Limestone from the monument (OL)**

#### 6.2.4. Porosimetry

The results of the open porosity and specific gravity for the different groups of tested samples are presented in the Tables 6-3, 4 & 5. The real density, the bulk density and the total open porosity of the selected historical and freshly quarried samples are presented in the Tables 6-6 & 7 while the average values of the bulk densities and the total open porosities are summarized in the Figs. 6-33 & 34.

The results of the open porosity and specific gravity measured on small irregular samples coming from the remaining walls of the monument give a first idea about the identified materials (see Table 6-3). The group Ooidal-Peloidal Limestones (Oolitic Limestones) shows the highest average value of open porosity with one of Shelly Limestones and Foraminifera-bearing Limestones following but almost with half of the value for Oolitic Limestones. Polimict Sandy Calcarenes (Sandy Calcarenes) and Travertines have a bit lower average value. Silica-cemented Red Sandstone has values already less than the one fourth of the Oolitic Limestones but the lowest measured values correspond to the Red Bio-micritic Limestones (Red Limestones), Marbles, and Granite.

The same measurement was also carried out on the cubic specimens of the eight selected samples from the monument (see Table 6-4) where the two Oolitic Limestones (OL and OL\_2) showed again the highest average values for open porosity and the two Shelly Limestones (SL and SL\_2) following with a relatively high open porosity, yet lower than the ones for OL and OL\_2. Sandy Calcarene (SC) presents an open porosity which is almost the half of the values for the Oolitic Limestones. Much lower results were given for the Red Limestone (RL) and the Marble (M) which are lower than 1%.

The different void spaces of the two freshly quarried Oolitic Limestones (OL-Q1 and OL-Q2) in comparison with the Red Limestone (RL-Q) are shown on the Table 6-5. Almost equal high open porosities were given for the OL-Q1 and OL-Q2 and much lower one for the RL-Q and those values are lower if compared with the ones for the same lithotypes (OL vs. OL-Q1 and RL vs. RL-Q) coming from the monument (Table 6-4).

Lithotypes	Sample Codes	N. of Samples	Open Porosity $P_0$				Specific Gravity SG	
			Min (%)	Max (%)	Mean (%)	St. Dev.	Mean	St. Dev.
Ooidal Peloidal Limestone	24, 12, 27, 8, 9, 10, 26, 17	8	27.92	57.42	41.90	9.11	1.74	0.10
Shelly Limestone	13, 3, 4A 14, 18A, 19	6	8.79	35.46	22.28	12.08	2.06	0.25
Polimict Sandy Calcarenite	1B, 1A, 20, 28	4	8.69	22.54	15.07	5.69	2.14	0.20
Red Bio-micritic Limestone	29, 25A, 25B	3	0.74	11.50	4.68	5.93	2.53	0.15
Travertine	5, 18B, 6, 4B	4	4.12	26.57	11.47	10.38	2.30	0.22
Marble	23, 15A, 15B	3	0.44	1.53	1.12	0.60	2.68	0.02
Foraminifera-bearing Limestone	11, 21	2	12.25	25.26	18.75	9.20	2.06	0.24
Silica-cemented Red Sandstone	16	1			8.25		2.01	2.01
Granite	tov	1			1.40		2.63	2.63

**Table 6-3: Open porosity and Specific Gravity for samples of irregular shape from the walls of the monument divided in the main groups of lithotypes**

Samples	Open Porosity $P_o$ (%)	St. Dev.	Specific Gravity SG	St. dev.
OL	27.97	0.80	1.80	0.02
OL_2	28.35	0.10	1.77	0.03
SL	22.74	1.45	1.90	0.06
SL_2	19.03	4.01	2.06	0.15
SC	12.60	0.69	2.26	0.04
RL	0.80	0.20	2.67	0.04
Rh	4.13	0.26	2.44	0.03
M	0.24	0.05	2.58	0.07

**Table 6-4: Open Porosity and Specific Gravity for cubic samples from the monument (see Table 4-2, p. 16 for abbreviations)**

Lithotypes	Open Porosity $P_o$ (%)	Specific Gravity SG
OL-Q1	27.14	1.83
OL-Q2	27.58	1.80
RL-Q	0.56	2.65

**Table 6-5: Open Porosity and Specific Gravity for cylindrical samples from the quarries (see Table 4-2, p. 16 for abbreviations)**

The results for the densities and total open porosity of the four more important historical lithotypes and the three freshly quarried stones are presented the Tables 6-6 and 7 accordingly.

For the samples coming from the monument, the lowest average bulk density corresponds to the OL and the highest to the RL. The values of the rest two lithotypes are in between the extreme ones with the SL being closer to the OL and the SC closer to the RL. In the same way, the average densities for the freshly quarried stones are lower for the OL-Q1 and OL-Q2 than the one for the RL-Q. (Fig. 6-10)

Regarding the total open porosity of the analysed materials (see Table 6-6 and 6-7) and the average values as shown on the Fig. 6-16 the OL has the highest void space among the historical samples, a lower value was measured for the SL, almost half of the one belonging to the OL corresponds to the SC and the finally the lowest volume belongs to RL. Referring to the fresh samples, OL-Q1 and OL-Q2 have much higher values than the RL-Q. Slightly lower percentages of total open porosity are observed for the fresh samples (OL-Q1 and RL-Q) in comparison with their petrographically similar ones from the monument (OL and RL).

Sample codes	Real density	Mean	St. Dev.	Bulk density	Mean	St. Dev.	Total open porosity	Mean	St. Dev.
	$\gamma_r$ (g/cm <sup>3</sup> )			$\gamma_b$ (g/cm <sup>3</sup> )			P%		
OL_a	2.71	2.72	0.01	1.85	1.84	0.02	31.70	32.50	0.92
OL_b	2.72			1.81			33.50		
OL_c	2.72			1.85			32.30		
SL_a	2.69	2.69	0.01	1.99	1.99	0.00	26.20	26.30	0.56
SL_b	2.70			1.99			26.90		
SL_c	2.68			1.99			25.80		
SC_a	2.71	2.71	0.01	2.27	2.27	0.00	16.10	16.30	0.26
SC_b	2.72			2.27			16.60		
SC_c	2.70			2.27			16.20		
RL_a	2.72	2.72	0.00	2.70	2.70	0.01	0.70	0.80	0.06
RL_b	2.72			2.70			0.70		
RL_c	2.72			2.69			0.80		

**Table 6-6: Real density, bulk density and total open porosity for the four most important historical lithotypes (see Table 4-2, p. 16 for abbreviations)**

Sample codes	Real density	Mean	St. Dev.	Bulk density	Mean	St. Dev.	Total open porosity	Mean	St. Dev.
	$\gamma_r$ (g/cm <sup>3</sup> )			$\gamma_b$ (g/cm <sup>3</sup> )			P%		
OL-Q1a	2.70	2.70	0.01	1.86	1.85	0.01	31.00	31.71	0.58
OL-Q1b	2.70			1.84			32.00		
OL-Q1c	2.71			1.84			32.00		
OL-Q2a	2.71	2.72	0.01	1.88	1.84	0.05	31.00	32.33	1.53
OL-Q2b	2.72			1.84			32.00		
OL-Q2c	2.72			1.79			34.00		
RL-Qa	2.69	2.69	0.01	2.68	2.68	0.01	0.34	0.34	0.01
RL-Qb	2.70			2.69			0.36		
RL-Qc	2.69			2.68			0.34		

**Table 6-7: Real density, bulk density and total open porosity for the three lithotypes from the quarries (see Table 4-2, p. 16 for abbreviations)**



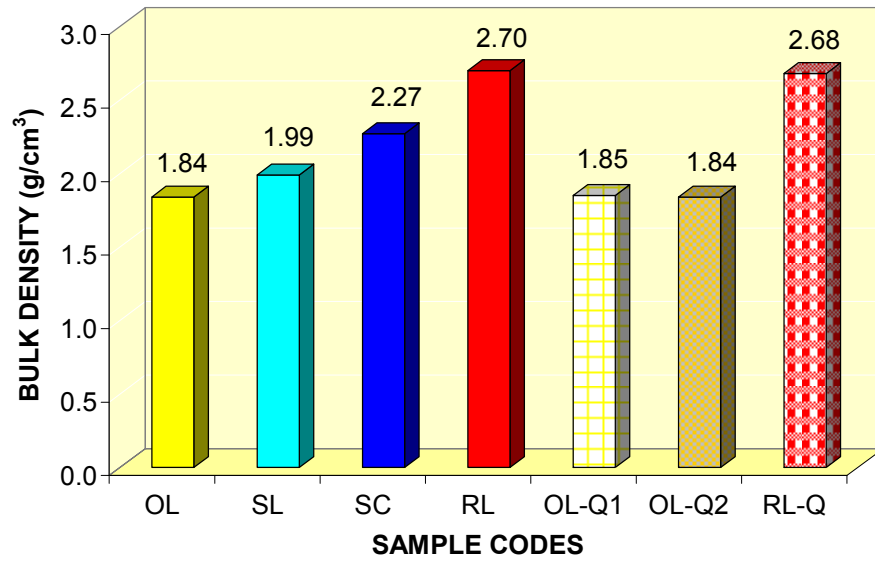


Fig. 6-33: Average bulk density values for both the historical and freshly quarried samples (see Table 4-2, p. 16 for abbreviations)

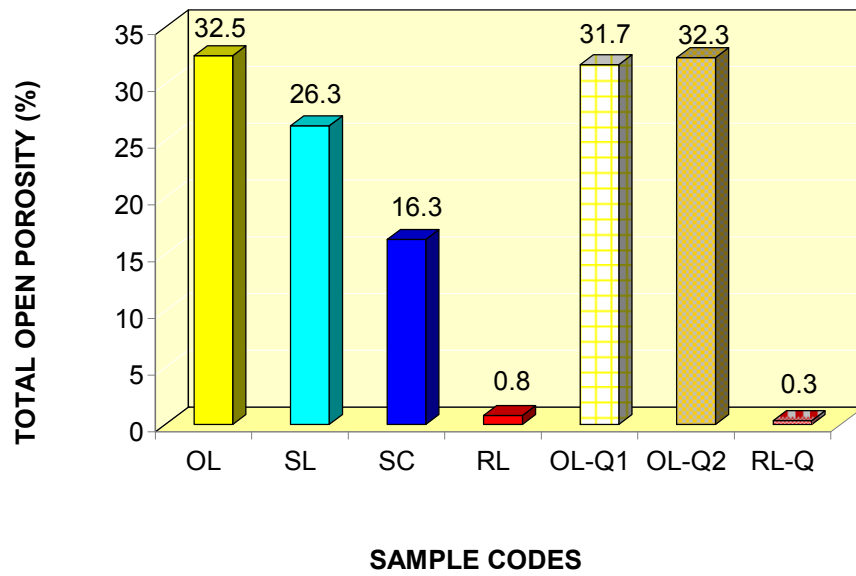
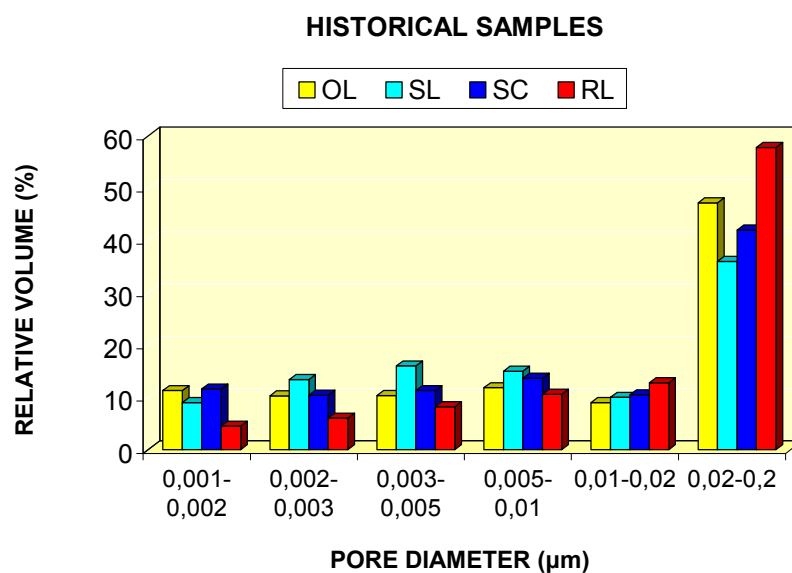
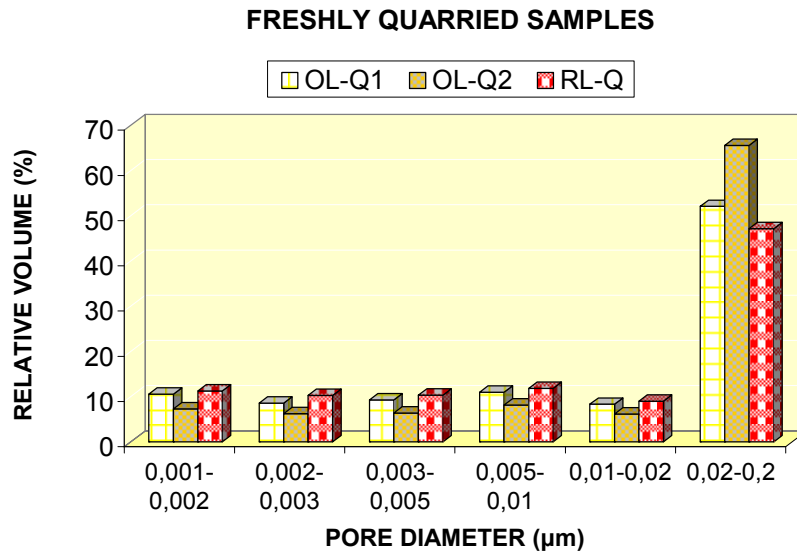


Fig. 6-34: Total Open Porosity for both the historical and the freshly quarried samples (see Table 4-2, p. 16 for abbreviations)

By observing the results which characterize the pores achieved by nitrogen adsorption, all of the tested samples show a unimodal distribution with their main pore volume accumulated in the diameter range of 0.02 to 0.2  $\mu\text{m}$ . The results for the four selected lithotypes from the monument (OL, SL, SC and RL) are presented in the Fig. 6-12 while the ones for the three freshly quarried lithotypes (OL-Q1, OL-Q2 and RL-Q) in the Fig. 6-35.



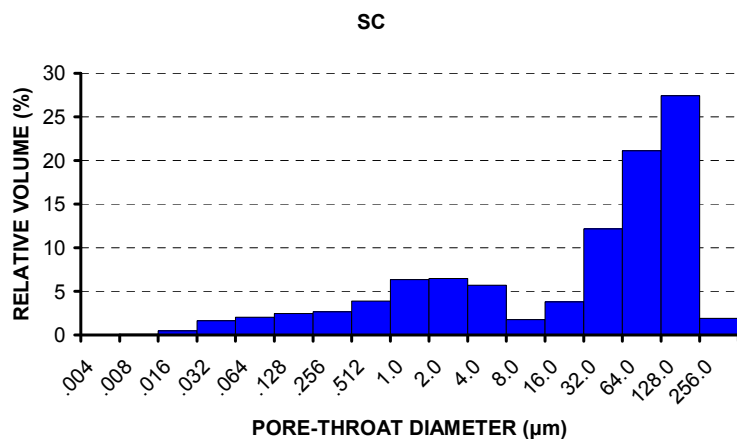
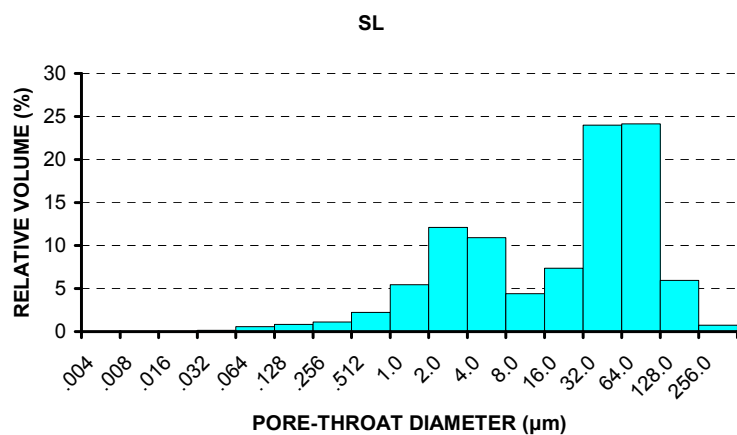
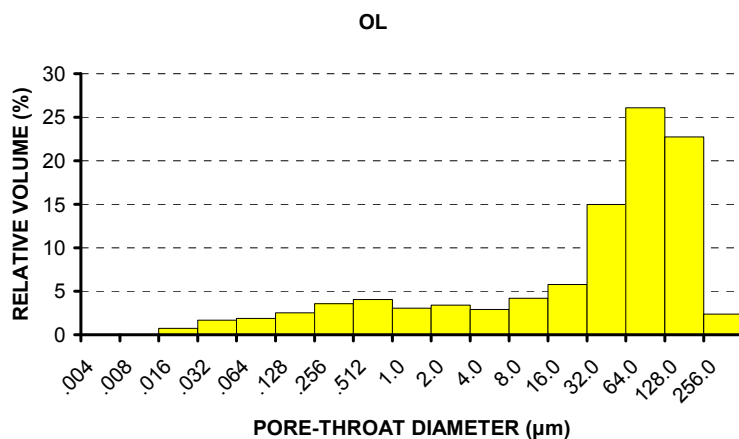
**Fig. 6-35: Pore size distribution by nitrogen adsorption for the four selected historical lithotypes (see Table 4-2, p. 16 for abbreviations)**



**Fig. 6-36: Pore size distribution by nitrogen adsorption for the three freshly quarried lithotypes (see Table 4-2, p. 16 for abbreviations)**

The mercury intrusion porosimetry (MIP) carried out on three specimens from each one of the four historical samples and the three fresh stone samples. The presented values are the average ones out of the three specimens for each lithotype. The results presented in the Figs. 6-37 & 39 show that the samples OL, SL, SC, OL-Q1 and OL-Q2 show the main volume accumulated in the diameter range between 16 to 256 μm. The RL and RL-Q show a bimodal distribution for which a second noticeable volume of pore sizes is observed in the diameter range between 0.004 to 0.256 μm (Figs. 6-37 and 6-39).

The relative volumes divided in four ranges of pore-throat diameter are presented in the Fig. 6-38 for the historical samples and Fig. 6-40 for the freshly quarried ones where the most intense difference in the distribution is clear for the RL and the RL-Q.



(see legend for Fig. 6-37 in the next page)

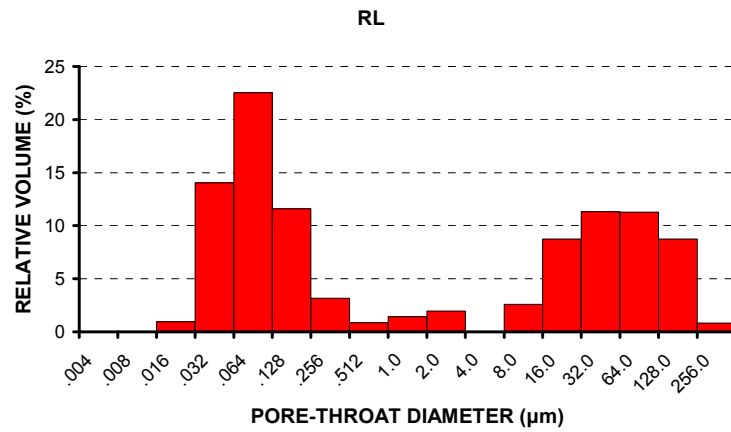


Fig. 6-37: Pore size distribution by MIP for historical Oolitic Limestone (OL), Shelly Limestone (SL), Sandy Calcarenite (SC) and Red Limestone (RL)

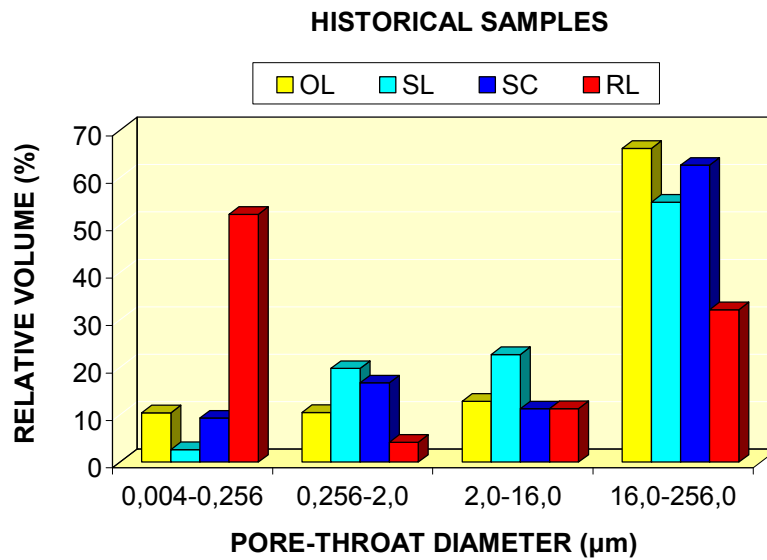
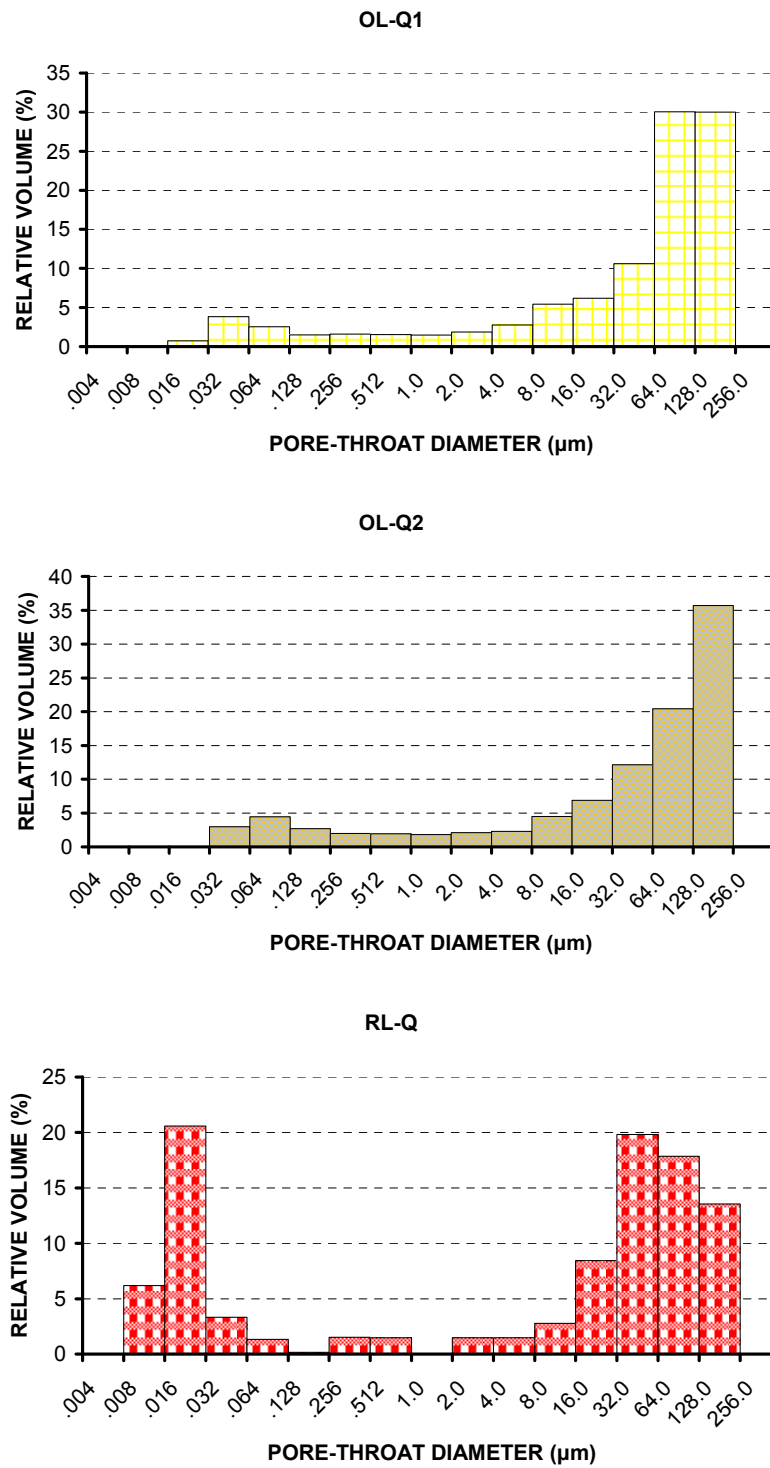
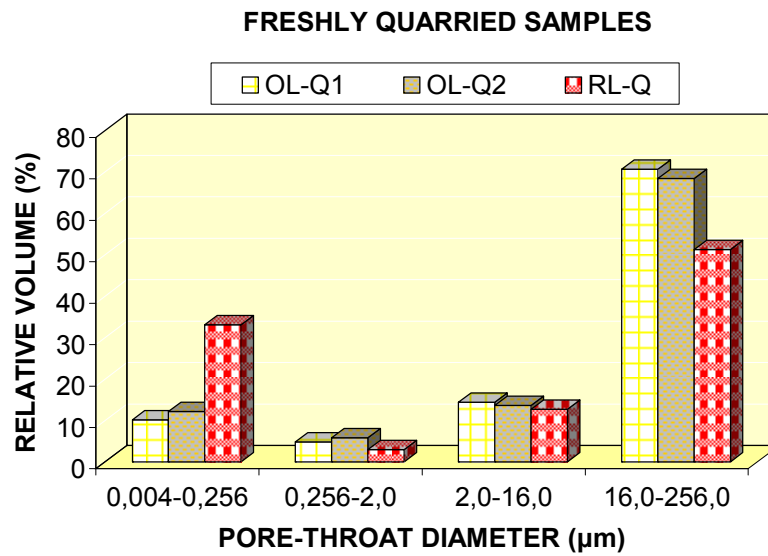


Fig. 6-38: Comparative graph of the distribution by MIP of the historical samples (OL, SL, SC and RL- see Table 4-2, p. 16 for abbreviations)



**Fig. 6-39: Pore size distribution by MIP for freshly quarried medium-grained Oolitic Limestone (OL-Q1), coarse-grained Oolitic Limestone (OL-Q2) and freshly quarried Red Limestone (RL-Q)**



**Fig. 6-40: Comparative graph of the pore size distribution by MIP of the freshly quarried samples (OL-Q1, OL-Q2 and RL-Q - see Table 4-2, p. 16 for abbreviations)**

The mesoporosity of all samples analysed by MIP was calculated and its average values out of three specimens for each lithotype are presented in Fig. 6-41. OL and SL have the highest void volume in the range of mesopores. Half of the aforementioned volume corresponds to the SC and the lowest one belongs to the RL. Regarding the fresh stone samples, high void volumes were measured for the OL-Q1 and the OL-Q2 with difference of about 5 % observed between them (lower percentage for the OL-Q2). Very low mesoporosity corresponds to the RL-Q and again, the comparison between the historical (OL and RL) and the fresh samples (OL-Q1 and RL-Q) shows slightly lower values for the case of the fresh ones.



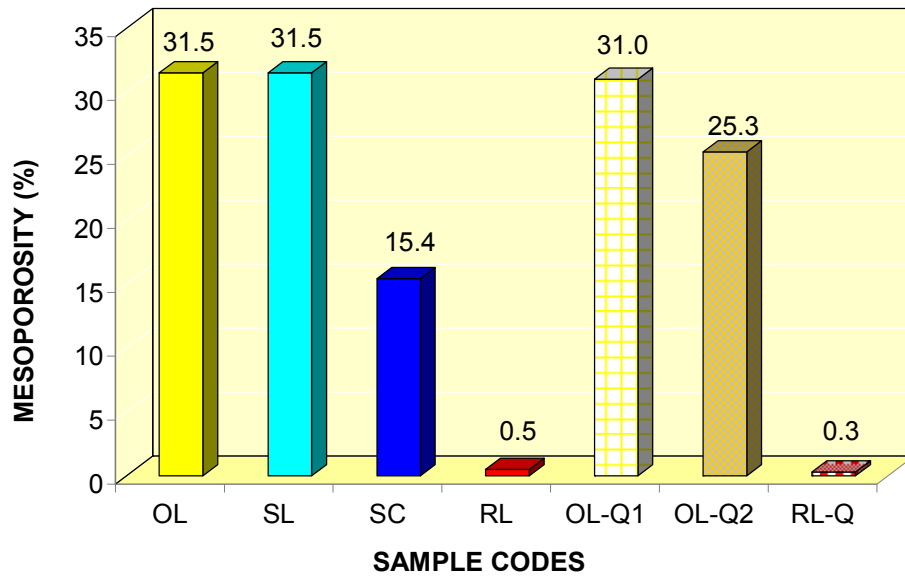


**Fig. 6-41: Mesoporosity for both the historical (OL, SL, SC and RL) and the freshly quarried samples (OL-Q1, OL-Q2 and RL-Q) - see Table 4-2, p. 16 for abbreviations**

#### **6.2.5. Water Absorption**

The water absorption by capillarity measured on three specimens for each type is presented as a plot of capillary height in function of time for the OL-Q1 and OL-Q2 in the Fig. 6-42.

In OL-Q1, water needed few more seconds in order to reach the top surface of the specimen than in the case of OL-Q2. For both lithotypes, the capillary absorption of water was gradually increased in function of time. Carrying out the measurement on the specimens of the RL-Q, no noticeable changes were observed.

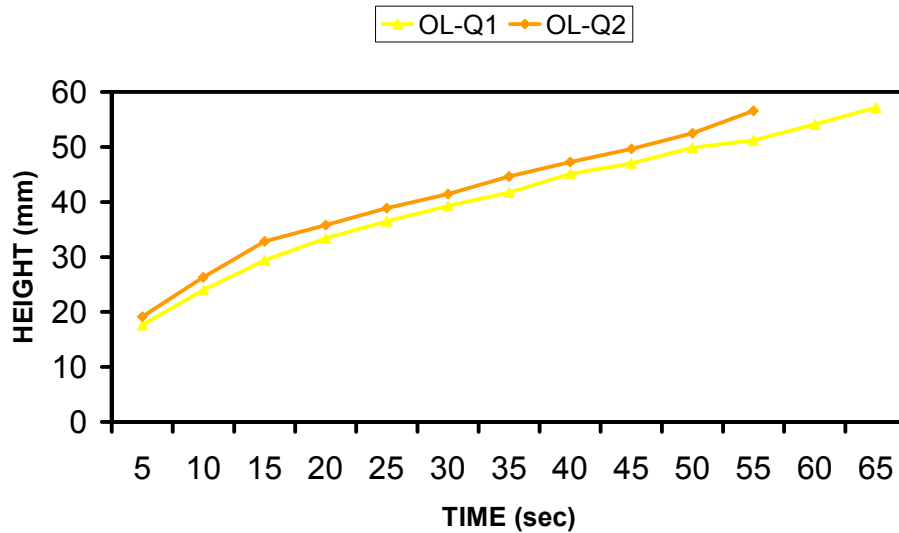


**Fig. 6-42: Capillary-rise absorption in function of time of representative samples for the freshly quarried medium-grained Oolitic Limestone (OL-Q1) and the coarse-grained one (OL-Q2)**

The water absorption at atmospheric pressure profiles for the three freshly quarried stone types OL-Q1, OL-Q2 and RL-Q are presented in the Fig. 6-43. Similar behaviour is observed between the OL-Q1 and the OL-Q2 yet a totally different one for the RL-Q; over sixteen days, the percentage of absorbed water is increasing with a much more rapid way in the case of the OL-Q1 and OL-Q2 than in the case of RL-Q. This difference in behaviour can be further clarified by having a look at the average values of total absorption for the three lithotypes after sixteen days of immersion in water (Fig. 6-44) where the percentages are much higher for the OL-Q1 and OL-Q2 than the one for the RL-Q.

The average results obtained by the porosimetric studies and the hydric tests are summarized in Table 6-8 for both the historical and the freshly quarried materials.

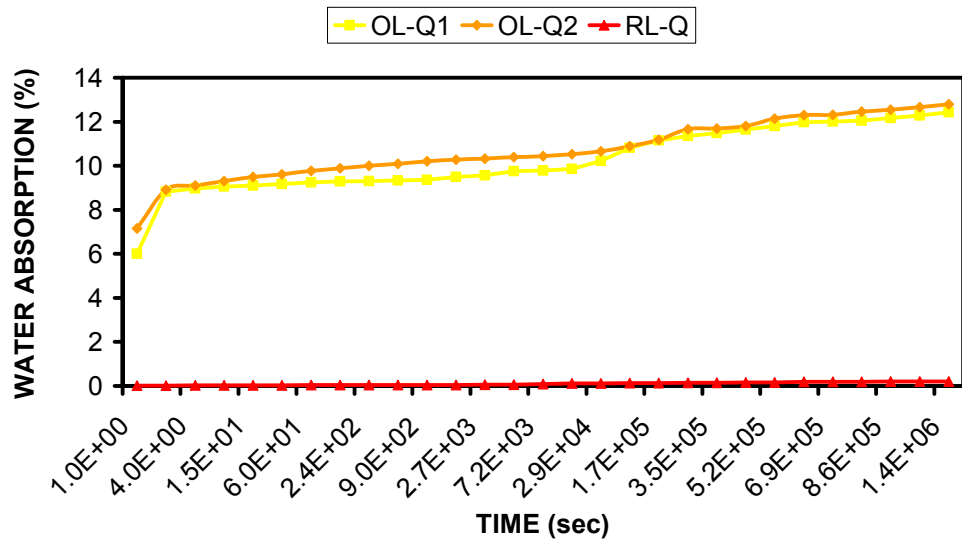


Fig. 6-43: Water absorption at atmospheric pressure in function of time for three representative specimens of the freshly quarried medium-grained Oolitic Limestone (OL-Q1), coarse-grained Oolitic Limestone (OL-Q2) and Red Limestone (RL-Q)

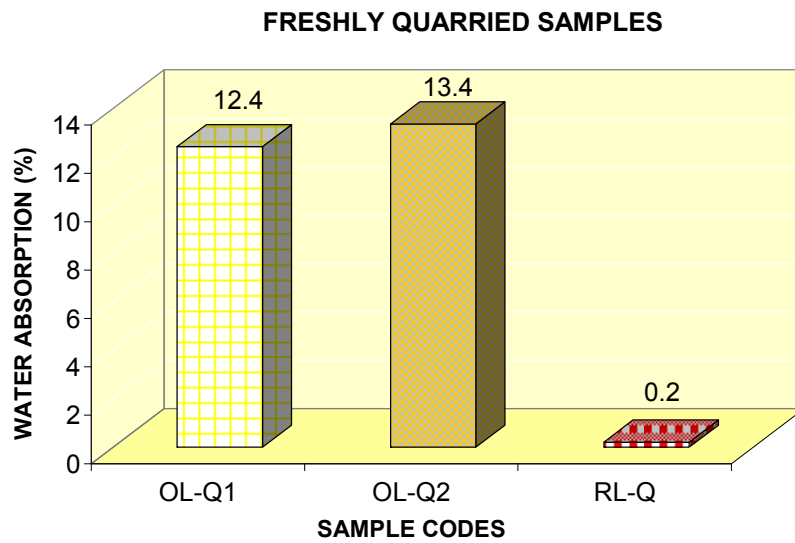


Fig. 6-44: Water absorption at atmospheric pressure after sixteen days; average value for three specimens of each freshly quarried lithotype (OL-Q1, OL-Q2 and RL-Q - see Table 4-2, p. 16 for abbreviations)

Sample Codes	apparent density (kg/m <sup>3</sup> )	real density (kg/m <sup>3</sup> )	bulk density (kg/m <sup>3</sup> )	open porosity (%)	specific gravity	total open porosity (%)	mesoporosity (%)	wat. abs. atmosph. pres. (%)
OL	1741.26	2717.50	1835.34	15.55	1.799	32.46	31.49	-
SC	2229.02	2710.07	2268.95	12.60	2.260	16.28	15.38	-
SL	1885.98	2961.10	1987.66	12.00	1.898	26.30	25.07	-
RL	2640.25	2718.60	2695.95	0.30	2.666	0.76	0.49	-
OL-Q1	1835.03	2703.90	1846.60	27.1	1.831	31.71	31.00	13.49
OL-Q2	1757.37	2716.42	1838.22	27.6	1.804	32.33	25.33	14.21
RL-Q	2687.27	2692.74	2683.16	0.56	2.650	0.34	0.30	0.21

**Table 6-8: Average values for the porosimetric and hydric studies for both historical and freshly-quarried lithotypes (see Table 4-2, p. 16 for abbreviations)**

#### 6.2.6. Pulse velocity, Strength, Elasticity and Artificial Frost Weathering

The average values of the sound speed propagation presented in the Fig. 6-45 was calculated after measuring three specimens for each stone type coming from the monument (OL, SL, SC and RL) and six for each fresh stone type (OL-Q1, OL-Q2 and RL-Q). The two extreme values for both the historical and the fresh samples belong to the Oolitic Limestones (OL, OL-Q1 and OL-Q2) and the Red Limestones (RL and RL-Q) with the lower velocity belonging to the first lithotypes and the highest belong to the second ones.

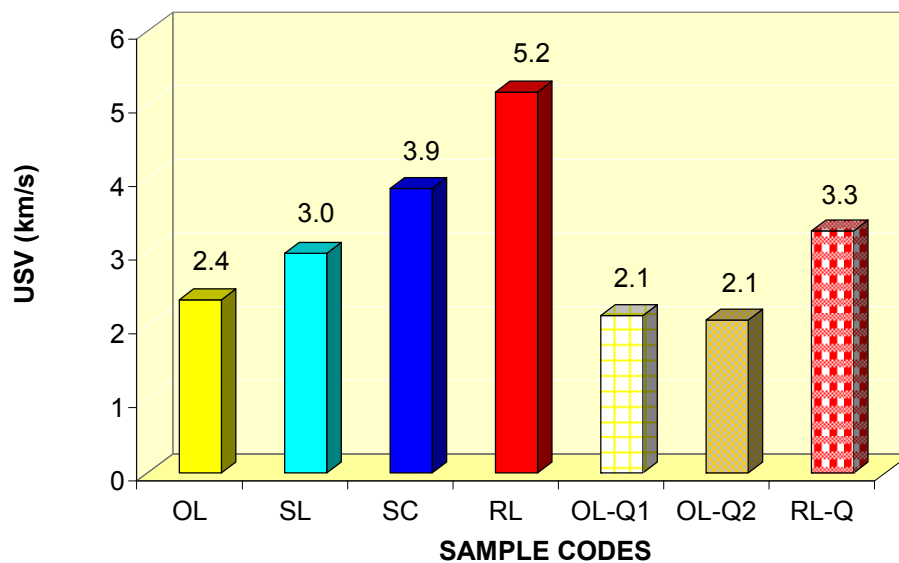


**Fig. 6-45: Average values for the ultrasound pulse velocity measured for both the historical (OL, SL, SC and RL) and the freshly quarried samples (OL-Q1, OL-Q2 and RL-Q) - see Table 4-2, p. 16 for abbreviations**

In Fig. 6-46, the average values for the ultrasound pulse velocity is shown for four different groups of specimens coming from the quarries divided based on their condition during the test: air dried as in Fig. 4-45 (six specimens), water saturated (six specimens), artificially weathered after eight freeze-thaw cycles and after twenty (six specimens for OL-Q2 and RL-Q and three for OL-Q1). The pulse velocity decreases over the artificial frost weathering in the case of OL-Q1 and OL-Q2 whereas it increases in the case of RL-Q.

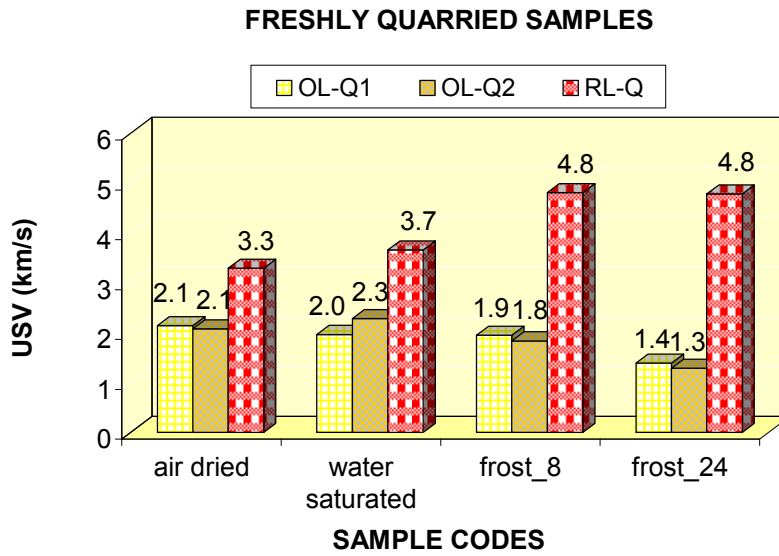


**Fig. 6-46: Average values for the ultrasound pulse velocity measured for four different groups of freshly quarried samples tested in different conditions: air dried, water saturated and artificially weathered by frost damage after eight and after twenty four cycles (see Table 4-2, p. 16 for abbreviations)**

For the same groups of specimens the values of the uniaxial compressive strength are presented in Fig. 6-47 & 48. The lowest strength values were measured for the OL and OL-Q1 and OL-Q2 and the highest ones for the RL and the RL-Q. Higher values are observed for the OL-Q than for the OL and for the RL-Q than the RL. During the artificial frost weathering (Fig. 6-48), a general decreasing trend is observed for the samples of OL-Q1 and OL-Q2 whereas the RL-Q shows higher strength after the completion of the test than at the beginning.

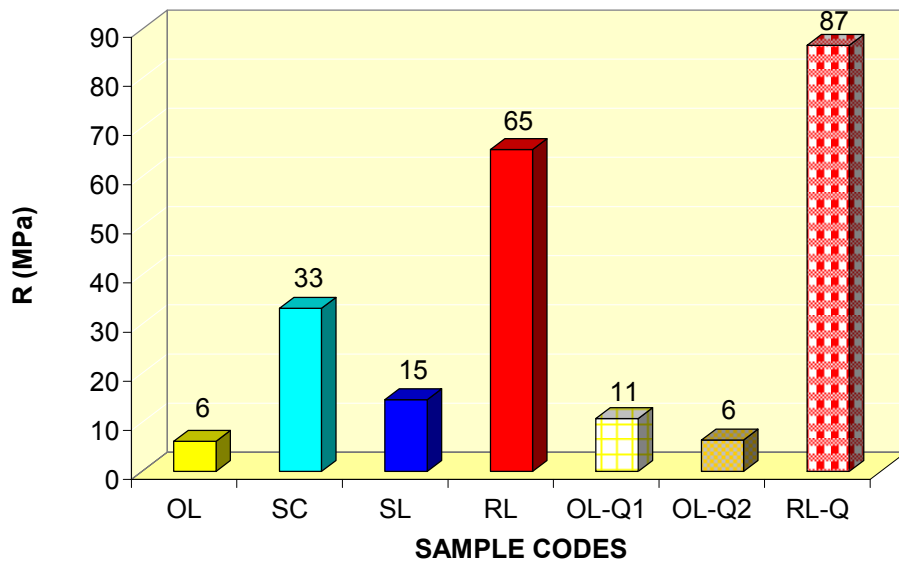


Fig. 6-47: Average values for the uniaxial compressive strength measured for both the historical (OL, SL, SC and RL) and the freshly quarried samples (OL-Q1, OL-Q2 and RL-Q - see Table 4-2, p. 16 for abbreviations)

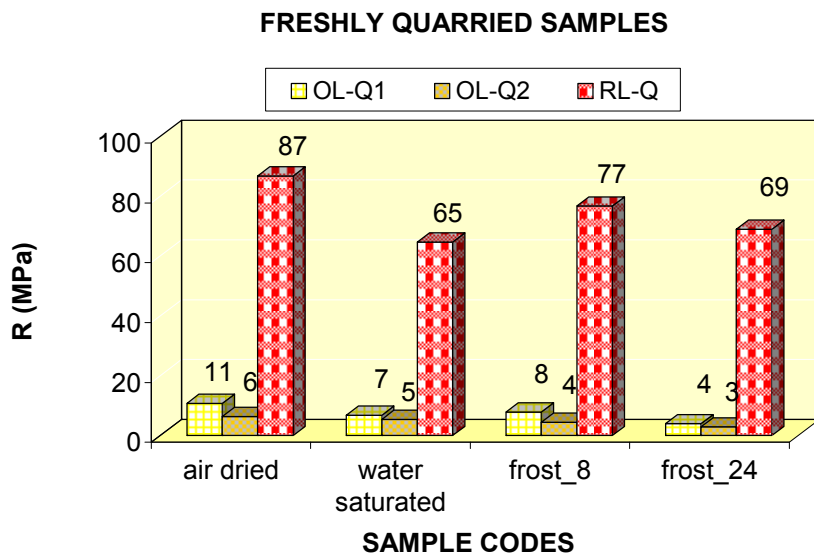
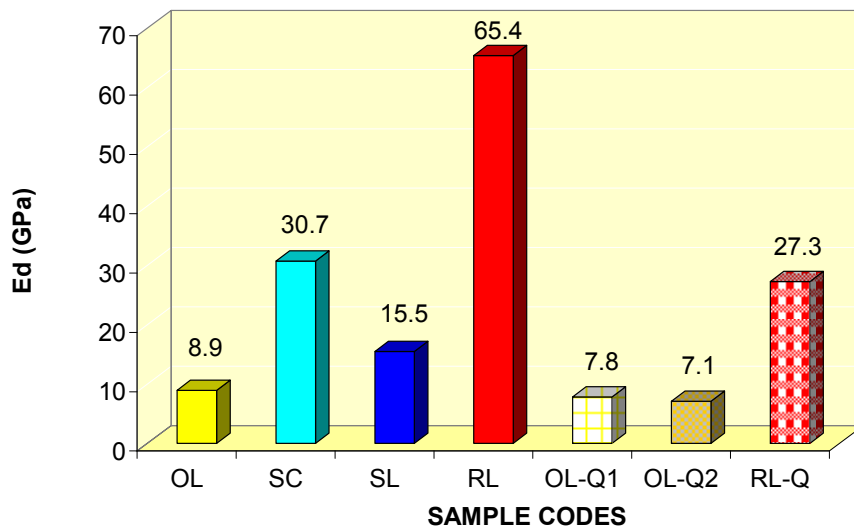


Fig. 6-48: Average values for the uniaxial compressive strength measured for four different groups of freshly quarried samples tested in different conditions: air dried, water saturated and artificially weathered by frost damage after eight and after twenty four cycles (see Table 4-2, p. 16 for abbreviations)



The dynamic modulus of elasticity was also calculated for the aforementioned groups of specimens (Figs. 6-49 & 50). The lowest values of elasticity belong to the OL, OL-Q1 and OL-Q2 and the highest to the RL and RL-Q.

Fig. 6-50 shows the different behaviour of the OL-Q1 and OL-Q2 in comparison with the one for RL-Q; for the first two lithotypes a decrease in elasticity values was recorded while the modulus of elasticity of the RL-Q was increased after the completion of the artificial frost weathering.



**Fig. 6-49: Average values for the dynamic modulus of elasticity measured for both the historical (OL, SL, SC and RL) and the freshly quarried samples (OL-Q1, OL-Q2 and RL-Q) - see Table 4-2, p. 16 for abbreviations**

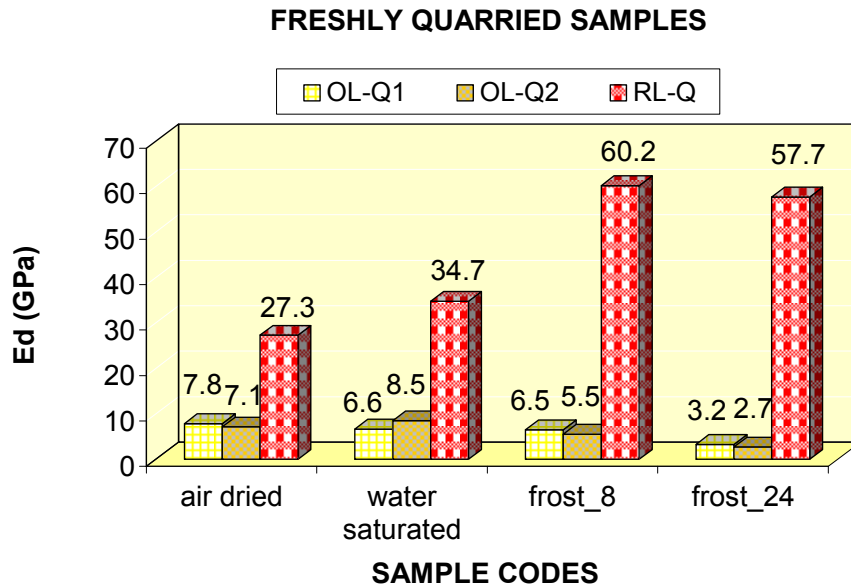


**Fig. 6-50: Average values for the dynamic modulus of elasticity measured for four different groups of freshly quarried samples tested in different conditions: air dried, water saturated and artificially weathered by frost damage after eight and after twenty four cycles (see Table 4-2, p. 16 for abbreviations)**

The changes in water saturated mass (Figs. 6-53 & 54) and ultrasound pulse velocity (Fig. 6-55) after each freeze thaw cycle are given for representative specimens of each lithotype. It should be clarified that the current interruptions before the completion of the twenty four cycles which are depicted in the graphs for the specimens 109 and 134 (OL-Q1), are due to their early failure. This early failure corresponds to score number 4 at the scale of visual inspection described by EN: 12371: 2001, which refers to a “specimen broken in two or with major cracks” (see Fig. 6-51 a & b). In the same scale, the specimens of the OL-Q2 scored number 2 (see Fig. 6-52 a & b) while RL-Q scored 0 (see Fig. 6-53 a and b). The description of the visual inspection is summarized in Table 6-9.

Lithotypes	score	description of score
OL-Q1	4	specimen broken in two or with major crack
OL-Q2	2	one or several minor cracks ( $\leq 0.1$ mm width) or detachment of small fragments ( $\leq 10$ mm <sup>2</sup> per fragment)
RL-Q	0	specimen intact

**Table 6-9: Visual inspection according to the scale of the EN 12371: 2001**

(see Table 4-2, p. 16 for abbreviations)

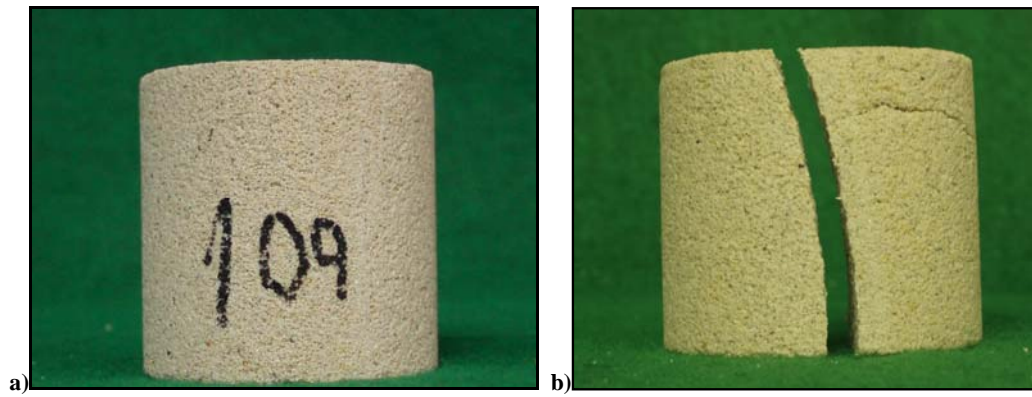


Fig. 6-51: specimen of OL-Q1 before and after eleven freeze-thaw cycles (see Table 4-2, p. 16 for abbreviations)

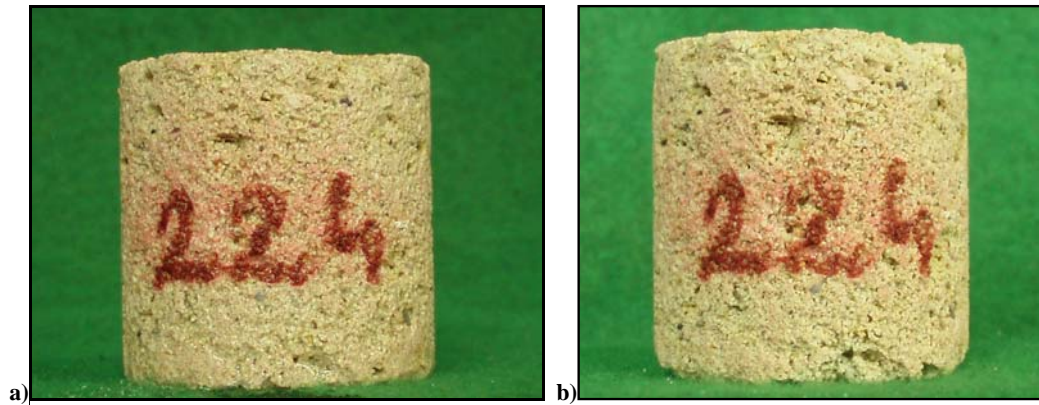


Fig. 6-52 a) and b): specimen of OL-Q2 before and after twenty four freeze-thaw cycles (see Table 4-2, p. 16 for abbreviations)

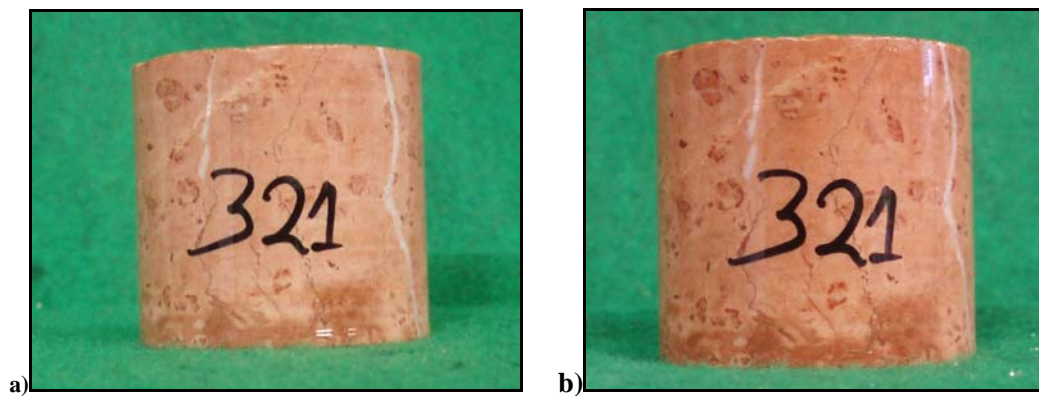
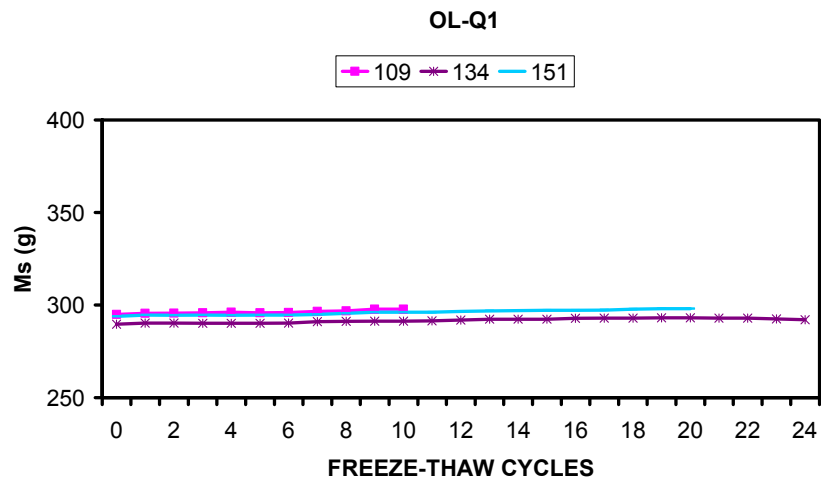
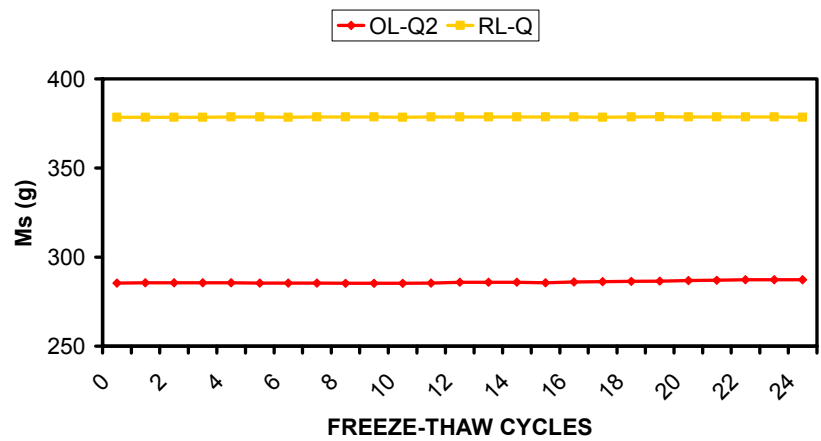


Fig. 6-53: specimen of RL-Q before and after twenty four freeze-thaw cycles (see Table 4-2, p. 16 for abbreviations)

The water saturated masses in air after each complete artificial freeze-thaw cycle is given for representative specimens which belong to the OL-Q1 in Fig. 6-54 and for OL-Q2 and RL-Q in Fig. 6-55. No remarkable differences are observed in terms of changes in water saturated mass.



**Fig. 6-54: Water saturated masses during the artificial frost weathering of selected specimens of freshly quarried medium-grained Oolitic Limestone (OL-Q1)**



**Fig. 6-55: Water saturated masses during the artificial frost weathering of representative specimens of freshly quarried coarse-grained Oolitic Limestone (OL-Q2) and Red Limestone (RL-Q)**

For the same representative samples the changes in ultrasound pulse velocity during the artificial frost weathering are depicted in Fig. 6-56. As it is clearly visible on the graphs, the pulse velocity is decreasing during the twenty four freeze cycles in the case of OL-Q1 and OL-Q2. It is also observed that after the completion of the test, the decrease is higher for the OL-Q2 for the specimens of OL-Q1 that could resist to the frost deterioration. The opposite trend is recorded in the case of RL-Q and the anodic profile shows the increase in pulse velocity during the test.

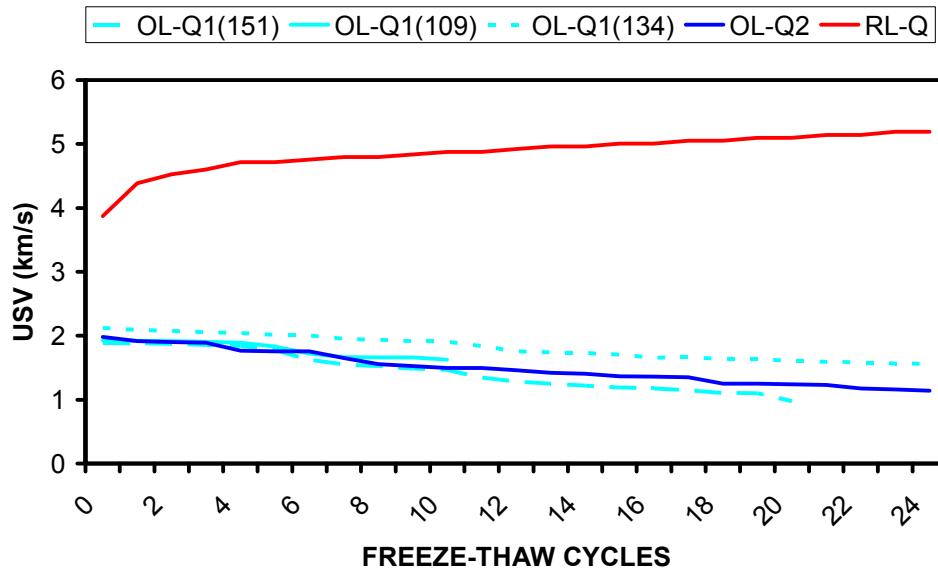


**Fig. 6-56: Profiles of the ultrasound pulse velocity for five representative specimens of the freshly quarried limestones (OL-Q1, OL-Q2 and RL-Q) during the artificial frost weathering (see Table 4-2, p. 16 for abbreviations)**

The average physical and mechanical properties of the four more important historical lithotypes (air dried) and the freshly quarries stones (air dried, water saturated, after eight and twenty four freeze-thaw cycles) are gathered in Table 6-10.

Sample Codes	USV (km/s)	R (MPa)	Ed (GPa)
OL air dried	2.4	6	8.9
SC air dried	3.9	33	30.7
SL air dried	3.0	15	15.5
RL air dried	5.2	65	65.4
OL-Q1 air dried	2.1	11	7.8
OL-Q1 saturated	2.0	7	6.6
OL-Q1 frost 8 cycles	1.9	8	6.5
OL-Q1 frost 24 cycles	1.4	4	3.2
OL-Q2 air dried	2.1	6	7.1
OL-Q2 saturated	2.3	5	8.5
OL-Q2 frost 8 cycles	1.8	4	5.5
OL-Q2 frost 24 cycles	1.3	3	2.7
RL-Q air dried	3.3	87	27.3
RL-Q saturated	3.7	65	34.7
RL-Q frost 8 cycles	4.8	77	60.2
RL-Q frost 24 cycles	4.8	69	57.7

**Table 6-10: Average physical and mechanical properties of both historical and freshly quarried specimens tested in different conditions (see Table 4-2, p. 16 for abbreviations)**

### 6.2.7. Dynamic Mechanical Analyser

Fig. 6-57 shows the changes in length and temperature of RL-Q by cooling measured by a dynamical mechanical analyser. Observing the results, there is no measured expansion of the tested material by cooling up to approximately 30 °C. On the contrary, the depicted sample just contracts while the temperature decreases.

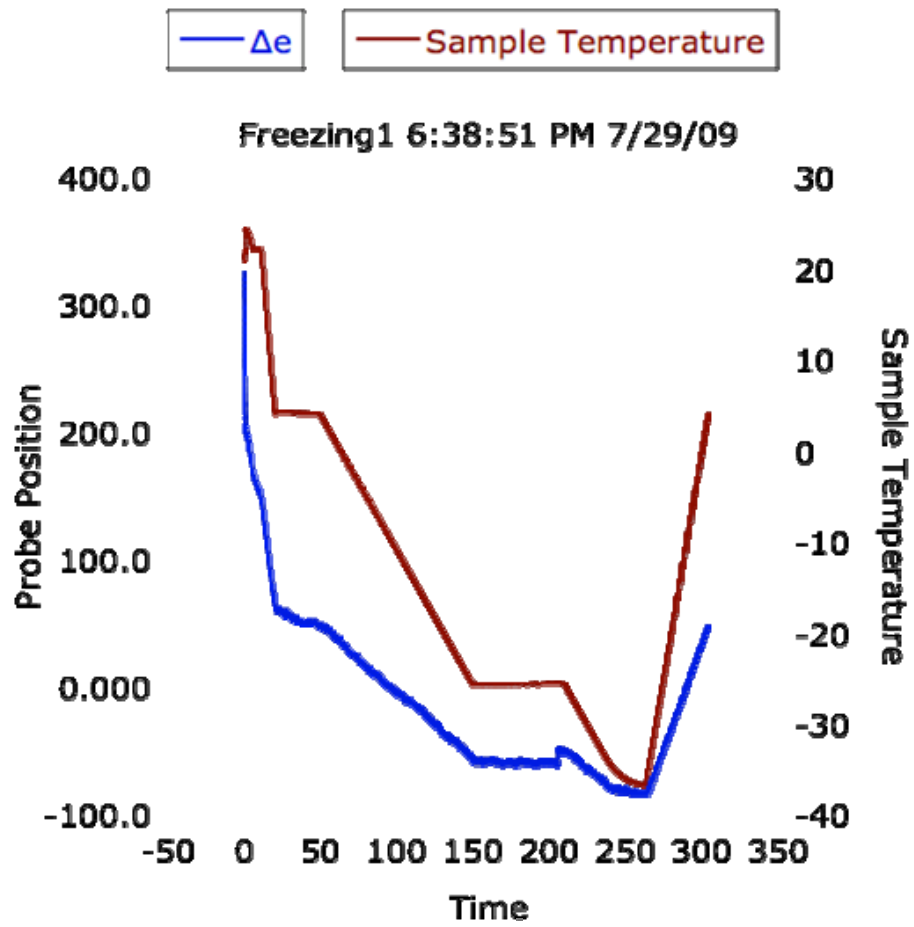


Fig. 6-57: Changes in length and temperature of the freshly quarried Red Limestone (RL-Q)



## 7. DISCUSSION

---

Limestone is the most common building stone of the historic structures at Székesfehérvár Ruin Garden. From a variety of limestone lithotypes the Oolitic Limestone (OL) is the prevailing one (Table 6-2), while the use of other types such as Shelly Limestone (SL) and Red Limestone (RL) is also remarkable (Table 6-2). Additionally, several blocks of other lithologies such as Sandy Calcarene (SC), Rhyolite (Rh), Marble (M), Travertine (T) and other types of Fossiliferous Limestones (FL) have been also identified (Table 6-2). In terms of the use of stone materials, there is a clear distinction between construction periods. OL was used throughout the entire history of the construction (Figs. 6-2, 5, 8, 11 & 14), while RL appears only in the reconstruction period, that took place in the 12<sup>th</sup> century (Fig. 6-8). This observation is in good correlation with the previous findings (Kertész & Szabó-Balog 1988), since the use of RL in Hungarian monuments dated back to 12<sup>th</sup> – 18<sup>th</sup> centuries was relatively common (Pintér et al. 2004, Török 2007a). The RL which is analogous to Italian Rosso di Ammonitico was a popular dimension stone not only in Hungary, but throughout the Mediterranean Basin (Lazarini 2004). In Central Europe, quarries of red limestones are known not only from Hungary, but also from Austria (eg. Adnet) and from Romania (Pintér et al. 2004). The oolitic limestone (OL) or better to define as porous limestone is also widespread in other monuments in Hungary (Kertész 1982). The so-called Leitha Limestone, which is a Miocene porous limestone type, is known from Austria, Czech Republic and Hungary (Török et al. 2004). In Hungary several porous limestone lithotypes are known and historic quarries that could have provided the stone for Székesfehérvár can be found in the vicinity (Öskü) or a distance of few tens of kilometres from the Ruin Garden (Budapest, or Fertőrákos) (Török 2004). Petrographic description of samples provide useful information on the possible source quarry (Prikryl 2007) but due to the significant variations in depositional environments and lithologies in a quarry scale it is often very difficult to identify the provenance area of this porous limestones (Török 2004). Nevertheless based on micro-fabric analyses it is very probable that oolitic limestone (OL), which was used at Székesfehérvár, was quarried in Budapest region (probably at Sósút area), while shelly limestone (SL) and sandy calcarenite (SC) is from Öskü area. At the latter locality, no more active quarries exist and the former ones are abandoned and often difficult to identify, which hampers the provenance analyses. The provenance of the other stones used at Székesfehérvár is very likely

to be found in the present territory of Hungary, with one exception, which is marble. The travertine is from the North, from Süttő area (see Kertész 1982, Török 2007a) and the red limestone is from Tardos (Kertész 1982, Pintér et al. 2004). The rhyolite (RH) is most likely from the nearby igneous area of Velence Mountains, but at present, no similar volcanic stones are exposed in quarries. The marble (M) is very probably coming from other territories than present day Hungary, but further studies such as geochemical analyses would be needed to find the source area.

The long-term behaviour of stone structures depends on the durability of the stone (Macmillan 1967, Kieslinger 1968, Richardson 1991, Ordóñez et al. 1997) and on the environmental conditions. When various lithotypes of the studied Ruin Garden are compared it seems that Oolitic Limestone (OL), which is the most common one is less durable, than other lithologies at the site. Based on the in-situ observation OL display various forms of decay such as cracks, crumbling, granular disintegration, multiple scaling and flaking, black and white crust and biological colonization (Figs. 6-3, 6, 9, 12 & 15). The Bioclastic Limestone also shows decay forms such as micro-cracks, crumbling, rounded surface, black crust and in the case of blocks totally exposed to the exterior environment (Fig. 6-6) biological colonization is also observed. The same forms of biological colonization are observed on the blocks of Travertine, which is exposed to the outdoor environmental conditions in addition with cracks and micro-karstification (Fig. 6-12). Biological colonization is not restricted to outdoor environments. At the roof covered parts of the ruin green patches of microbial mats were observed (Figs. 6-3, 9 & 12). It is especially intense at low-lying blocks and in the joints, suggesting that capillary water rise of groundwater provides moisture for biological activity. A clear dependence on the substrate was also noticed, since porous stone types such as OL is preferentially covered while lower porosity stones such as travertine (T) or rhyolite (Rh) show far less intense biological colonisation (Figs. 6-9 & 12). Among the different types of limestones, the Red Limestone appears to be the most durable one since only minor alterations were observed, such as decolourization of the surface (Fig. 6-9). In some cases, when the granitic blocks are found uncovered and exposed, cracks and multiple flaking develops even on these durable stones (Fig. 6-6). Rhyolite (Rh) seems to be also relatively resistant to decay since besides a few micro-cracks no major decay forms were observed at blocks (Fig. 6-9). Former studies on most of the aforementioned local stones show similar behaviour of the materials used in historical

structures found in other locations of the country (Kertész 1988, Török 2003, 2006, 2007b, Török et al. 2007b).

The stone decay and especially the deterioration of limestone monuments is a commonly reported phenomenon from other countries, too. It is caused either by environmental conditions such as freeze-thaw or thermal stresses or by pollution plumes. The air pollution related soiling have been reported from cities with heavy traffic load such as Athens (Moropoulou et al. 1998), London (Trudgill et al. 1991, Bonazza et al. 2007) or Budapest (Török 2002). Exposed limestone facades located in smaller urban areas with heavy pollution fluxes also show intense blackening in cities such as Venice (Amoroso & Fassina 1984, Sabbioni 1995), Oxford (Viles 1993, Smith & Viles 2006). At Székesfehérvár the local transport related pollution is less intense and the Ruin Garden is located in a pedestrian area, therefore gypsum-rich black crust formation is subordinate. The major decay processes are related to climatic conditions. The annual 70-75 freeze-thaw cycles are responsible for the granular disintegration of porous limestones (OL) as well as for scaling and flaking. Similar processes of porous limestone decay and frost damages were also reported from Budapest (Török 2003). Micro-cracks and micro-fractures observed on other lithologies are also related to freeze-thaw. Therefore the planned new roof could be beneficial in terms of regulating climatic conditions and reducing frost damage at the Ruin Garden. Salt-related decay, which is common in maritime environments are not observed under the continental climate of Székesfehérvár. The use of de-icing salts is not a common practice at the monument, therefore minor salt efflorescence observed at some blocks are very probably related to the use of cement mortar as repair materials in the 60's.

As it well known, the characterization of strength parameters is very important for understanding the behaviour of stone materials and for the judgement of long-term durability of stone structures. For the determination of strength parameters both in-situ and laboratory methods are known. For many of the laboratory strength tests such as uniaxial compressive strength determination, high amount of samples are needed and the use of this destructive techniques are very often not allowed at heritage sites due to limitations of sampling. Therefore non-destructive or micro-destructive techniques are preferentially used at monuments. Among others in-situ micro-drilling resistance and Schmidt hammer tests were used at székesfehérvár in order to detect the strength parameters of historically used stones. Several published studies in the past have shown that a good estimation of the strength

properties is possible by the application of these techniques e.g. by, Exadaktylos et al. 2000, Tiano et al. 2000b, Delgado Rodrigues et al. 2002, Pamplona et al. 2008 compared micro-drilling resistance with strength. Christaras 1996, Kahraman 2001, Török 2004 used the Schmidt hammer to estimate rock strength. Moreover, the aforementioned techniques have been applied for the evaluation of the weathering processes and for the judgement of the efficacy of consolidation treatments of monumental stones (e.g. Christaras 1991, Tiano et al. 2000a, Török 2003, Ferreira Pinto & Delgado Rodrigues 2008).

In the current research, the average demanded drilling forces gave a good estimation of the strength parameters of the tested materials. The drilling profiles correspond to the micro-fabric of the materials close to the surface e.g. higher heterogeneity for the Sandy Calcarenite due to the presence of grains in comparison with the compact Red Limestone (Fig. 6-26). Moreover, the results achieved by in-situ measurements depict the occurring weathering phenomena such as the presence of crust on the surface of Oolitic Limestone by showing higher drilling resistance on the top-most millimetre. At greater depth the samples showed lower values (Fig. 6-25, 26 & 28). The total evaluation of our results is in agreement with the aforementioned published studies related to the application of this method.

Drawbacks of the micro-drilling technique have been already mentioned together with relevant suggested solutions such as the influence of using different drill bits in-situ (Tiano et al. 2000b, Pamplona et al. 2007), the dust accumulation during drilling (Mimoso & Costa 2006), the virtual increase of drilling resistance in case of abrasive stones (Pfefferkorn 2000, Singer et al. 2000, Delgado Rodrigues 2004) and the problem in drilling hard materials due to the limitation of the drilling system (maximum measurable drilling force equal to 100N). The latter problem was faced in this current study since micro-drilling of Rhyolite (Fig. 6-28) and in some cases of Red Limestone was impossible. However, possible solutions to this issue have been already published by Mimoso & Costa 2008 and Pamplona et al. in 2008. Finally, during the evaluation of the technique it should be always taken into account the fact that the applied tool only provided data for the top most 10 mm which does not detect deep weathering profiles.

Regarding the Schmidt hammer application (Figs. 6-21, 22, 23, 24 & 25), the results contributed to a quick and non-destructive estimation of the materials strength properties. Furthermore, weathering of the materials surfaces could be detected by the changes in surface

strengths measured by the method as for instance the increase in surface strength due to the formation of weathering crusts. This decay pattern of Oolitic Limestone was also recorded in previous studies (Török 2003). It should be also clarified that despite the fact that the technique is considered a non-destructive one, small impound marks are the result on the surface of tested stones. Hence, the application of the test was avoided on deeply weathered stone blocks.

The moisture content of the stone blocks in-situ is one of the most crucial factors for the long-term behaviour of stones (Török 2009). Several methods are known for measuring this value such as conductometry and thermographic imagery (Meinhardt-Degen et al. 2008), field dielectrometry and unilateral nuclear magnetic resonance (Olmi et al. 2008). However, the high costs of applying some of the aforementioned techniques in-situ might be an obstacle. In our case, the Gann Hydromette Uni was used, which despite the fact that it gives only relative and not absolute values, it can give a profile of the different values in different measured points. The achieved measurements (Figs. 6-21, 22, 23, 24 & 25) presented a good indicator of the influence of climatic conditions for each block e.g. higher moisture content values for the same lithotype in case of blocks located closer to the ground or in areas that are constantly in shadow. Many of the measured points with higher moisture content values have already presented salt efflorescence and/or biological colonization. Therefore, the use of this low-cost technique can contribute significantly to the identification of endangered zones.

Mineralogical analyses have shown that the purest limestone is the Red Limestone with minor amount of impurities. On the contrary, the Oolitic Limestone contains detectable amount of quartz, mica and clay minerals but not in equal quantities in medium and coarse-grained varieties. These small differences in mineralogical composition influence less the durability than the physical parameters such as porosity, pore-size distribution and strength.

SEM analyses confirmed that due to weathering not only dissolution but also the precipitation of secondary calcite occur in porous Oolitic Limestone (Fig. 6-32).

Fabric and texture of rock materials are related to their physical and mechanical properties (Montoto 1978). Among the different rock components, voids have the clearest influence on the physical properties of rocks. This is explained by the double function of the voids, which not only affect the mechanical behaviour due to the absence of solid but is directly connected

with the water content capacity of the rock and the water pathways in the rock matrix. Therefore, the void space is one of the most crucial parts of any petrophysical study (Mondoto 2004). The durability of a material often depends on water circulation inside porous solids (Charola & Lazzarini 1986, Kowalski 1975, Winkler 1997, Scherer et al., 2001). As a consequence, the interpretation of the results achieved by hydric tests is of a high importance. MIP and water absorption tests are based on the intrusion of liquids into the microstructure, which ultimately relates the results to the connectivity of the pore system and its access to the external surfaces (Cnudde 2009).

The analytical investigations related to the porosity of the four more important lithotypes from the monuments and the three freshly quarried lithotypes showed in all cases higher percentages for the OL, OL-Q1 and OL-Q2 which are approximately 30%, relatively high for the SL, almost half for the SC in comparison with the OL and less than 1% for the RL and RL-Q (Tables 6-4, 5, 6 & 7 and Fig. 6-41). This is in complete accordance with the observed characteristics of the materials texture and their calculated density (Fig. 6-33). Almost equal values are observed for the two different types of Oolitic Limestones coming from the quarries: OL-Q1 and OL-Q2. Slight differences in the pore volumes were identified between the historical and the fresh specimens with similar characteristics (OL and OL-Q1, RL and RL-Q) with the fresh ones having lower values with a difference of less than 1%. Good correlation is observed among the porosimetric results achieved by different methods which it self suggests that methods with much lower costs, such as the calculation of the open porosity by vacuum assisted water absorption can give a good estimation of the materials pore volume. Similar methods have been used for estimating the open porosity of various building materials, such as natural and artificial stones. These techniques were applied in order to check the compatibility (Papayianni et al. 2008), the behaviour of natural stone in artificial weathering processes (Stefanidou & Papayianni 2008), the correlation of strength with porosity in lime-pozzolan mortars (Papayianni & Stefanidou 2006) and the role of aggregate on the structure and properties of lime mortars (Papayianni & Stefanidou 2005).

Looking in the pore distribution of both the historical and the fresh lithotypes, all of the types show low relative volumes in the range of micropores (pore's diameter  $<0.0074\ \mu\text{m}$  as defined by Barsottelli et al. 1998) that could be identified by nitrogen adsorption. The highest volume for all the lithotypes is accumulated in the range of  $0.02$  to  $0.2\ \mu\text{m}$  pore diameter, which is the highest one measured by this method. The comparison of the OL with the OL-Q1

and the RL with the RL-Q confirms the lower pore volumes measured in the case of the freshly quarried stones. (Fig. 6-36)

The distribution of the mesopores (0.0074-300  $\mu\text{m}$  diameter), defined by the MIP is similar for the OL, SL, SC, OL-Q1 and OL-Q2 in the sense of showing the main relative volume of pore space in the highest range measured by this method, whereas the results for the RL and the RL-Q show an additional volume accumulated in the range of smaller mesopores. (Figs. 6-37, 38, 39 & 40)

Regarding the two methods that have been used for the characterization of the pore size distribution, important notes have to be taken always into account. One of the main assumptions in BET theory is that the surface of a particle is covered by a multilayer of multimolecular thickness of adsorbent due to vapour tension and that all the adsorption sites are identical in terms of energy without any lateral interaction between adjacent molecules (Beck et al. 2003). Sing (2001) concluded that nitrogen adsorption can be used as the first stage in the characterization of microporous and mesoporous solids but it should be expected to give only a semi-quantitative evaluation of the pore size distribution of micropores. A very important and well known aspect of MIP has to be repeated at this point highlighting one of the major drawbacks of the method. MIP misrepresents the size of these pores as having the diameter of their throats. This bias is referred to as the “ink bottle” effect and it results to an increase in the volume of the small pores against the large pores consequently, the distribution is shifted to the small pores. This phenomenon has been described by many authors (Renault 1988, Abell et al. 1999, Fitzner 1999, Rouquerol et al. 1999). MIP cannot provide information on closed pores, nor can it give detailed information on pore connectivity (Cnudde et al. 2009). However, both techniques give useful information for the characterisation of porous media but good understanding of their limits and their use is crucial (Roels et al. 2001, Benavente et al. 2004).

The water absorption by capillarity was very rapid fast for the two porous Oolitic Limestones being slightly faster for OL-Q2 slightly faster than for OL-Q1 (Fig. 6-42). Taking into account the aforementioned results for the measured void volumes of the two lithotypes which are almost equal in terms of total porosity and total open porosity, the only difference, which might be connected to this phenomenon is related to pore structure identified by MIP; the OL-Q2 has about 5% higher relative volume in the range of 128 to 256  $\mu\text{m}$  pore diameter

than the OL-Q1, but about 10% in the range of 64 to 128  $\mu\text{m}$ . In total, the mesoporosity of the OL-Q2 is about 5% lower than the one of OL-Q1. (Figs. 6-39 & 41). No similar difference was observed in the behaviour of the two oolitic limestones during the determination of water absorption at atmospheric pressure (Fig. 6-43) but these differences might reflect the variations in the durability of the two lithotypes under artificial weathering (Figs. 6-51 & 52).

The totally different behaviour of the RL-Q became obvious already by the accomplishment of the hydric tests where no remarkable water absorption by capillary imbibition was observed and the percentages of the void spaces accessible by water or mercury are significantly lower than the ones for OL-Q1 and OL-Q2 (Fig. 6-43).

For the former one (RL-Q) the smaller intergranular pores are related to clayey stylolitic seams (Gómez-Heras et al. 2006).

Referring to the pulse velocity (USV) (Figs. 6-45 & 46), dynamic modulus of elasticity (Ed) (Figs. 6-49 & 50) and uniaxial compressive strength (UCS) (Figs. 6-47 & 48) measured under laboratory conditions, the more porous the material is, the higher values of USV and Ed and lower of UCS are observed. Therefore, the different behaviour between the OL-Q1 & OL-Q2 and the RL-Q is clear as expected by the interpretation of the porosity values. Moreover, the difference between the OL-Q1 and OL-Q2 is highlighted in a better way with the latter performing lower strength values despite the fact of having similar mineralogical composition and void space volume. It should be also mentioned that the UCS for the lithotypes coming from the monument, OL & RL, in comparison with their similar lithotypes coming from the quarries, OL-Q1 & RL-Q respectively, is lower (Fig. 6-47), suggesting the influence of the weathering to their mechanical properties. In addition, the UCS of the lithotypes measured under laboratory conditions (Fig. 6-47) is in complete accordance with the Schmidt Hammer values (e.g. Fig. 6-18) and the average micro-drilling forces of the similar lithotypes measured in-situ (Figs. 6-23 & 24).

The simulation of frost damage under laboratory conditions supports the higher durability of RL-Q in comparison with the OL-Q1 and OL-Q2. Regarding the OL-Q1 and OL-Q2, a markedly different behaviour was recorded. Although the OL-Q1 had higher UCS values comparing to the OL-Q2 (Fig. 6-48), the first one showed much earlier and more severe failure than the latter presenting major cracks and in some cases being broken into two or



more pieces already after the completion of the eleventh freeze-thaw cycle (Figs. 6-51, 52). Moreover, only the one fourth of the total number of specimens reached the end of the twenty fourth cycle without failing while all of the specimens belonging to the OL-Q2 and RL-Q did.

One of the most outstanding results that came out from the durability test was the increase of USV and UCS for the RL-Q after the completion of the test (Figs. 6-46, 48). Former studies indicated the possibility of having contraction of a material during freeze-thaw cycles despite the 9% expansion in volume of water due to its transformation to ice (Powers & Helmuth 1953, Prick et al. 1993, Prick 1995), which could be only related to the migration of unfrozen water within the pores of the material. To verify that this could be the case of the RL-Q, specimens were submitted to the DMA. Indeed, by cooling even up to about -30°C there was no measured expansion. An expansion would be the result that water freezes and ice exert a pressure on the pore wall that can break the stone. However, the specimen of the RL-Q just contracted by cooling (Fig. 6-57). This can explain why the elastic modulus did not decrease after each freeze-thaw cycle however it cannot explain why it increased.

Due to the limited specimens that were subjected to the test, we can only assume that no frost damage is expected for this lithotype (Red Limestone). The effect can be contributed to the migration of the water from the water-saturated pores to air voids (empty pores) that are presented in the material. Consequently, the hydraulic pressure is negligible and so was the expansion. However, we cannot declare that there is an additional significant contraction that “protects” the stone, which would explain the increase of the modulus. This contraction would result from "entropic" effects when ice forms in the large pores and sucks water from the small pores. Therefore, further testing and analysis is crucial and expected in the future.

The evaluation of the effects of the artificial frost weathering, taking into account the weathering forms which were observed on the historical materials in-situ, indicates that the laboratory test is much more aggressive causing more severe and/or faster damages on the stone materials. This can be attributed to many reasons, which are the evidence for the differences between the real conditions and the ones held in the laboratory. First of all, before the beginning of the test and during thawing, the specimens were fully immersed in water which resulted to much higher water content than the one that a block of stone might reach due to the environmental conditions. Furthermore, the size of the laboratory specimens is much smaller than a common building stone found in historical constructions. Also, the

micro-environmental conditions in the monument might differ from one point to another, while in the laboratory the conditions around the surfaces of the same specimen are identical. Therefore, it is obvious that the results of the artificial weathering test are not reliable in terms of estimating the reality. However, the correct interpretation of them can provide very important dataset related to the long-term behaviour of the materials which is crucial in conducting guidelines for conservation.

## 8. CONCLUSIONS

---

The use of several lithotypes such as different kinds of limestone, rhyolite and granite, was identified in the Ruin Garden of Székesfehérvár throughout its several construction periods between the 11<sup>th</sup> and the 15<sup>th</sup> century. Few blocks of other lithotypes whose origin is most probably out of the borders of the Carpathian Basin such as marble were also found. Oolitic Limestone is the prevailing type among the different types of limestones used in the several construction periods of the monument which is in accordance with its generally wide use in historic constructions. Moreover, the Red Limestone which was found in the part that was constructed in the 12<sup>th</sup> century and its very similar to the Italian Rosso di Ammonitico is another popular dimension stone in monumental constructions. Both of the aforementioned materials can be found in Hungarian quarries, which are very close to the location of the studied site such as the quarry in Sóskút which provides Oolitic Limestone and the quarry in Tardos for the Red Limestone.

In-situ observations suggest that Ooolitic Limestone suffers the most in terms of weathering since several decay patterns were identified such as black crust, scaling, crumbling, flaking, granular disintegration, rounded surfaces and biological colonization. Whereas Red Limestone seems to be relatively durable with decolourization of the surface being its main observed weathering form. This is in accordance with the results of the in-situ measurements by means of Schmidt hammer and micro-drilling. Moisture content measurements proves the influence of micro-environmental conditions on the stones seeing that higher values coincide with more intense decay forms as for instance in the case of biological colonization.

The porosimetric study of more important materials highlighted the differences in pore structures. Oolitic Limestone showed the highest value of void space and the Red Limestone the lowest one. In terms of their pore-size distribution, a further difference was noticed; the main volume of identified mesopores of the Oolitic Limestone was accumulated in the range of “larger” pores measured by MIP while the Red Limestone presented two main volumes, one in the range of “large” pores and one in the “smaller” ones.

High uniaxial compressive strength, ultrasonic pulse velocity and modulus of elasticity values were measured for the Red Limestone in comparison with ones for the Oolitic Limestone.

Among the two Oolitic Limestones coming from the quarry, the medium-grained had higher values than the coarse-grained one. This is not in accordance with the results related to the durability of the stones determined by means of artificial frost weathering since the medium-grained one deteriorated much earlier and in a more severe way than the coarse-grained one. Therefore, the initial aforementioned values are not necessarily considered as good indicators of durability. Red Limestone showed minor increases in values of both strength and pulse velocity when water saturated and freeze-thaw treated samples were compared. Indeed, dynamic mechanical analysis proved that this type of stone is only contracts by cooling even up to -30 °C, which is most probably related to the migration of unfrozen water within the pores of the material. However, further investigation is needed to fully understand the behaviour of this material.

A comparison between the effects of artificial frost weathering in the laboratory and the weathering state of the historical materials in-situ indicates the problem in terms of how reliable the laboratory results are when durability under natural conditions is assessed, since the artificial weathering has a more dramatic effect. This can be attributed to the different water content of the materials in the two cases and the different micro-environmental conditions. However, the proper interpretation of the results can be very important in giving information about the long-term behaviour of the tested materials.

In general, good correlation was observed between the in-situ and under laboratory measurements which suggests the importance of the application of in-situ measurements especially in the case of structures of a historical importance where sampling is limited.

Regarding the importance of the current research in terms of the conservation of the studied site, these in-situ and laboratory tests provide an overview of the present state of the stones of the Ruin Garden prior to the construction of a new roof system. The results will serve as a database for the future comparison of long term behaviour of stones before and after the planned reconstruction of the entire area.

## 9. REFERENCES

---

- Abell A. B., Willis K. L. & Lange D. A. 1999. Mercury intrusion porosimetry and image analysis of cement-based materials. *Journal of Colloid and Interface Science*, 211, pp. 39-44
- Altmann J., Biczó P., Buzás G., Horváth I., Kovács A., Siklósi G. & Végh A. 1996, in English 1999. *Medium Regni. Nap Kiadó, Budapest*, 212p
- Amoroso G.G., Fassina V. 1983. *Stone Decay and Conservation*. Elsevier, Amsterdam, pp. 1-453
- ASTM C597 2004. Standard test method for pulse velocity through concrete. Annual book for ASTM Standards, Vol. 04.02, American Society for Testing and Materials, West Conshohocken
- Barsottelli M., Cellai G. F., Fratini F. & Manganelli Del Fà C. 2001. The hygrometric behaviour of some artificial stone materials. *Materials and Structures*, 34, pp. 211-216
- Barsottelli M., Fratini F., Giorgetti G. & Manganelli Del Fà C. M. 1998. Microfabric and alteration in the Carrara marble: a preliminary study. *Science and Technology for Cultural Heritage*, 7, 2, pp. 109-120
- Barton N. & Choubey V., 1977. The shear strength of rock joints in theory and practice. *Rock Mechanics and Rock Engineering*, 10, pp. 1-54
- Bartos G., Biczó P., Buzás G., Lővei P., Mentényi K. & Tóth M. 2004. *The provostry and church of the Virgin Mary. King St. Stephen Museum, Székesfehérvár*, 44p.
- Beaudoin J. J. 1979. Porosity measurement of some hydrated cementitious systems by high pressure mercury intrusion: Microstructural limitations. *Cement and Concrete Research*, 9, pp. 771-781
- Beck K., Al-Mukhtar M., Rozenbaum O., Rautureau M. 2003. Characterization, water transfer properties and deterioration in tuffeau building material in the Loire valley – France. *Building and Environment*, 38, pp. 1151 – 1162

- Bell F. G. 1993. Durability of carbonate rock as a building stone with comments on its preservation. *Environmental Geology*, 21, pp. 187-200
- Benavente D, García del Cura M. A., Fort R., Ordóñez S. 2004. Durability estimation of porous building stones from pore structure and strength. *Engineering Geology*, 74, pp. 113-127
- Biczó P. 2005. Székesfehérvár. Nemzeti Emlékhely I–II. [The Székesfehérvár National Monument I-II]. *Tájak–Korok–Múzeumok Kiskönyvtára* 309–310, szám. TKM Egyesület (in Hungarian)
- Bonazza A, Brimblecombe P., Grossi C., Sabbioni C. 2007. Carbon in Black Crusts from the Tower of London. *Environmental Science and Technology* 41, 12, pp. 4199-4204
- Charola A.E., Lazzarini L. 1986. Material degradation caused by acid rain. In: Baboian R. (Ed.) *ACS Symposium Series n. 318*. American Chemical Society, Washington, pp. 250–258
- Chrastaras B. 1991. Durability of building stones and weathering of antiquities in Crete/Greece. *Bulletin of the International Association of Engineering Geology*, 44, pp. 17-25
- Chrastaras B. 1996. Non destructive methods for investigation of some mechanical properties of natural stones in the protection of monuments. *Bulletin of the International Association of Engineering Geology*, 54, pp. 59-63
- Cnudde V., Cwirzen A., Masschaele B., Jacobs P.J.S. 2009. Porosity and microstructure characterization of building stones and concretes. *Engineering Geology*, 103, pp. 76–83
- Csorba C., Estók J & Salamon K. 2005. *Illustrated History of Hungary*. Helikon Kiadó, Budapest, 254p
- Delgado Rodrigues J., Costa D. 2004. A new method for data correction in drilling resistance. Tests for the effect of drill bit wear. *International Journal for Restoration of Buildings and Monuments*, 10, pp. 1-18
- Delgado Rodrigues J., Ferreira Pinto A., Rodrigues da Costa D. 2002. Tracing of decay profiles and evaluation of stone treatments by means of microdrilling techniques. *Journal of Cultural Heritage*, 3, pp. 117-125

Dercsényi D. 1943. A székesfehérvári királyi bazilika. Magyarország művészeti emlékei I. [The Székesfehérvár Royal Basilica. In: Relics of art in Hungary I.]. Műemlékek Országos Bizottsága, Budapest (in Hungarian)

EN 12371: 2001. Natural stone methods. Determination of frost resistance. European Committee for Standardization, Brussels

EN 12407: 2000. Natural stone test methods – Petrographic examination. European Committee for Standardization, Brussels

EN 13755: 2001. Natural stone test methods. Determination of water absorption at atmospheric pressure. European Committee for Standardization, Brussels

EN 14579: 2004. Natural stone test methods. Determination of sound speed propagation. European Committee for Standardization, Brussels

EN 1925: 1999. Natural stone test methods. Determination of water absorption coefficient by capillarity. European Committee for Standardization, Brussels

EN 1926: 2006. Natural stone methods. Determination of uniaxial compressive strength. European Committee for Standardization, Brussels

EN 1936: 2006. Natural stone test methods. Determination of real density and apparent density, and of total and open porosity. European Committee for Standardization, Brussels

Exadactylos G., Tiano P., Filareto C. 2000. Validation of a model of rotary drilling of Rocks with the drilling force measurement. International Journal for Restoration of Buildings and Monuments, 3, pp. 307-340

Ferreira Pinto A. P., Delgado Rodrigues J. 2008. Stone consolidation: The role of treatment procedures. Journal of Cultural Heritage, 9, pp. 38-53

Fitzner B. 1993. Porosity properties and weathering behavior of natural stones – methodology and examples. In: Proc. Second course on Stone material in monuments: diagnosis and conservation. Heraklion – Crete, pp. 45-53

Fitzner B. 1999. Porosity analysis - a method for the characterization of building stones in different weathering states. In: P.G. Marinos and G.C. Koukis, Eds., *Engineering Geology of Ancient Works, Monuments and Sites*, Balkema, Rotterdam, pp. 2031–2037

Fitzner B., Heinrichs K. & La Bouchardiere D. 2002. Damage index for stone monuments. In: Galan E. & Zezza F. (Eds.) *Protection and Conservation of the Cultural Heritage of the Mediterranean Cities*, Proceedings of the 5th International Symposium on the Conservation of Monuments in the Mediterranean Basin, Sevilla, Swets & Zeitlinger, Lisse, The Netherlands, pp. 315-326

Fitzner B., Heinrichs K. 2002. Damage diagnosis on stone monuments - weathering forms, damage categories and damage indices. In: Prikryl R. & Viles H. A. (Eds.): *Understanding and managing stone decay*, Proceeding of the International Conference Stone weathering and atmospheric pollution network (SWAPNET 2001), Charles University in Prague, The Karolinum Press, pp.11-56

Fitzner B., Heinrichs K., & Kownatzki R. 1997. Weathering forms at natural stone monuments - classification, mapping and evaluation.- *International Journal for Restoration of Buildings and Monuments*, Vol. 3, No. 2 pp. 105-124

Gómez-Heras M., Alvarez de Buergo M., Fort R., Hajpál M, Török Á., Varas M. J. 2006. Evolution of porosity in Hungarian building stones alter simulated burning. In: Fort, Alvarez de Buergo, Gómez-Heras & Vasquez-Calvo (Eds.) *Heritage, Weathering and Conservation*, Taylor & Francis Group, London, pp. 513-519

Hull A. W. 1919. A new method of chemical analysis. *Journal of the American Chemical Society*, 41 (8), pp. 1168-1175

ICOMOS-ISCS 2008. Illustrated glossary on stone deterioration patterns / Glossaire illustré sur les formes d'altération de la pierre. Vergès-Belmin V. (Ed.), Ateliers 30 Impression, Champigny/Marne, France, 78p.

Kahraman S. 2001. Evaluation of simple methods for assessing the uniaxial compressive strength of rock. *International Journal of Rock Mechanics and Mining Sciences*, 38, pp. 981-994



- Katz O., Reches Z. & Roegiers J. C. 2000. Evaluation of mechanical rock properties using a Schmidt hammer. *International Journal of Rock Mechanics and Mining Sciences*, 37, pp. 723-728
- Kertész P. 1982. A műemléki kőanyagok bányahelyeinek kutatása. Építés- és Építészettudomány (Research of mounumental stones and historic quarries), 1-2, pp. 193-228 (in Hungarian)
- Kertész P. 1988. Decay and conservation of Hungarian building stones. In: Marinos P.G. & Koukis G.C. (Eds.): *The Engineering Geology of Ancient Works, Monuments and Historical Sites*. IEAG Conference Proceedings, Athens, Vol. II, pp. 755-761, Rotterdam (Balkema)
- Kertész P., Szabó-Balog A. 1988. Provenance and petrographical problems of the building and ornamental stone materials of Hungarian Renaissance architecture. *Periodica Polytechnica*, 32, 3-4, pp. 169-193
- Kieslinger A. 1968. Les principaux facteurs des pierres à bâtir. *ICOMOS Monum.*, 11, pp. 61-65
- Kowalski W. C. 1975. L'influence des variations de teneur en eau sur la résistance mécanique et la déformation des roches dans la zone d'altération. *Bull. Assoc. Intern. Geol. Ingen.*, 12, pp. 37-43
- Lazzarini L. (Ed) 2004. *Pietre e Marmi Antichi*. CEDAM, Castenaso (Bologna)
- Lővei P., Farbaky P., Kelényi, Sisa J., Sabján T., Gerle J. & Ferkai A. 1998. Wiebenson N. & Sisa J. (Eds.): *The Architecture of Historic Hungary*. Massachusetts Institute of Technology, 328p
- Mamillan M. 1967. La gélivité des materiaux. *Suppl. Ann. Inst. Tech. Bâtiment Trav. Publics*, 6, pp. 1017-1024
- Maravelaki-Kalaitzaki P., Biscontin G. 1999. Origin, characteristics and morphology of weathering crusts on Istria stone in Venice. *Atmospheric Environment*, 33, pp. 1699-1709
- Maucha L., Sárváry I. 1998. A székesfehérvári romterület talajviz viszonyainak vizsgálata/A vizsintsüllyesztési terv kiértékelő bírálata. [Examinations concerning the soil water at the Székesfehérvár ruin garden/comments on the plans for decreasing the water table].

Manuscript, Vízgazdálkodási Tudományos Kutató Rt., Hidrológiai Intézet, Budapest (in Hungarian)

Meinhardt-Degen J., Franzen C., Löther T., Weise S. 2008. Application of active infrared thermography for the detection of sub-surface defects in historic wall paintings and the assessment of their backfilling. In: Lukaszewicz, J. & Niemcewicz P. (Eds.) Proceedings of the 11th International congress on deterioration and Conservation of Stone, ICOMOS Poland, Torun, 1, pp. 441-448

Meyer K., Lorenz P., Böhl-Kuhn B., Klobes P. 1994. Porous solids and their characterization. *Crystal Research and Technology*, 29, pp. 903–930

Miller R.P. 1965. Engineering classification and index properties for intact rock. PhD Thesis, University of Illinois

Mimoso J., Costa D. 2006. The DRMS drilling technique with pilot holes. In: Proceedings of the International Heritage, Weathering & Conservation Conference, Consejo Superior de Investigaciones Científicas, Madrid, pp. 651-656

Mimoso J., Costa D. 2008. A new technique for using DRMS in hard materials. Application to the study of the consolidation action. In: Delgado Rodrigues & Mimoso (Eds.) Proceedings of the International Symposium for Stone consolidation in cultural heritage – research and practice, LNEC, Lisbon, pp. 359-368

Montoto M. 1978. Fabric and texture of rock materials in relation to their engineering properties. In: Proceedings of the 3<sup>rd</sup> International Congress of the Association of Engineering Geology, Madrid, S. II, v. 2, pp. 51-60

Montoto M. 2004. Petrophysics at the rock scale: hydraulic properties and petrographic interpretation. ENRESA, Madrid, 297p.

Moropoulou A, Bisbikou K, Torfs K, Van Grieken R, Zezza F, Macri F. 1998. Origin and growth of weathering crusts on ancient marbles in industrial atmosphere. *Atmospheric Environment* 32, pp. 967-982

Moyzes A. 1995. Székesfehérvár, Nemzeti Emlékhely-építéshidrológiai vizsgálata [Hydrogeological survey of the Székesfehérvár National Monument]. Manuscript,

NATURAQUA, Kutató, Tervező és Szolgáltató bt. és szakértői csoportja, Budapest (in Hungarian)

Olmi R., Riminesi C., Priori S., Proietti N., Capitani D., Segre A. L., Giani E., Santopadre P. 2008. An integrated approach to mapping moisture and salt content in two frescoes in the Basilica of San Clemente. In: Tiano P. & Pardini C. (Eds.): *In situ Monitoring of Monumental Surfaces*. Edifir-Editzioni, Florence, pp. 239-246

Oravecz J. 1997. Jelentés a székesfehérvári romkert feltárt építőköveinek földtani vizsgálatáról. [Report on the excavated building stones of the Székesfehérvár ruin garden]. Manuscript, Szent István Király Múzeum Adattára, ltsz. 6980/99, Székesfehérvár (in Hungarian)

Pamplona M., Kocher M., Snethlage R., Aires-Barros L. 2007. Drilling resistance: overview and outlook. *Zeischrift der Deutshen Gesellscahft für Geowissenschaften*, 158/3, pp. 665-676

Pamplona M., Kocher M., Snethlage R. 2008. Micro drilling reseistance – How can satisfying correlations with mechanical properties be found? In: Tiano P. & Pardini C. (Eds.): *In situ Monitoring of Monumental Surfaces*. Edifir-Editzioni, Florence, pp. 341-346

Papayianni I., Stefanidou M. 2005. The role of aggregates on the structure and properties of lime mortars, *Cement and Concrete Composites*, 27, pp. 914-919

Papayianni I., Stefanidou M. 2006. Strength-porosity relations in lime-pozzolan mortars, *Construction and Building Materials*, 20, pp. 700-705

Papayianni I., Stefanidou M. & Pachta V. 2008. Design and application of artificial stone compatible to the existing old one in the archaeological site of Pella. In: Lukaszewicz, J. & Niemcewicz P. (Eds.) *Proceedings of the 11th International congress on deterioration and Conservation of Stone*, ICOMOS Poland, Torun, 2, pp. 709-716

Pfefferkorn S. 2000. Correction functions for eliminationg drill bit abrasion and blocked drill dust transport. In: Tiano P. (Ed.) *Proceedings of the Workshop DRILLMORE – Drilling Methodologies for Monuments Restoration*, Centro Stampa Toscana Nuova, Firenze, pp. 67-74

- Pintér F. et al. 2004. The provenance of “red marble” monuments from the 12th – 18th centuries in Huééengary. *European Journal of Mineralogy*, 16, pp. 619-629
- Powers T.C., Helmuth R.A. 1953. Theory of volume changes in hardened Portland Cement Paste during freezing. *Mater. Constr.*, 46, pp. 285-297
- Prick A. 1995. Dilatometrical behaviour of porous calcareous rock samples subjected to freeze-thaw cycles. *Catena*, 25, pp. 7-20
- Prick A., Pissart A., Ozouf J.-C. 1993. Variations dilatométriques de cylindres de roches calcaires subissant des cycles de gel-dégel. *Permafrost Periglacial Process.*, 4, pp. 1-15
- Prykril R. 2007. Understanding the Earth scientists's role in the pre-restoration research of monuments: an overview. In: Prykril R. & Smith J.B. (Eds.): *Building Stone Decay: From Diagnosis to Conservation*, Geological Society, London, Special Publications 271, pp. 9-21
- Qasrawi H.Y. 2000. Concrete strength by combined nondestructive methods - Simply and reliably predicted. *Cement and Concrete Research*, 30, pp. 739-746
- Ordóñez S., Fort R., García del Cura M. A., 1997. Pore size distribution and the durability of a porous limestone. *Quarterly Journal of Engineering Geology*, 30, pp. 221– 230
- Renault P. 1988. Theoretical studies of mercury intrusion in some networks: testing the applicability of mercury intrusion in the size characterisation of the lacunar pore space of soil samples. *Transport in Porous Media*, 3, pp. 529–547
- Richardson B. A. 1991. The durability of porous stones. *Stone Ind.*, 12, pp. 22–25
- Rilem CPC11.3 1984. Absorption d’eau par immersion sous vide / Absorption of water by immersion under vacuum. *Rilem Publications SARL, Materials and Structures*, 17, Issue 101, pp. 391-394
- Roels S., Elsen J., Carmeliet J., Hens H. 2001. Pore volume distribution of limestone combining mercury porosimetry and micrography. *Materials and Structures (RILEM)*, 34, pp. 76-82
- Rouquerol F, Rouquerol J, Sing K. 1999. Assessment of microporosity. In: *Adsorption by powders and porous solids*. London: Academic Press, pp. 219–236

- Sabbioni C 1995. Contribution of atmospheric deposition to the formation of damage layers. *The Science of the Total Environment* 167, pp. 49-55
- Sachpazis C.I. 1990. Correlating Schmidt hardness with compressive strength and Young's modulus of carbonate rocks. *Bulletin of Engineering Geology and the Environment*, 42, pp. 75-83
- Scherer G.W., Flatt R., Wheeler G. 2001. Materials science research for the conservation of sculpture and monuments. *MRS Bulletin*, 26, pp. 44-50
- Schmidt E. 1951. A non-destructive concrete tester. *Concrete*, 59 (8), pp. 34-35
- Sing K. 2001. Review. The use of Nitrogen adsorption for the characterization of porous materials. *Journal of Colloids and Surfaces, A* 187-188, pp. 3-9
- Singer B., Hornschild I., Snethlage R. 2000. Strength profiles and correction functions for abrasive stones. In: Tiano P. (Ed.) *Proceedings of the Workshop DRILLMORE – Drilling Methodologies for Monuments Restoration*, Centro Stampa Toscana Nuova, Firenze, pp. 35-42
- Smith B.J., Viles H.A. 2006. Rapid catastrophic decay of building limestones: Thoughts on causes, effects and consequences. In: Fort R, Alvarez de Buego M, Gomez-Heras M. and Vazquez-Calvo C. (Eds): *Heritage Weathering and Conservation*, Taylor & Francis/Balkema, London, Vol. I, pp. 191-197
- Stefanidou M., Papayianni I. 2008. The porosity of limestone and its behaviour to salt cycles. In: Lukaszewicz, J. & Niemcewicz P. (Eds.) *Proceedings of the 11th International congress on deterioration and Conservation of Stone*, ICOMOS Poland, Torun, 1, pp. 283-290
- Suryanarayana C., Norton M. G. 1998. *X-Ray Diffraction: A Practical Approach*, Plenum Press, New York, p. 238
- Theodoridou M., Török Á. 2008. Conservation Science and the role of Engineering Geology in studying material properties; a case study of the Székesfehérvár Ruin Garden. In: Török Á. Vásárhelyi B. (Eds.) *Engineering-Geology and Rock Mechanics 2008 (Mérnökgeológia-Közetmechanika 2008)*, Műegyetemi Kiadó, Budapest, pp. 225-236

Theodoridou M. 2007. Preliminary petrographic investigation of building stones in the Szekesfehervar Ruin Garden, Hungary. Problems encountered in the preservation of monuments, Archeometriai Műhely/Archaeometry Workshop, 2007/3, Budapest, pp. 53-59 (in Hungarian with English abstract)

Theodoridou M. 2008. The significance of a broad investigation on monumental building stones, preceding consolidation. Székesfehérvár Ruin Garden, Hungary. In: Delgado Rodrigues & Mimoso (Eds.) Proceedings of the International Symposium for Stone consolidation in cultural heritage – research and practice, LNEC, Lisbon, pp. 427-434

Theodoridou M., Biczó P., Józsa S., Kázmér M., Szakmány G. 2008a. Petrographic results and possible provenance of medieval building stones, Székesfehérvár Ruin Garden, Hungary. Problems encountered in the preservation of monuments. In: Book of abstracts of the 37th International Symposium on Archaeometry, Siena, p. 254

Theodoridou M., Stefanidou M., Józsa S. 2008b. Mechanical and physical properties of medieval building stones in relation to the state of conservation. Székesfehérvár Ruin Garden, Hungary. In: Proceedings of the 9th International (CICOP) Congress of Architectural Heritage Rehabilitation and Building, Seville, vol. I, pp. 289-295

Tiano P. 2001. The use of microdrilling techniques for the characterization of stone materials, in site control and non destructive evaluation of masonry structures and materials. In: L. Binda and R.C. de Vekey (Eds.) (Rilem PRO26, 2003): Proceedings of the RILEM TC177 MDT International Workshop, Mantova, pp. 203-214

Tiano P., Delgado Rodrigues J., De Witte E., Vérges Belmin V., Massey S. Snethlage R., Costa D., Cadot-Leroux L., Carrod E., Singer B. 2000a. The conservation of monuments: A new method to evaluate consolidating treatments. Internationale Zeitschrift für Bauinstandsetzen und Baudenkmalpflege, Geowissenschaften 6, Jahrgang, Heft 2, pp. 133-150

Tiano P., Filareto C., Ponticelli S., Ferrari M., Valentini E. 2000b. Drilling force measurement system, a new standardisable methodology to determine the stone cohesion: Prototype design and validation. Internationale Zeitschrift für Bauinstandsetzen und Baudenkmalpflege, Geowissenschaften 6, Jahrgang, Heft 2, pp. 115-132

- Török Á. 2002. Oolitic limestone in polluted atmospheric environment in Budapest: weathering phenomena and alterations in physical properties. In: Siegesmund S., Weiss T. S., Vollbrecht A (Eds.), *Natural Stones, Weathering Phenomena, Conservation Strategies and Case Studies*. Geological Society, London, Special Publications, 205, pp. 363-379
- Török Á. 2003. Surface strength and mineralogy of weathering crusts on limestone buildings in Budapest. *Building and Environment*, 38, pp. 1185-1192
- Török Á. 2004. Leithakalk-type limestones in Hungary: an overview of lithologies and weathering features. In: Prikryl R., Siegel P. (Eds): *Architectural and sculptural stone in cultural landscape*. The Karolinum Press, Prague, pp. 157-172
- Török Á. 2006. Hungarian travertine: Weathering forms and durability. In: Fort, Alvarez de Buergo, Gómez-Heras & Vasquez-Calvo (Eds.) *Heritage, Weathering and Conservation*, London, pp. 199-204
- Török Á. 2007a. Hungarian dimensional stones: an overview. *Zeischrift der Deutshen Gesellscahrt für Geowissenschaften*, 158/3, pp. 361-374
- Török Á. 2007b. Morphology and detachment mechanism of weathering crusts of porous limestone in the urban environment of Budapest. *Central European Geology*, 50/3, pp. 225-240
- Török Á. 2008. Schmidt hammer and duroscope tests in assessing surface properties of stones. In: Tiano P. & Pardini C. (Eds.): *In situ Monitoring of Monumental Surfaces*. Edifir-Editzioni, Florence, pp. 207-214
- Török Á. 2009. In situ methods of testing stone monuments and the application of non-destructive physical properties testing in masonry diagnosis. In: M. Bostenaru Dan et al. (Eds.): *Materials, Technologies and Practice in Historic Heritage Structures*, Springer Science+Business Media B.V., London, pp. 177-193
- Török Á., Rozgonyi N, Prikryl R., Prikrylová J. 2004. Leithakalk: the ornamental and building stone of Central Europe, an overview. In: Prikryl, R. (ed), *Dimension stone*. Balkema, Rotterdam, pp. 89-93

Török Á., Siegesmund S., Müller C., Hüpers A., Hoppert M., Weiss T. 2007a. Differences in texture, physical properties and microbiology of weathering crust and host rock: a case study of the porous limestone of Budapest (Hungary). In: Přikryl R. & Smith B. J. (Eds.) *Building Stone Decay: From Diagnosis to Conservation*, Geological Society, London, Special Publications, 271, pp. 261-276

Török Á., Stück H., Quetscher A., Glätzner P. 2007b. Comparative study of weathering features of stones in Hungarian castles: morphological characteristics and changes in physical properties. *Zeischrift der Deutshen Gesellscahft für Geowissenschaften*, 158/4, pp. 931-955

Török Á., Weiss T., Hüpers A., Müller C. & Siegesmund S. 2004. The decay of oolitic limestones controlled by atmospheric pollution: a case study from the Parliament and Citadella in Budapest, Hungary. In: Kwiatkowski D. & Löfvendal R. (Eds.): *Proceedings of the 10th International Congress on Deterioration and Conservation of Stone*, ISOMOS Sweeden, Stockholm, 2, pp. 947-954

Tóth M. 1995. Székesfehérvár Nemzeti Emlékhely régészeti feltárásából származó kőanyagok ásvány-kőzettani kutatásáról. [On the mineralogical and petrographical examination of the lithic materials of the Székesfehérvár National Monument]. Manuscript, Jelentés a KMB 317/G/1995 GKL számú kutatási szerződés keretében végzett, MTA Geokémiai Kutatólaboratóriumában, Budapest (in Hungarian)

Trudgill S.T., Viles H.A., Cooke R.U., Inkpen R.J., Heathwaite L.A. and Houston J. 1991. Trends in stone weathering and Atmospheric pollution at St Paul's Cathedral, London, 1980-1990. *Atmospheric Environment* 25A, 12, pp. 2851-2853

Varjú E. 1930. Szent István koporsója. [St. Stephen's coffin]. *Magyar Művészet* 6, pp. 372-379

Viles H., Camuffo D., Fitz S., Fitzner B., Lindquist O., Livingston R.A., Maravellaki P.V., Sabbioni C. & Warscheid T. 1997. What is the state of our knowledge of the mechanisms of deterioration and how good are our estimations of rates of deterioration? In: Dahlem Workshop "Saving our architectural heritage - the conservation of historic stone structures", John Wiley & Sons Ltd, UK, pp. 95-112



Viles H. A. 1993. The Environmental Sensitivity of Blistering of Limestones Walls in Oxford, England: A Preliminary Study. In: Thomas DSG, Allison RJ (Eds.) Landscape Sensitivity. John Wiley, Chichester, pp 309-326

Washburn E. N. 1921. Note on a Method of Determining of Pores Sizes in a Porous Material. In: Proceedings of the National Academy of Science, 7, pp. 115-116

Weiss J. 2006. Elastic properties, creep and relaxation. In: Lamond J. F. & Pielert J. H. (Eds.): Significance of tests and properties of concrete and concrete-making materials. American Society for Testing and Materials, Committee C-9 on Concrete and Concrete Aggregates, pp. 194-206

Winkler E.M. 1997. Stone in Architecture: Properties, Durability, 3rd edition. Springer-Verlag, Berlin

Winslow D. N., Diamond S. 1970. A mercury porosimetry study of the evaluation of porosity in cement. ASTM J. Materials, 5 (3), pp. 564-585

Wojnárovits L. 1995. Mészke minták higany-penetrációs porozitás és elektronmikroszkópi vizsgálata. [Mercury penetration porosity and SEM investigation of limestone samples]. Manuscript, SZIKKTI Labor Kft., Budapest (in Hungarian)

Internet links:

Working group "Natural stones and weathering". RWTH Aachen University.  
[www.stone.rwth-aachen.de](http://www.stone.rwth-aachen.de).

The limestone project: Understanding the catastrophic decay of building limestone. Queen's University of Belfast, Oxford University, City University of London.  
[www.qub.ac.uk/geomaterials/epsr/](http://www.qub.ac.uk/geomaterials/epsr/)

## 10. ACKNOWLEDGEMENTS

---

The presented research is a part of the European PhD in Science for Conservation (EPISCON-project) which has been financially supported by the Marie Curie Actions (6th Framework Programme's Human Resources and Mobility - HRM, European Union).

First of all, I would like to thank my supervisors Prof. Ákos Török and Dr. Sándor Józsa who helped me in carrying out this research project and overcoming all the obstacles. Especially, I would like to express my gratitude to Prof. Török Ákos who accepted to collaborate within the frames of this project and therefore guide and supervise my research till the end. I am also grateful to Dr. Szakmány György for his assistance, Dr. Biczó Piroska for her help in everything related to the historical site, Dr. Katalin Biró, Dr. Márta Kissné and Dr. Farkas Pintér for their continuous collaboration.

I am indebted to my colleagues from ELTE and BME Universities for their assistance both in the theoretical and experimental part of the research: Dr. Görök Péter, Dr. Kopecskó Katalin, Árpás Endre, Emszt Gyula, Szemerey-Kiss Balázs, Bálint Pálkás, Zsolt Bedő. The help of Rita Kókey in all the administrative part of the project is very much appreciated.

Prof. Ioanna Papayianni and Dr. Maria Stefanidou from the Aristotle University of Thessaloniki are highly acknowledged for their useful advices and the access to the equipment of the Laboratory of Building Materials. The application of the DRMS in-situ was a part of MOLAB which was financially supported by the Eu-Artech project and represented in Hungary by Dr. Piero Tiano, Dr. Susanna Bracci and Dr. Barbara Sacci from ICVBC in Florence. Dr. Silvia Rassic from ICVBC is also acknowledged for the MIP. I am grateful to Dr. Rosa Espinosa for carrying out the DMA measurement at the Princeton University.

The freshly quarried materials that were submitted to the tests were a kind offer of the Sósút Limestone Quarry and the Tardos Stein Ltd.

Many thanks to the persons that made my life pleasant and fun in these past three years and were always a real support both psychologically and practically: Efi, Theodoros, Eleni, Timea, Louise, the friends and colleagues from EPISCON project and last but not least Anna, for sharing together all the good and bad moments and a priceless and sincere friendship.

Finally, I would like to dedicate this dissertation to my parents Theodoros and Sofia and my brother Giannis, since without their continuous help and support in all these years of my studies this PhD would have never been feasible.